STRUCTURE-PRESERVING ISOGEOMETRIC ANALYSIS FOR COMPUTATIONAL FLUID DYNAMICS

BY STEVIE-RAY JANSSEN

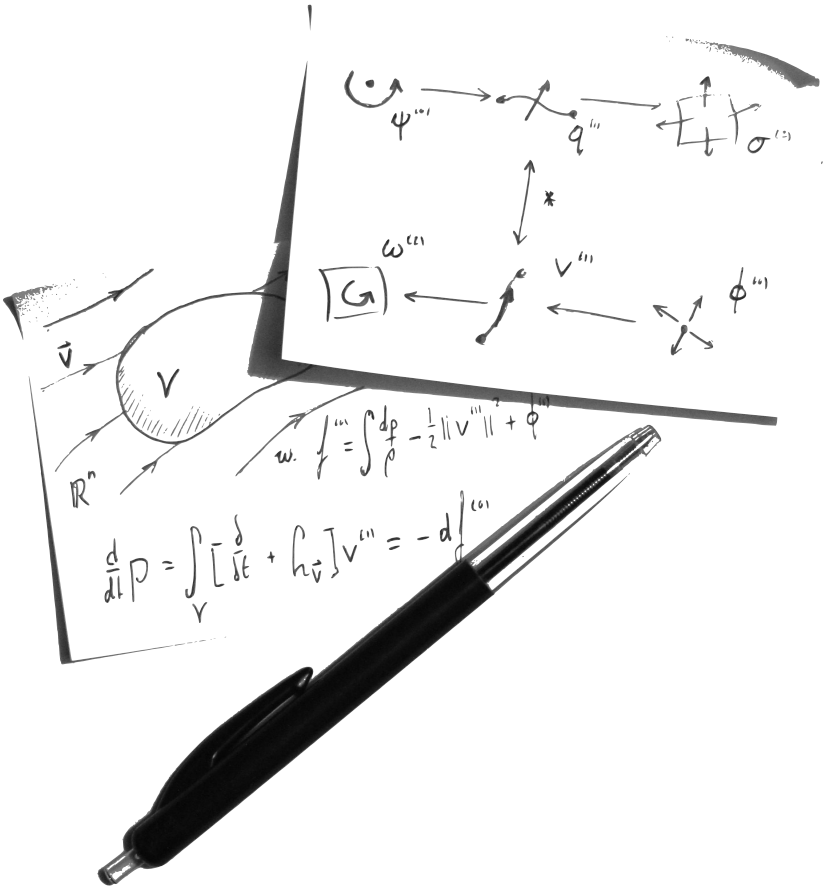

M.SC. THESIS

November 7th, 2016

Structure-Preserving Isogeometric Analysis for Computational Fluid Dynamics

M.Sc. Thesis

To obtain the degree Master of Science at Delft University of Technology,

by

Stevie-Ray Janssen

Student of Aerospace Engineering and Applied Mathematics,
Delft University of Technology,
Delft, The Netherlands.

Thesis Committee:

Aerospace Engineering:

Dr. ir. M.I. Gerritsma	TU Delft, supervisor
Prof. dr. S. Hickel	TU Delft
Dr. ir. A. Palha	TU Eindehoven

Applied Mathematics:

Dr. M. Möller,	TU Delft, supervisor
Prof. dr. ir. C. Vuik	TU Delft
Prof. dr. J.M.A.M. van Neerven	TU Delft

November 7th, 2016

An electronic version of this dissertation is available at
http://repository.tudelft.nl/.

Contents

PREFACE

Man, I went through this thesis project like a loose cannon. I finally found myself near the battlefront of knowledge! I was excited to learn, to develop new ideas, and I wanted to do everything. Call it a young man's hubris. I've looked at space-time discretisations, the variational multiscale method, discontinuous Galerkin, Lagrangian and Eulerian meshing techniques, symplectic time integrators, and, of course, isogeometric analysis and structure-preserving discretisation techniques. Unsurprisingly, I struggled somewhat with combining this all into one thesis, which resulted in the fact that some material has been removed or moved to appendices to improve both consistency and readability. I encourage any reader to check the appendices as well.

In 2013 I attended dr. Gerritsma's course on structure-preserving discretisations for CFD. The mathematics fascinated me even though I barely understood what he was talking about (pseudo-differential form-coboundary-operator-mumbo-jumbo). I wanted to learn more about this stuff, and asked him if I could do my thesis project with him. He, being a nice man and all, accepted my request. He brought me into contact with dr. Möller, who was organising biweekly seminars on isogeometric analysis at that time. Since this stuff was also pretty interesting, I ended up combining both topics into structure-preserving isogeometric analysis for CFD.

I would like to thank them both for guiding me along the way. I would like to thank some of my predecessors, Hiemstra, dr. Kreeft, Natale, dr. Palha, Rebelo, Toshniwal, old students of dr. Gerritsma, whose theses inspired me and helped me mastering the material. I'd like to thank prof. Hughes for having me over at ICES in Austin for a few months. Thank you for your great lectures on isogeometric analysis. Special thanks to René and Deepesh for your guidance and friendship. I really enjoyed working with you guys. I'd also like to thank the other guys at ICES for letting me kick their asses at fußbal. Finally, I'd like to thank my girlfriend, Mariel, who has taken such good care of me.

Stevie-Ray Janssen
Rotterdam, November 2016

1

INTRODUCTION

Computational Fluid Dynamics (CFD), the field of computer simulations of fluid flows, has established itself as one of the pillars of modern fluid flow research. The field has a wide range of theoretical applications which include the research of turbulence, tidal dynamics, and blood flows, but also knows important industry applications as the design of aircraft, micro-processors, or submarines. The Navier-Stokes equations govern many fluid flows. The underlying geometric structure of these equations facilitates structures and symmetries. Classical solution methods often neglect these structures. As a result, these methods fail to conserve invariant quantities, and are unable to simulate the desired physical behaviour, [1]. Recently it is shown that solution techniques can be constructed that do preserve the underlying geometry of physics. These techniques are known as *structure-preserving techniques*.

"In discretising the incompressible Navier-Stokes' one encounters two difficulties, p.265 [2]". The first difficulty is the discretisation of the non-linear convective term. The second difficulty used to be the treatment of the saddle-point problem that describes the relation between pressure and velocity. Structure-preserving methods have reduced the second difficulty to a triviality. These methods aim at preserving fundamental structures of operators and operands found in partial differential equations (PDE's). Concepts from differential geometry and algebraic topology are used to analyse these structures. In this approach we distinguish between relations that depend on metric and those that are purely topological. The topological relations can be described using algebraic equations, which allows exact representation in the discrete setting as argued by Tonti [1]. Satisfying these topological relations lies at the heart of structure-preserving discretisation techniques.

The application of differential geometry and algebraic topology has resulted in the development of a wide variety of structure-preserving discretisation techniques. Roughly speaking, they can be split in two groups, each having a different approach of discretising the Hodge-$\star$ operator. In the first approach one defines an explicit primal- and dual-grid on which the action of the Hodge-$\star$ operator is approximated. This approach leads more to a finite-differencing, or finite-volume type methods. Fundamental works include the

work on mimetic finite difference by Hyman, [3], and the work on discrete exterior calculus by Desbrun et al., [4]. In another approach one uses the inner product definition of the Hodge-$\star$ operator in a variational approach, leading to finite-element type methods. Fundamental works in are the ones on finite element exterior calculus by Arnold et al., [5], conforming mimetic discretisations by Bochev and Hyman, [6], and mimetic spectral element method Gerritsma et al, [7].

Isogeometric analysis (IGA) was pitched by Hughes et al. in 2005 to bridge the gap between CAD design and analysis, [8]. In this approach *Non-Uniform Rational B-spline*s (NURBS) are used for both representation of the physical geometry and variational analysis. It was shown that NURBS posses superior approximation behaviour in analysis over Lagrange polynomials, classically used in finite elements analysis, [9, 10]. Buffa et al. developed a theoretical framework of structure-preserving isogeometric analaysis for elliptic PDE problems, [11]. Variety of successful implementations include the Maxwell equations by Buffa, [12], and the unsteady Navier-Stokes' equations by Evans, [13]. These works deal with similar discretisation challenges, e.g. unsteadiness, non-linearity and asymmetric operators, that are also present in the proposed model problem.

The incompressible Euler equations have a rich geometric structure as described in [14]. The Hamiltonian structure of these was unveiled in the classical work by V. Arnold [15]. An interesting discretisation was introduced by L. Rebholz in which velocity and vorticity are treated as independent variables [16]. The structure-preserving discretisation by Palha makes use of this idea [17]. The study proposed will contribute to these developments, and will aim at the further development and analysis of structure-preserving techniques for the Euler equations. The main challenge is to discretise the non-linear convective operator in a structure-preserving manner, i.e. preserving global quantities as kinetic-energy, vorticity, and enstrophy.

This thesis is the result of a research project on discretisation techniques for CFD. This thesis was written to obtain the degree of Master of Science at the faculties of Aerospace Engineering (AE) and Applied Mathematics (AM) at Delft University of Technology. The project was divided in three objectives. The first objective was to study the existing existing structure-preserving IGA framework for elliptic PDE's, (chapter 2 and chapter 3). The objective for AM was to expand this theoretical framework to discretise hyperbolic PDE's (chapter 4). The objective for AE was to construct a structure-preserving IGA discretisation for the incompressible Euler equations, chapter 5. All results are combined in this single thesis document.

In line with the mentioned works we will analyse the PDE's using concepts from differential geometry, exterior calculus, and algebraic topology. Fundamental concepts and theorems from these fields will be introduced and reviewed in chapter 2. We will identify the DeRham complex, which can also be constructed in a discrete setting, and formulate elliptic PDE problems. In chapter 3 we will introduce a variational framework, the foundation of the finite-elements method, introduce concepts from isogeometric analysis, and construct a framework of structure-preserving isogeometric analysis, using the concepts introduced in chapter 2. We will use these results to discretise various formulations of the scalar Poisson problem. In chapter 4 we expand our exterior calculus toolbox, and introduce variational formulations for hyperbolic PDE's. We study the scalar transport equation, and discuss various discretisation strategies. Finally, in chapter 5 we introduce

the Euler equations for incompressible fluids, and derive structure-preserving discretisations that conserve integral invariants over time. Conclusions and future directions will be discussed in chapter 6

2

EXTERIOR CALCULUS

The laws of physics are generally analysed using the language of vector calculus. Following the works mentioned in the introduction, we will analyse physical relations using *differential geometry*, *exterior calculus*, and *algebraic topology*. The first advantage of this approach is that analysis is performed on arbitrary geometries, which are known as *manifolds*. Results that will be introduced do not depend on some local description of physics. The second and main advantage of this approach, is that it enables a clear distinction between relations that do depend on the description of local geometry, i.e. that depend on *metric*, and those that are purely topological, i.e. that are independent of metric. In the discrete setting local geometry is approximated on some mesh, which induces an approximation error for metric-dependent relations. Topological relations can be described using algebraic equations, which allows exact representation in the discrete setting. Satisfying these topological relations lies at the heart of structure-preserving discretisations techniques.
In this chapter we will introduce fundamental concepts from the fields, and aim to relate these concepts to numerical analysis. In section 2.1 we introduce *manifolds* and *coordinate systems* on which we define *primal* and *dual* vector spaces. Dual vectors, known as *differential forms*, are used to describe physical quantities. Basic operations as the *wedge product* $\wedge$ and the *exterior derivative d* on differential forms are presented in section 2.2. The exterior derivative is a generalisation of the grad, curl, and div operations from vector calculus. Relations between differential forms that are governed by the exterior derivative are topological, and can be satisfied exactly by discrete spaces using *chains* and *cochains*. In section 2.3 we define these chains and cochains from the field of algebraic topology. We show that differentiation is exact in the discrete setting. Metric-dependent relations are introduced in the next section, section 2.4. Here we define an inner product through the *Hodge-$\star$ operator*. In the final section, section 2.5, we return to the physics, and formulate PDE's on arbitrary geometries using the formalisms introduced in this chapter.

2.1. MANIFOLDS AND COORDINATE SPACES

In this section we will introduce *manifolds* and *coordinate bases*. A manifold is a topological description of some geometry. One needs to introduce a coordinate system to measure metrics, i.e. positions, distances, or angles on a specific manifold. For example, a disk in $\mathbb{R}^2$ is a manifold, one can measure metric using the Cartesian or the equivalent polar coordinate system. Derivatives of the coordinate system's mapping form a basis. This basis is used to describe quantities known as *vectors*. There exists a dual basis which is used to describe quantities known as *differential forms*. Differential forms are coordinate invariant containers of quantities that are associated with points, lines, surfaces, or volumes. We will use these differential forms as the variables in our coordinate invariant description of PDE's.

A n-dimensional *manifold* $\mathcal{M}$ is a topological space which is locally homeomorphic to Euclidean space $\mathbb{R}^n$. We define *charts* $\mathcal{U}_\alpha$ to be the open subsets that cover the manifold $\mathcal{M}$, i.e.

$$\mathcal{M} = \bigcup_{\alpha \in A} \mathcal{U}_\alpha. \tag{2.1}$$

For each chart $\mathcal{U}_\alpha$, there exists a bijective coordinate map $\varphi_{\mathcal{M},\alpha} : \mathcal{U}_\alpha \to \mathbb{R}^m$, with $m \geq n$. The coordinate map $\varphi_{\mathcal{M},\alpha}$ associates coordinates to each point $p \in \mathcal{U}_\alpha$,

$$p = (x_1, x_2, \cdots, x_m) = \varphi^{-1}_{\mathcal{M},\alpha}(\hat{x}_1, \hat{x}_2, \cdots, \hat{x}_m), \tag{2.2}$$

with $(\hat{x}_1, \hat{x}_2, \cdots, \hat{x}_m) \in \varphi_{\mathcal{M},\alpha}(\mathcal{U}_\alpha)$. The pair $(\mathcal{U}_\alpha, \varphi_{\mathcal{M},\alpha})$ defines a *local coordinate system*. We require that local coordinate systems are compatible in regions where charts overlap. Hence, on the overlap of charts $\mathcal{U}_\alpha \cap \mathcal{U}_\beta$ we demand existence of a *diffeomorphism*, which is the map,

$$\varphi_{\mathcal{M},\beta} \circ \varphi^{-1}_{\mathcal{M},\alpha} : \varphi_{\mathcal{M},\alpha}(\mathcal{U}_\alpha \cap \mathcal{U}_\beta) \to \varphi_{\mathcal{M},\beta}(\mathcal{U}_\alpha \cap \mathcal{U}_\beta). \tag{2.3}$$

A diffeomorphism is essentially a transformation from one coordinate system to another. We illustrate these concepts in Figure 2.1. The collection of all pairs $\mathcal{A} = \{(\mathcal{U}_\alpha, \varphi_{\mathcal{M},\alpha})\}_{\alpha \in A}$ is known as the *atlas* of $\mathcal{M}$. We formally define a manifold using the atlas as follows.

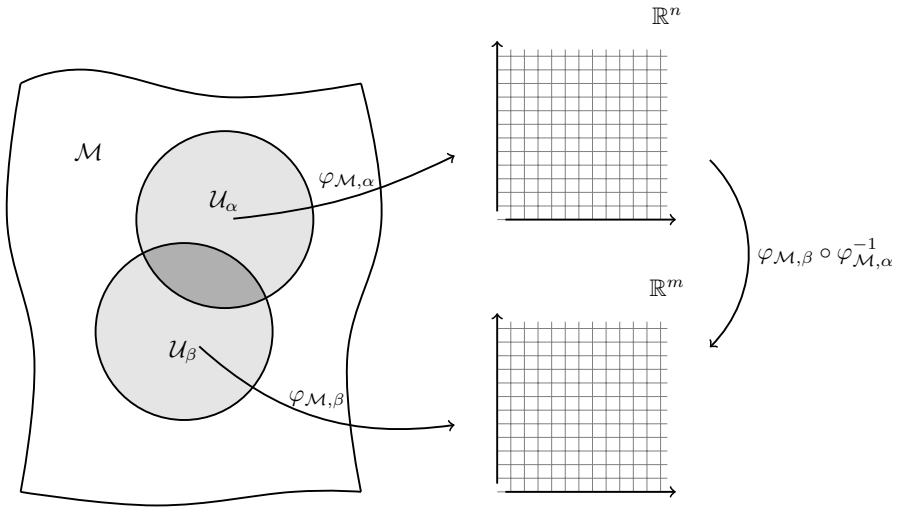

Figure 2.1: Differentiable manifold $\mathcal{M}$ with charts $\mathcal{U}_\alpha$, and $\mathcal{U}_\beta$. $\mathcal{U}_\alpha \cap \mathcal{U}_\beta \neq \emptyset$. Points in $\mathcal{U}_\alpha$ are described by the map $\varphi_{\mathcal{M},\alpha} : \mathcal{U}_\alpha \to \mathbb{R}^n$, similarly for $\mathcal{U}_\beta$. On $\mathcal{U}_\alpha \cap \mathcal{U}_\beta$ there exists diffeomorphism $\varphi_{\mathcal{M},\beta} \circ \varphi^{-1}_{\mathcal{M},\alpha}$.

Definition 2.1 (Differentiable manifold, (Sec. 1.2 [18]))**.**
A n-dimensional k-differentiable manifold is a topological space for which there exists an atlas $\mathcal{A} = \{(\mathcal{U}_\alpha, \varphi_{\mathcal{M},\alpha})\}$, whose coordinate maps are k-times differentiable, i.e. $\varphi_{\mathcal{M},\alpha} \in \mathcal{C}^k$. A smooth manifold is a manifold with $\varphi_{\mathcal{M},\alpha} \in \mathcal{C}^\infty$.

The continuity constraints are required to perform analysis on manifolds. Each point p in $\mathcal{M}$ is either an *interior point* or a *boundary point*. We call $p = (x_1, x_2, \cdots, x_n) \in \mathcal{M}$ an interior point if there exists an open ball around p that is fully contained in $\mathcal{M}$, i.e.

$$\exists\, \epsilon > 0 \quad \text{s.t.} \quad \{x \in \mathcal{M} : d(x,p) < \epsilon\} \subset \mathcal{M},$$

where $d(x,p)$ is the distance measured in some metric. A point p is a boundary point if it is not an interior point. The set of boundary points of $\mathcal{M}$ denoted by $\partial\mathcal{M}$.
We can use a coordinate system to locally define a linear vector space. First consider a point p on the local coordinate system (U,φ) on n-dimensional differentiable manifold $\mathcal{M}$. Consider a curve $\gamma(s) = (x_1(s), x_2(s), \cdots, x_n(s))$ through p, with parametric coordinate $s \in (-\epsilon, \epsilon)$, such that $\gamma(0) = p$, as shown in Figure 2.2. The derivative with respect to parametrisation parameter s, known as the *tangent vector* at p along $\gamma(s)$, is given by,

$$\dot{\gamma}(p) = \left.\frac{d\gamma}{ds}\right|_p = \left.\frac{dx_1}{ds}\frac{\partial}{\partial x_1}\right|_p + \left.\frac{dx_2}{ds}\frac{\partial}{\partial x_2}\right|_p + \cdots + \left.\frac{dx_n}{ds}\frac{\partial}{\partial x_n}\right|_p. \tag{2.4}$$

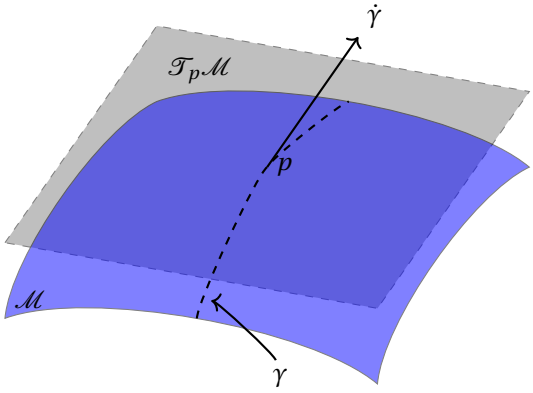

Figure 2.2: Tangent vectors $\dot{\gamma}$ of curves γ through p define the tangent space $\mathcal{T}_p\mathcal{M}$ on differentiable manifold $\mathcal{M}$.

The collection of all possible tangent vectors through p span a linear vector space, which we call the *tangent space* of $\mathcal{M}$ at p, denoted by $\mathcal{T}_p\mathcal{M}$. The collection of all tangent spaces on $\mathcal{M}$ is known as the *tangent bundle*, denoted by $\mathcal{T}\mathcal{M}$ with,

$$\mathcal{T}\mathcal{M} := \bigcup_{p\in\mathcal{M}} \mathcal{T}_p\mathcal{M}. \tag{2.5}$$

Now we can construct a *coordinate basis* at p. Consider n linearly independent curves $(\gamma_1, \gamma_2, \cdots, \gamma_n)$ through p given by,

$$\begin{aligned}
\gamma_1(x_1) &= (x_1, 0, \cdots, 0),\\
\gamma_2(x_2) &= (0, x_2, \cdots, 0),\\
&\vdots\\
\gamma_n(x_n) &= (0, 0, \cdots, x_n).
\end{aligned}$$

The corresponding n tangent vectors define a basis $\frac{\partial}{\partial x^i}$ at a point p.

Definition 2.2 (Basis $\frac{\partial}{\partial x^i}$, (Sec. 1.3 [18]))**.**
Given a n-dimensional differentiable manifold $\mathcal{M}$ we can define basis vectors at a point $p \in \mathcal{M}$,

$$\frac{\partial}{\partial x^i} := (0, \cdots, 0, \frac{dx_i}{ds}, 0, \cdots, 0). \tag{2.6}$$

A given basis induces *orientation* locally on $\mathcal{M}$, i.e the sign of the determinant of the components of the basis is considered positive or negative. We call a manifold $\mathcal{M}$ *orientable* if the orientation is globally consistent. This means that any locally induced orientation at a point p can be mapped continuously along any closed curve in $\mathcal{M}$ such that the orientation is not reversed at the endpoint in p.

A vector $\boldsymbol{v}$ can be expanded in some basis at p,

$$\begin{aligned}\boldsymbol{v}_p &= v^1(p)\frac{\partial}{\partial x^1} + v^2(p)\frac{\partial}{\partial x^2} + \cdots + v^n(p)\frac{\partial}{\partial x^n} \\ &= \sum_i v^i(p)\frac{\partial}{\partial x^i}.\end{aligned}$$

The action of a vector on a smooth scalar function on the manifold, $f \in C^\infty(\mathcal{M})$, along curve $\gamma(s)$, is equivalent to the directional derivative of f in $\gamma(s)$,

$$\boldsymbol{v}_p(f) = \sum_i v^i(p)\frac{\partial f}{\partial x^i} = \sum_i \frac{dx_i}{ds}\bigg|_p \frac{\partial f}{\partial x^i} = \frac{df(\gamma(s))}{ds}.$$

Note that this operation is a derivation. The dual space of the tangent space is known as *cotangent space*. The cotangent space at p, denoted by $\mathcal{T}_p^*\mathcal{M}$, consists of linear functionals acting on the tangent space. The collection of all cotangent spaces on $\mathcal{M}$ is known as the *cotangent bundle*, and is denoted by $\mathcal{T}^*\mathcal{M}$, with

$$\mathcal{T}^*\mathcal{M} := \bigcup_{p\in\mathcal{M}} \mathcal{T}_p^*\mathcal{M}. \tag{2.7}$$

The contangent space $\mathcal{T}_p^*\mathcal{M}$ is also a linear vector space. We define the basis $(dx^1, dx^2, \cdots, dx^n)$ for $\mathcal{T}_p^*\mathcal{M}$ as the dual of the vector basis in the tangent space $\mathcal{T}_p\mathcal{M}$.

Definition 2.3 (Dual basis dx^i, (Sec. 2.1 [18]))**.**
Given a n-dimensional differentiable manifold $\mathcal{M}$ we define dual basis vectors at a point $p \in \mathcal{M}$, such that

$$dx^i\left(\frac{\partial}{\partial x^j}\right) = \delta^i_j, \tag{2.8}$$

where δ^i_j is the Kronecker delta. The expansion of a dual vector α, in some dual basis at p is given by,

$$\begin{aligned}\alpha_p &= \alpha_p(p)dx^1 + \alpha_2(p)dx^2 + \cdots + \alpha_n(p)dx^n \\ &= \sum_i \alpha_i(p)dx^i.\end{aligned}$$

The action of a dual vector $\alpha(x) = \alpha_1(x)dx^1 + \alpha_2(x)dx^2 + \cdots + \alpha_n(x)dx^n$ on a vector $\boldsymbol{v}(x) = v^1(x)\frac{\partial}{\partial x^1} + v^2(x)\frac{\partial}{\partial x^2} + \cdots + v^n(x)\frac{\partial}{\partial x^n}$, is given by,

$$\alpha(\boldsymbol{v}) = \sum_i^n \sum_j^n \rho_i v^j \frac{\partial}{\partial x^j} dx^i = \sum_i^n \sum_j^n \rho_i v^j \delta^i_j = \sum_i^n \rho_i v^i.$$

Dual vectors, known as a *differential* 1*-forms*, will be used as the objects that hold physical quantities in our formulation of physics. The space of differential 1-forms on $\mathcal{M}$ is denoted by $\Lambda^{(1)}(\mathcal{M})$, with $\alpha^{(1)} \in \Lambda^1(\mathcal{M})$. Scalar functionals, known as *differential* 0*-forms*, are denoted by $\beta^{(0)} \in \Lambda^{(0)}(\mathcal{M})$. In our analysis, vectors will be used to describe variables which are intimately related to the geometric mapping, e.g. deformation and velocity. Differential forms will play the role of physical variables living on the geometries. In the next section we expand the concept of differential forms, and introduce tools and techniques required for analysis.

2.2. FORMS AND OPERATIONS

The differential 1-form resembles the integrand of a line integral. It is a description of a quantity defined along a line, which can be measured by integrating it along a curve. The *wedge product* $\wedge$, that will be introduced shortly hereafter, is used to construct higher dimensional forms that resemble integrands of surface- and volume integrals. In this section we will introduce the fundamental tools required for differentiation and integration of differential forms. Differentiation of forms is governed by the *exterior derivative* d. The exterior derivative is used to differentiate forms, and acts like the grad, curl, or div operator depending on the dimension of the specific form. The exterior derivative induces important topological connections on the spaces of differential forms, which is encoded in the *DeRham sequence*. Proper understanding of its structures is key to the development of structure-preserving discretisations. The *Stokes' theorem* is the fundamental theorem for integration of forms, and will be introduced at the end of this section.
We will introduce a product operator to build higher dimensional objects like surfaces or volumes. Higher dimensional differential forms can be constructed using the *wedge product* $\wedge$.

Definition 2.4 (Wedge product $\wedge$, (Sec. 2.5 [18]))**.**
Let $\Lambda^{(k)}$, and $\Lambda^{(l)}$ be spaces of k-forms and l-forms on $\mathcal{M} \subset \mathbb{R}^n$. The wedge product $\wedge$ is the mapping,

$$\wedge : \Lambda^{(k)}(\mathcal{M}) \times \Lambda^{(l)}(\mathcal{M}) \rightarrow \Lambda^{(k+l)}(\mathcal{M}) \tag{2.9}$$

that satisfies,

$$\begin{aligned}
(\alpha^{(k)} + \beta^{(l)}) \wedge \gamma^{(m)} &= \alpha^{(k)} \wedge \gamma^{(m)} + \beta^{(l)} \wedge \gamma^{(m)} \\
(\alpha^{(k)} \wedge \beta^{(l)}) \wedge \gamma^{(m)} &= \alpha^{(k)} \wedge (\beta^{(l)} \wedge \gamma^{(m)}) \\
f\alpha^{(k)} \wedge \beta^{(l)} &= \alpha^{(k)} \wedge f\beta^{(l)} = f(\alpha^{(k)} \wedge \beta^{(l)}) \\
\alpha^{(k)} \wedge \beta^{(l)} &= (-1)^{kl} \beta^{(l)} \wedge \alpha^{(k)},
\end{aligned}$$

with $\alpha^{(k)} \in \Lambda^{(k)}, \beta^{(l)} \in \Lambda^{(l)}, \gamma^{(m)} \in \Lambda^{(m)}$, and $f \in \Lambda^{(0)}$.

Example 2.1 (Action of the wedge product $\wedge$)**.**
The action of the wedge product is similar to that of the cross- and dot-product in vector

calculus. Consider 1-forms $\alpha^{(1)}, \beta^{(1)} \in \Lambda^1(\mathscr{M})$ with $\mathscr{M} \subset \mathbb{R}^3$.

example 1:

$$dx^1 \wedge dx^1 = -dx^1 \wedge dx^1$$
$$\Leftrightarrow\ dx^1 \wedge dx^1 = 0$$

example 2:

$$\begin{aligned}\alpha^{(1)} \wedge \beta^{(1)} &= (\alpha_1 dx^1 + \alpha_2 dx^2 + \alpha_3 dx^3) \wedge (\beta_1 dx^1 + \beta_2 dx^2 + \beta_3 dx^3)\\ &= \alpha_1\beta_2 dx^1 \wedge dx^2 + \alpha_1\beta_3 dx^1 \wedge dx^3\\ &+ \alpha_2\beta_1 dx^2 \wedge dx^1 + \alpha_2\beta_3 dx^2 \wedge dx^3\\ &+ \alpha_3\beta_1 dx^3 \wedge dx^1 + \alpha_3\beta_2 dx^3 \wedge dx^2\\ &= (\alpha_1\beta_2 - \alpha_2\beta_1) dx^1 \wedge dx^2\\ &+ (\alpha_2\beta_3 - \alpha_3\beta_2) dx^2 \wedge dx^3\\ &+ (\alpha_3\beta_1 - \alpha_1\beta_3) dx^3 \wedge dx^1\end{aligned}$$

example 3:

$$\begin{aligned}\alpha^{(1)} \wedge \beta^{(1)} \wedge \gamma^{(1)} &= (\alpha_1\beta_2\gamma_3 - \alpha_2\beta_1\gamma_3) dx^1 \wedge dx^2 \wedge dx^3\\ &+ (\alpha_2\beta_3\gamma_1 - \alpha_3\beta_2\gamma_1) dx^2 \wedge dx^3 \wedge dx^1\\ &+ (\alpha_3\beta_1\gamma_2 - \alpha_1\beta_3\gamma_2) dx^3 \wedge dx^1 \wedge dx^2\\ &= \det\begin{vmatrix}\alpha_1 & \alpha^2 & \alpha_3\\ \beta_1 & \beta_2 & \beta_3\\ \gamma_1 & \gamma_2 & \gamma_3\end{vmatrix} dx^1 \wedge dx^2 \wedge dx^3\end{aligned}$$

Note that the result $\alpha^{(1)} \wedge \beta^{(1)}$ is a 2-form with components similar to $\boldsymbol{a} \times \boldsymbol{b}$, which describes a surface in vector calculus. Furthermore, $\alpha^{(1)} \wedge \beta^{(1)} \wedge \gamma^{(1)}$ is a 3-form with components similar to $\boldsymbol{a} \times \boldsymbol{b} \cdot \boldsymbol{c}$, which describes a volume (parallelepiped) in vector calculus.

The example reveals a connection between differential forms and geometric objects. Moreover, we observe that forms resemble integrands of line-, surface-, and volume integrals. In $\mathscr{M}(\mathbb{R}^3)$ we associate 3-forms with volumes, 2-forms with surfaces, 1-forms with lines, and 0-forms with points. Each differentiable k-form can be interpreted as some quantity that is to be measured (integrated) in some structure, e.g. flux is measured through surface, and density in volume, and so on. Each physical quantity also has some natural orientation with respect to its underlying structure. We distinguish between *tangential* (inner-oriented) forms, and *normal* (outer-oriented) forms (sec. 28 of Burke [19]). A flux is defined normal through a surface, while vorticity is defined tangential to the surface. Further elaboration on the physical interpretation of differential forms will follow in section 2.5. We present some examples.

$\Lambda^{(k)}$	**geometry**	**example**	
$\Lambda^{(0)}$	points	pressure	$p^{(0)} = p(x,y,z)$
$\Lambda^{(1)}$	lines	velocity	$v^{(1)} = v_x(x,y,z)dx + v_y(x,y,z)dy + v_z(x,y,z)dz$
$\Lambda^{(2)}$	surfaces	flux	$\sigma^{(2)} = \sigma_z(x,y,z)dx \wedge dy$
			$+\sigma_y(x,y,z)dz \wedge dx + \sigma_x(x,y,z)dy \wedge dz$
$\Lambda^{(3)}$	volumes	density	$\rho^{(3)} = \rho(x,y,z)dx \wedge dy \wedge dz.$

Definition 2.5 (Exterior derivative d, (Sec. 2.6 [18]))**.**
Differentiation of differential forms is governed by the *exterior derivative* d. The exterior derivative d is the mapping,

$$d : \Lambda^{(k)}(\mathcal{M}) \to \Lambda^{(k+1)}(\mathcal{M}), \tag{2.10}$$

satisfying,

$$\begin{aligned} &d(\alpha^{(k)} + \beta^{(k)}) = d\alpha^{(k)} + d\beta^{(k)} \\ &d(\alpha^{(k)} \wedge \beta^{(m)}) = d\alpha^{(k)} \wedge \beta^{(m)} + (-1)^k \alpha^{(k)} \wedge d\beta^{(m)} \\ &d^2\alpha^{(k)} := d \circ d\alpha^{(k)} = 0, \end{aligned}$$

The action of the exterior derivative on a 0-form $\alpha^{(0)} \in \Lambda^{(0)}$ is given by,

$$d\alpha^{(0)} := \sum_{i=1}^{n} \frac{\partial \alpha}{\partial x^i} dx^i. \tag{2.11}$$

The exterior derivative generalises the grad, curl, and div operators from multivariate calculus. Furthermore, the fact that $d^2 = 0$, known as the *nilpotency* property, is equivalent to the curl $\circ$ grad $= 0$ and div $\circ$ curl $= 0$ relations. The exterior derivative defines a sequence of mappings, known as the *DeRham complex*. For $\mathcal{M} \subset \mathbb{R}^n$ we have

$$\mathbb{R} \longrightarrow \Lambda^{(0)} \xrightarrow{d} \Lambda^{(1)} \xrightarrow{d} \cdots \xrightarrow{d} \Lambda^{(n)} \xrightarrow{d} \emptyset$$

The action of the exterior derivative on various forms is shown below.

Example 2.2 (Action of the exterior derivative d in $\mathbb{R}^3$)**.**
The action of the exterior derivative is very similar to the grad, curl and div operators. Using the properties of the wedge product $\wedge$, and the exterior derivative d, we find for $\mathcal{M} \subset \mathbb{R}^3$,

0-form:

$$d\phi^{(0)} = \frac{\partial \phi}{\partial x_1} dx^1 + \frac{\partial \phi}{\partial x_2} dx^2 + \frac{\partial \phi}{\partial x_3} dx^3$$

1-form:

$$\begin{aligned} du^{(1)} &= \left(\frac{\partial u_1}{\partial x_1} dx^1 + \frac{\partial u_1}{\partial x_2} dx^2 + \frac{\partial u_1}{\partial x_3} dx^3\right) \wedge dx^1 \\ &+ \left(\frac{\partial u_2}{\partial x_1} dx^1 + \frac{\partial u_2}{\partial x_2} dx^2 + \frac{\partial u_2}{\partial x_3} dx^3\right) \wedge dx^2 \\ &+ \left(\frac{\partial u_3}{\partial x_1} dx^1 + \frac{\partial u_3}{\partial x_2} dx^2 + \frac{\partial u_3}{\partial x_3} dx^3\right) \wedge dx^3 \\ &= \left(\frac{\partial u_3}{\partial x_2} - \frac{\partial u_2}{\partial x_3}\right) dx^2 \wedge dx^3 + \left(\frac{\partial u_1}{\partial x_3} - \frac{\partial u_3}{\partial x_1}\right) dx^3 \wedge dx^1 + \left(\frac{\partial u_2}{\partial x_1} - \frac{\partial u_1}{\partial x_2}\right) dx^1 \wedge dx^2 \end{aligned}$$

2-form:

$$\begin{aligned} d\omega^{(2)} &= \left(\frac{\partial \omega_1}{\partial x_1} dx^1 + \frac{\partial \omega_1}{\partial x_2} dx^2 + \frac{\partial \omega_1}{\partial x_3} dx^3\right) \wedge dx^2 \wedge dx^3 \\ &+ \left(\frac{\partial \omega_2}{\partial x_1} dx^1 + \frac{\partial \omega_2}{\partial x_2} dx^2 + \frac{\partial \omega_2}{\partial x_3} dx^3\right) \wedge dx^3 \wedge dx^1 \\ &+ \left(\frac{\partial \omega_3}{\partial x_1} dx^1 + \frac{\partial \omega_3}{\partial x_2} dx^2 + \frac{\partial \omega_3}{\partial x_3} dx^3\right) \wedge dx^2 \wedge dx^3 \\ &= \left(\frac{\partial \omega_1}{\partial x_1} + \frac{\partial \omega_2}{\partial x_2} + \frac{\partial \omega_3}{\partial x_3}\right) dx^1 \wedge dx^2 \wedge dx^3 \end{aligned}$$

Hence $d\phi^{(0)}$ defines a 1-form with components of grad operator in Cartesian coordinates, $du^{(1)}$ defines a 2-form with components of curl operator, and $d\omega^{(2)}$ defines a 3-form with component of the div operator.
Important topological connections are encoded in the exterior derivative and the DeRham sequence. Connections between exterior derivative's kernel and range, subspaces of the $\Lambda^{(k)'}s$, have an important role in the existence and uniqueness of PDE solutions. More on the structure of the DeRham sequence can be found in Appendix A. From the nilpotency of the exterior derivative it follows that if $d\alpha^{(k)} = \beta^{(k+1)}$, then $d\beta^{(k+1)} = 0$. The converse is true on *contractible manifolds.* Contractible manifolds can be continuously reduced to a point. Examples include any (star) domain in Euclidean space.

Theorem 2.1 (Poincaré Lemma, (Sec. 5.4 [18]))**.**
Let $\beta^{(k)}$ be a k-form on contractible manifold $\mathcal{M}$, such that $d\beta^{(k)} = 0$. There exists a non-unique $\alpha^{(k-1)}$, such that,

$$d\alpha^{(k-1)} = \beta^{(k)}. \tag{2.12}$$

Often $\alpha^{(k-1)}$ is referred to as a potential function.

The theorem proofs existence of solutions for balancing relations is physics. These relations, often of the form $\text{grad}(\phi) = f$, $\text{curl}(\vec{\omega}) = \vec{g}$, and $\text{div}(\vec{v}) = h$, are fundamental in

the description physics. Furthermore, note that the theorem proofs existence of potentials for every volume form, as $d\rho^{(n)} = 0$ for any volume form $\rho^{(n)}$. In vector calculus this result is known as the surjectiveness of the div operator.

Example 2.3 (Potential flow)**.**
Irrotational (inviscid) flow satisfies $\nabla \times \vec{V} = 0$, or in terms of differential geometry, $dv^{(1)} = 0$. Hence by the Poincaré lemma, there exists a velocity potential function $\phi^{(0)} \in \Lambda^{(0)}$ s.t. $d\phi^{(0)} = v^{(1)}$. Flow solutions satisfying $d\phi^{(0)} = v^{(1)}$ are known as potential flow solutions. We will discuss potential flow in more detail in section 2.5.

We measure a differential form by pairing it with an equidimensional submanifold, e.g. a 2-form is measured by pairing it with some surface S, a 3-form with some volume V, and so on. We present a few examples.

$\Lambda^{(k)}$	**geometry**	**example**	
$\Lambda^{(0)}$	point: x	pressure	$P = \int_x p^{(0)}$
$\Lambda^{(1)}$	curve: γ	circulation	$\Gamma = \oint_\gamma v^{(1)}$
$\Lambda^{(2)}$	surface: S	flux	$\Phi = \int_S \sigma^{(2)}$
$\Lambda^{(3)}$	volume: V	mass	$M = \int_V \rho^{(3)}$.

Integration is governed through the *generalised Stokes' theorem* .

Theorem 2.2. *Generalised Stokes' Theorem, (Sec. 3.3 [18])*
Let $\alpha^{(k)} \in \Lambda^{(k)}$ be a k-form, and $\mathcal{M}$ be a $(k+1)$-dimensional submanifold. Then,

$$\int_{\mathcal{M}} d\alpha^{(k)} = \int_{\partial\mathcal{M}} \alpha^{(k)}. \tag{2.13}$$

The theorem generalises the classical Stokes', Green's and divergence theorem from multivariate calculus, as well as the fundamental theorem of calculus. The theorem states that the boundary operator ∂ is the formal adjoint of the exterior derivative d, i.e.

$$\langle \mathcal{M}, d\alpha^{(k)} \rangle = \langle \partial\mathcal{M}, \alpha^{(k)} \rangle. \tag{2.14}$$

Note that this result is purely topological. In the next section we will introduce the discrete analogue of the generalised stokes theorem.

2.3. CHAINS AND COCHAINS

In discretisation techniques we find the formation of some a *cell complex*, i.e. a grid of vertices, edges, faces, and volumes. These components, known as k-cells. Using k-cells we can define discrete counter-parts of submanifolds, *chains*, and differential forms, *cochains*. Cochains can be integrated by pairing them with chains. We can apply the generalised Stokes' theorem, Equation 2.13, to these structures to derive a discrete version of the exterior derivative, the coboundary operator δ. The coboundary operator satisfies the same topological structure as the exterior derivative. Its action is encoded in incidence matrices $\mathbb{E}^{(k,k-1)}$. These incidence matrices are the foundation of our discretisation approach.

Definition 2.6 (k-cell, (Appx. B.a [18]))**.**
A k-cell, $\tau_{(k)}$, is a k-dimensional submanifold of n-dimensional manifold $\mathscr{M}$ which is homeomorphic to k-dimensional unit ball.

Essentially k-cells are k-dimensional contractible spatial objects. From here on we will form a grid of k-cells which will act as a discrete manifold on which we can define a discrete counterpart of differential forms. Grids are generally constructed using simplexes, or simplicial structures. In this work we follow [6, 20] and use k-dimensional cuboids, k-dimensional objects for which there exists a bijection to the unit k-cube, $\{x \in [-1,1]^k\}$. These cuboids are convenient because of their ability to hold tensor-product structures, and because Gaussian quadrature rules are defined on its interior.

Example 2.4 (n-dimensional cuboids)**.**
A 3-dimensional cuboid is a convex polytope bounded by 6 quadrilateral faces, each face is bounded by 4 edges, and each edge is bounded by 2 nodes. Hence each 3-dimensional cuboid consists of $\{8,12,6,1\}$ $\{0,1,2,3\}$-dimensional objects. A 4-dimensional cuboid consists of $\{16,32,24,8,1\}$ $\{0,1,2,3,4\}$-dimensional objects.

Definition 2.7 (Cell Complex, (Appx. B.a [18]))**.**
A cell complex $\mathscr{D}$ on a n-dimensional differentiable manifold $\mathscr{M}$ is a finite collection of sets of $\{n, n-1, \cdots, 0\}$-cells such that,

i The collection of n-cells form a cover $\mathscr{M}$.

ii Every face of a k-cell is contained in $\mathscr{D}$.

iii Any two k-cells $\tau_{(k)}, \sigma_{(k)} \in \mathscr{D}$,

$$\tau_{(k)} \cap \sigma_{(k)} = \begin{cases} \upsilon_{(k-1)}, & \text{i.e. } \tau_{(k)}, \sigma_{(k)} \text{ share a boundary } \upsilon_{(k-1)} \\ \sigma_{(k)} = \tau_{(k)}, & \text{i.e. they indicate the same k-cell} \\ \emptyset \end{cases} \tag{2.15}$$

The cell complex forms the collection of nodes, lines, surfaces, volumes that is equivalent to grid structures in numerical methods. It will also form a discrete manifold structure on which we can perform numerical analysis. For a cell complex to act like a manifold, we will need to provide orientation to its k-cells. Oriented k-cells act as a basis. Sets of oriented k-cells are known as *k-chains*. These k-chains can be interpreted as discrete submanifolds.

Definition 2.8 (k-Chains $\boldsymbol{c}_{(k)}$, (Appx. B.a [18]))**.**
The space of k-chains on a cell complex $\mathscr{D}$, denoted by $C_{(k)}(\mathscr{D})$, is the space of all sets of k-cells. Hence each k-chain $\boldsymbol{c}_{(k)} \in C_{(k)}(\mathscr{D})$ can be written as,

$$\boldsymbol{c}_{(k)} = \sum_i c^i \tau_{(k),i}, \text{ with } \tau_{(k)} \in \mathscr{D}, \tag{2.16}$$

with c^i the expansion coefficients. We use k-chains to describe k-dimensional paths through oriented cell complexes. In our analysis we consider coefficients $c^i \in \{0, \pm 1\}$, where $c^i = \pm 1$ provides relative orientation of the i-th k-cell with respect to a global orientation, and $c^i = 0$ indicates that i-th k-cell is not within the considered path.

Example 2.5 (1-chains)**.**
Consider the oriented cell complex $\mathscr{D}$ shown in Figure 2.3. Closed paths around surfaces s_1, s_2 are described by 1-chains $\boldsymbol{c}_{(1)}, \boldsymbol{c}_{(2)} \in C_{(1)}(\mathscr{D})$,

$$\begin{aligned}\boldsymbol{c}_1 &= l_1 + l_6 - l_3 - l_5,\\ \boldsymbol{c}_2 &= l_2 + l_7 - l_4 - l_6.\end{aligned}$$

The space of $C_{(1)}(\mathscr{D})$ is a linear vector space, hence we are able to add $\boldsymbol{c}'_{(k)}s$ to construct new paths. For example, $\boldsymbol{c}_{(1)} + \boldsymbol{c}_{(2)}$ describes the path that encloses $s_1 \cup s_2$. Next, we introduce the boundary operator δ, which relates a k-chain to its boundary $(k-1)$-cells.

Definition 2.9 (Boundary operator ∂, (Appx. B.a [18]))**.**
The boundary operator is the mapping,

$$\partial : C_{(k)} \to C_{(k-1)},\ \partial \boldsymbol{c}_{(k)} = \sum_j c^j \partial \tau_{(k),j}, \tag{2.17}$$

where the boundary operator ∂ acting on the j-th k-cell $\tau_{(k),j}$ is given by,

$$\partial \tau_{(k),j} = \sum_i e^i_j \tau_{(k-1),i},$$

with,

$$e^i_j = \begin{cases} +1, & \text{if orientation of } \tau_{(k-1),i} \text{ is the same as the boundary of } \tau_{(k),j}\\ -1, & \text{if orientation of } \tau_{(k-1),i} \text{ is opposed to that of the boundary of } \tau_{(k),j}\\ 0, & \text{if } \tau_{(k-1),i} \text{ is no face of } \tau_{(k),j}\end{cases}.$$

The boundary operator acting on a k-cell is encoded in an incidence matrix $\mathbb{E}_{(k-1,k)}$ with entries $\mathbb{E}_{(k-1,k)_{(i,j)}}$ given by e^j_i. The boundary operator satisfies $\forall \boldsymbol{c}_{(k)} \in C_{(k)}(\mathscr{D})$,

$$\begin{aligned}\partial \boldsymbol{c}_{(0)} &= \boldsymbol{0},\\ \partial \circ \partial \boldsymbol{c}_{(k)} &= \boldsymbol{0},\end{aligned}$$

for which the latter property translates to matrix notation as $(\mathbb{E}_{(k-2,k-1)}\mathbb{E}_{(k-1,k)})\boldsymbol{c}_{(k)} = \boldsymbol{0}$. Finally, the boundary operator defines a sequence of mappings

$$\emptyset \xleftarrow{\partial} C_{(0)} \xleftarrow{\partial} C_{(1)} \xleftarrow{\partial} \cdots \xleftarrow{\partial} C_{(n)} \longleftarrow \mathbb{R}$$

Example 2.6 (Boundary operator ∂)**.** Consider again the oriented cell complex $\mathscr{D}$ in Figure 2.3. We find that

$$\begin{aligned}\partial s_1 &= l_1 + l_6 - l_3 - l_5,\\ \partial s_2 &= l_2 + l_7 - l_4 - l_6.\end{aligned}$$

Now take chains $\boldsymbol{c}_{(2)} = [s_1, s_2]^T$, $\boldsymbol{c}_{(1)} = [l_1, l_2, \cdots, l_7]^T$, and $\boldsymbol{c}_{(0)} = [p_1, p_2, \cdots, p_6]^T$. We could obtain $\boldsymbol{c}_{(1)}$ through $\boldsymbol{c}_{(1)} = \mathbb{E}_{(1,2)}\boldsymbol{c}_{(2)}$, and $\boldsymbol{c}_{(0)}$ through $\boldsymbol{c}_{(0)} = \mathbb{E}_{(0,1)}\boldsymbol{c}_{(1)}$, with

$$\mathbb{E}_{(0,1)} = \begin{bmatrix} 1 & 0 & 0 & 0 & 1 & 0 & 0 \\ -1 & 1 & 0 & 0 & 0 & 1 & 0 \\ 0 & -1 & 0 & 0 & 0 & 0 & 1 \\ 0 & 0 & 1 & 0 & -1 & 0 & 0 \\ 0 & 0 & -1 & 1 & 0 & -1 & 0 \\ 0 & 0 & 0 & -1 & 0 & 0 & -1 \end{bmatrix}, \quad \mathbb{E}_{(1,2)} = \begin{bmatrix} 1 & 0 \\ 0 & 1 \\ -1 & 0 \\ 0 & -1 \\ -1 & 0 \\ 1 & -1 \\ 0 & 1 \end{bmatrix},$$

where, for example, the 6-th row of $\mathbb{E}_{(1,2)}$ corresponds to l_6 for which orientation is similar to the face of s_1, but opposite to the face of s_2. One could check that $\mathbb{E}_{(0,1)}\mathbb{E}_{(1,2)}\boldsymbol{c}_{(2)} = \mathbf{0}$, i.e. the nilpotency $\partial \circ \partial \boldsymbol{c}_{(2)} = \mathbf{0}$ of the boundary operator is exact in these discrete structures. This is of great importance, as it will preserve the topological relations between exact and closed forms, introduced in the previous section, in the discrete setting. We will now introduce the discrete differential forms, known as *cochains* , which assign real values to the k-chains introduced.

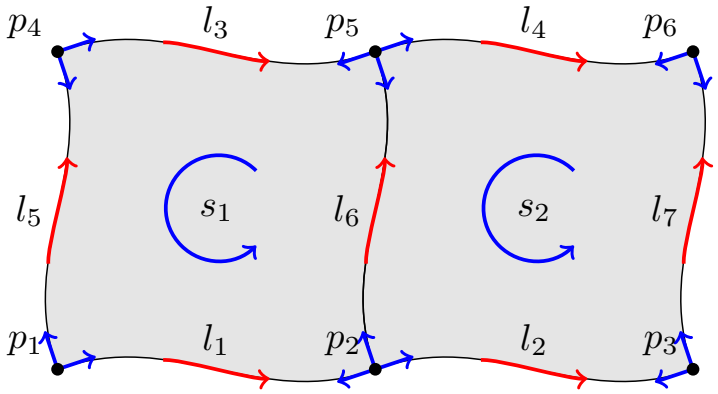

Figure 2.3: Cell complex $\mathscr{D}$ on a 2-dimensional manifold. Positive orientation of k-cells is indicated by direction of the arrows.

Definition 2.10 (k-Cochains $\boldsymbol{c}^{(k)}$, (Appx. B.b [18]))**.**
The space of k-cochains on a cell complex $\mathscr{D}$, denoted by $C^{(k)}(\mathscr{D})$, is the space that is dual to the space of k-chains $C_{(k)}(\mathscr{D})$. A k-cochain $\boldsymbol{c}^{(k)}$ expands in basis $\tau^{(k)}$,

$$\boldsymbol{c}^{(k)} = \sum_i c_i \tau^{(k),i}, \tag{2.18}$$

where $\tau^{(k)}$ is dual to a k-cell such that $\tau^{(k),i}(\tau_{(k),j}) = \delta^i_j$. The action of a k-cochain is the

mapping $\boldsymbol{c}^{(k)} : C_{(k)}(\mathscr{D}) \to \mathbb{R}$, with

$$\langle \boldsymbol{c}^{(k)}, \boldsymbol{c}_{(k)} \rangle := \boldsymbol{c}^{(k)}(\boldsymbol{c}_{(k)}) = \sum_i \sum_j c_i c^j \tau^{(k),i} \tau_{(k),j} = \sum_i c_i c^j.$$

2

Note that we could have chosen any other dual basis $\tau^{(k),i}$ that spans $C^{(k)}$. Cochains act as discrete differential forms, as will be shown. We now introduce the *coboundary operator* δ, which is the discrete equivalent of the differential operator.

Definition 2.11 (Coboundary operator δ)**.**
The coboundary operator $\delta : C^{(k)} \to C^{(k+1)}$ is the formal adjoint of the boundary operator,

$$\langle \boldsymbol{c}_{(k)}, \delta \boldsymbol{c}^{(k)} \rangle = \langle \partial \boldsymbol{c}_{(k)}, \boldsymbol{c}^{(k)} \rangle . \tag{2.19}$$

It follows that we can also encode the action of the coboundary operator in an incidence matrix,

$$\langle \mathbb{E}_{(k-1,k)} \boldsymbol{c}_{(k)}, \boldsymbol{c}^{(k)} \rangle = \langle \boldsymbol{c}_{(k)}, (\mathbb{E}_{(k-1,k)})^T \boldsymbol{c}^{(k)} \rangle .$$

Hence we define,

$$\mathbb{E}^{(k,k-1)} := (\mathbb{E}_{(k-1,k)})^T. \tag{2.20}$$

The coboundary operator inherits nilpotency property $\delta \circ \delta = 0$ from the boundary operator,

$$\langle \boldsymbol{c}_{(k)}, \delta\delta \boldsymbol{c}^{(k)} \rangle \overset{2.19}{=} \langle \partial \boldsymbol{c}_{(k)}, \delta \boldsymbol{c}^{(k)} \rangle \overset{2.19}{=} \langle \partial\partial \boldsymbol{c}_{(k)}, \boldsymbol{c}^{(k)} \rangle = 0,$$

and it defines a sequence of mappings,

$$\mathbb{R} \longrightarrow C^{(0)} \xrightarrow{\delta} C^{(1)} \xrightarrow{\delta} \cdots \xrightarrow{\delta} C^{(n)} \xrightarrow{\delta} \emptyset.$$

We can now connect the continuous differential forms from the previous section to the discrete cochain structures defined in this section.

Example 2.7 (Discretisation of $v^{(1)} = d\phi^{(0)}$)**.**
Consider again the oriented cell complex shown in Figure 2.3. Now consider the equation $v^{(1)} = d\phi^{(0)}$, defined on some manifold that is covered by the cell-complex. We can integrate over any line element l and use Stokes's theorem to find,

$$\int_l v^{(1)} = \int_l d\phi^{(0)} \overset{2.13}{=} \int_{\partial l_1} \phi^{(0)}$$

Next we discretise the variables $v^{(1)}, \phi^{(0)}$ through integration,

$$\boldsymbol{v}^{(1)} = \left[\int_{l_1} v^{(1)}, \int_{l_2} v^{(1)}, \cdots, \int_{l_7} v^{(1)} \right]^T,$$
$$\boldsymbol{\phi}^{(0)} = \left[\phi^{(0)}(p_1), \phi^{(0)}(p_2), \cdots, \phi^{(0)}(p_6) \right]^T.$$

The $\boldsymbol{v}^{(1)}$, and $\boldsymbol{\phi}^{(0)}$ are cochains, each coefficient assigns a real value to an oriented k-cell, just as a differential form assigns a real value to a manifold. We can now solve the discrete equation using the coboundary operator. Consider any 1-chain $\boldsymbol{c}_{(1)}$, we find

$$\begin{aligned}
&\int_{\boldsymbol{c}_{(1)}} v^{(1)} = \int_{\partial \boldsymbol{c}_{(1)}} \phi^{(0)} \\
\Leftrightarrow\ &\langle \boldsymbol{v}^{(1)}, \boldsymbol{c}_{(1)} \rangle = \langle \boldsymbol{\phi}^{(0)}, \partial \boldsymbol{c}_{(1)} \rangle = \langle \delta \bar{\phi}^{(0)}, \boldsymbol{c}_{(1)} \rangle \\
\Leftrightarrow\ &\langle \boldsymbol{v}^{(1)} - \mathbb{E}^{(1,0)} \boldsymbol{\phi}^{(0)}, \boldsymbol{c}_{(1)} \rangle = 0.
\end{aligned}$$

So we can solve the equation by evaluating $\boldsymbol{v}^{(1)} = \mathbb{E}^{(1,0)} \boldsymbol{\phi}^{(0)}$. The result is exact, no approximation has been made in this derivation, although information of the continuous forms have been lost in the process. In fact, any relation of the form $\alpha^{(k)} = d\beta^{(k-1)}$ can be discretised and solved using this approach, which preserves exactness of the exterior derivative, Appendix A.

We are able to preserve the exactness of the topological structure of our equations when we go to the discrete setting. However, the discretisation of the continuous forms to the discrete cochains came at a cost. We were able to conserve the global quantity at the cost of information concerning local behaviour. If we want to go back to a continuous form, we need to reconstruct the solution, performing some kind of interpolation. Bochev and Hyman introduced a framework to encode this process [6], which depends on the *reduction*- and *reconstruction*-operators.

Definition 2.12 (Reduction Operator $\mathscr{R}^{(k)}$)**.**
The reduction operator $\mathscr{R}^{(k)}$ is a mapping

$$\mathscr{R}^{(k)} : \Lambda^{(k)}(\mathscr{M}) \to C^{(k)}(\mathscr{D}), \tag{2.21}$$

that satisfies commutativity $\delta \mathscr{R}^{(k)} = \mathscr{R}^{(k+1)} d$, illustrated below.

$$\begin{array}{ccc}
\Lambda^{(k)} & \xrightarrow{\ d\ } & \Lambda^{(k+1)} \\
\downarrow{\scriptstyle \mathscr{R}^{(k)}} & & \downarrow{\scriptstyle \mathscr{R}^{(k+1)}} \\
C^{(k)} & \xrightarrow{\ \delta\ } & C^{(k+1)}
\end{array}$$

Definition 2.13 (Reconstruction Operator $\mathscr{I}^{(k)}$)**.**
The reconstruction operator $\mathscr{I}^{(k)}$ is a mapping

$$\mathscr{I}^{(k)} : C^{(k)}(\mathscr{D}) \to \Lambda_h^{(k)}(\mathscr{M}), \tag{2.22}$$

where $\Lambda_h^{(k)}(\mathscr{M}) \subset \Lambda^{(k)}(\mathscr{M})$ is an approximate finite-dimensional subspace of $\Lambda^{(k)}(\mathscr{M})$. The reconstruction operator needs to satisfy the same commutative property, $\delta \mathscr{I}^{(k)} = \mathscr{I}^{(k+1)} d$, illustrated below.

$$\begin{array}{ccc} C^{(k)} & \xrightarrow{\delta} & C^{(k+1)} \\ \downarrow{\scriptstyle \mathscr{I}^{(k)}} & & \downarrow{\scriptstyle \mathscr{I}^{(k+1)}} \\ \Lambda_h^{(k)} & \xrightarrow{d} & \Lambda_h^{(k+1)} \end{array}$$

Using the reduction and reconstruction operators it is possible to describe the discretisation process through the commuting diagram in Figure 2.4. Successful discretisation needs to satisfy the following conditions;

i Consistency condition, $\mathscr{R}^{(k)}\mathscr{I}^{(k)} = I$,

ii Approximation condition, $\mathscr{I}^{(k)}\mathscr{R}^{(k)} = I + \mathscr{O}(h^{p+1})$,

where h is some measure of grid size, and p the polynomial order of the approximation. We can use operators $\mathscr{R}$, $\mathscr{I}$ to define discrete operators acting on cochain $\boldsymbol{c}^{(k)} \in C^{(k)}$. Consider any operator $\bigstar$ acting on $\Lambda^{(k)}$, s.t. $\bigstar : \Lambda^{(k)} \to \Lambda^{(l)}$. We can then define discrete operator $\bigstar_h$ through

$$\bigstar_h \boldsymbol{c}^{(k)} := \mathscr{R}^{(k)} \bigstar \mathscr{I}^{(l)} \boldsymbol{c}^{(k)}.$$

$$\begin{array}{ccc} \Lambda^{(k)} & \xrightarrow{d} & \Lambda^{(k+1)} \\ \downarrow{\scriptstyle \mathscr{R}^{(k)}} & & \downarrow{\scriptstyle \mathscr{R}^{(k+1)}} \\ C^{(k)} & \xrightarrow{\delta} & C^{(k+1)} \\ \mathscr{I}^{(k)} \downarrow \uparrow \mathscr{R}^{(k)} & & \mathscr{I}^{(k+1)} \downarrow \uparrow \mathscr{R}^{(k+1)} \\ \Lambda_h^{(k)} & \xrightarrow{d} & \Lambda_h^{(k+1)} \end{array}$$

Figure 2.4: Commuting diagram of the reconstruction and reduction operators $\mathscr{R}$ and $\mathscr{I}$.

Classic discretisation techniques can be described through the reduction and reconstruction operators. In finite differencing techniques, one reconstructs using Taylor series expansion, while in finite volume techniques, one often reconstructs using polynomial interpolation. In finite element techniques, forms are reconstructed using basis functions. In finite differencing, and finite volume techniques, an explicit grid is generated, and one can reduce the continuous forms using integration, as in Example 2.7. Grids structures in finite element techniques are less obvious. Explicit reduction in finite element techniques can be performed using dual basis functions or projection operators.

2.4. THE CODIFFERENTIAL AND THE INNER PRODUCT

So far we have treated relations that are topological. In the previous section, we have shown that the exterior derivative d can be discretised without loss of its structure. In this section we will introduce operations that depend on metric. In the discrete setting local geometry is approximated on some mesh, which induces an approximation error for metric-dependent relations. Fundamental is the Hodge-$\star$ operator, which maps an oriented form to its corresponding dual-oriented form. The Hodge-$\star$ operator defines an inner-product, which is a vital tool in variational analysis.

Definition 2.14 (Hodge-$\star$ operator, (Sec. 14.1 [18]))**.**
The Hodge-$\star$ operator in $\mathscr{M} \subset \mathbb{R}^n$ is a mapping $\star : \Lambda^{(k)} \to \Lambda^{(n-k)}$ with,

$$\star\alpha(x^1, \cdots, x^n) dx^{i_1} \wedge \cdots \wedge dx^{i_k} = \text{sign} \cdot \alpha(x^1, \cdots, x^n) dx^{j_1} \wedge \cdots \wedge dx^{j_{n-k}}, \tag{2.23}$$

where $\{i_1, \cdots i_k\} \subseteq \{1, \cdots, n\}$ and $\{j_1, \cdots j_{n-k}\}$ its complement, and

$$\text{sign} = \begin{cases} - & \text{, if } \{j_1, \cdots, j_{n-k}, i_1, \cdots, i_k\} \text{ is an even permutation of } \{1, \cdots, n\} \\ + & \text{, else} \end{cases}.$$

When applied twice to a differential k-form we find that $\star\star\,\alpha^{(k)} = (-1)^{k(n-k)}\alpha^{(k)}$. The Hodge-$\star$ defines a complex of sequences of mappings, known as the *double DeRham complex* , Figure 2.5.

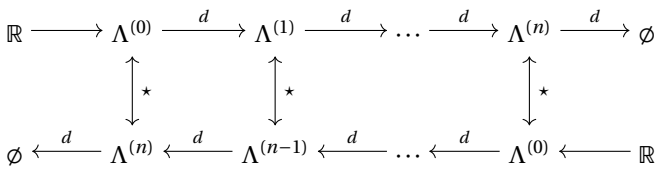

Figure 2.5: Double DeRham complex; two dual DeRham sequences are connected through the Hodge-$\star$ operator.

Example 2.8 (Geometrical Interpretation of the Hodge-$\star$ operator)**.**
The Hodge-$\star$ transforms differential forms to their dual forms . Its action doesn't affect the magnitude or direction of the components, but maps the basis to its dual configura-

tion. Some examples are given,

$$\mathbb{R}^2:$$
$$\star 1 = dx^1 \wedge dx^2$$
$$\star dx^1 = dx^2$$
$$\star dx^2 = -dx^1$$

$$\mathbb{R}^3:$$
$$\star 1 = dx^1 \wedge dx^2 \wedge dx^3$$
$$\star dx^1 = dx^2 \wedge dx^3$$
$$\star dx^2 \wedge dx^1 = -dx^3$$

Now consider the case $\mathbb{R}^2$, for which the double DeRham complex is shown in Figure 2.6. Any point value becomes a face value and vice versa. A value associated along a line, becomes a value associated through a line.

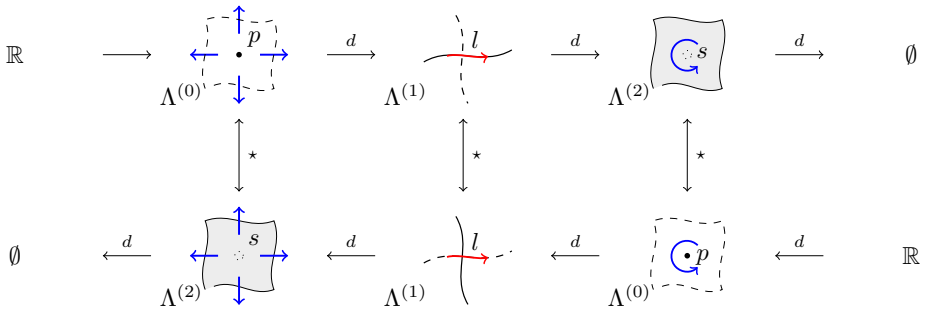

Figure 2.6: Double DeRham complex in $\mathbb{R}^2$.

The double-DeRham complex shows that we can identify two distinct orientations of a physical quantity on a geometric object. The top row in Figure 2.6 corresponds to *inner-orientated* object (or tangent orientated). From left to right we observe a source in a point, some quantity along a line, rotation in a surface. The bottom row corresponds to outer-oriented objects (or normal oriented). Here we see source through a face, flux through a surface, rotation around a point. Topological connections are shown horizontally, while metric-dependent relations are shown vertically.

Definition 2.15 (Inner Product $(\cdot,\cdot)_{\mathcal{M}}$, (Sec. 14.1 [18]))**.**
The Hodge-$\star$ operator defines an L^2-inner product $(\cdot,\cdot)_{\mathcal{M}} : \Lambda^{(k)} \times \Lambda^{(k)} \to \mathbb{R}$ by

$$(\alpha^{(k)}, \beta^{(k)})_{\mathcal{M}} := \int_{\mathcal{M}} \alpha^{(k)} \wedge \star \beta^{(k)}, \tag{2.24}$$

with $\alpha^{(k)}, \beta^{(k)} \in \Lambda^{(k)}$ on $\mathcal{M}$.

The inner product is essential in variational analysis, and plays a vital role in the construction of a finite-elements framework as we will see in the next chapter, chapter 3. With the Hodge-$\star$ operator we can define the adjoint of the differential operator, the *codifferential* d^* .

Definition 2.16 (Codifferential d^*, (Sec. 14.1 [18]))**.**
The codifferential d^* is a mapping $d^* : \Lambda^{(k)}(\mathscr{M}) \to \Lambda^{(k-1)}(\mathscr{M})$ for which

$$d^*\alpha^{(k)} = (-1)^{n(k-1)+1} \star d \star \alpha^{(k)} \tag{2.25}$$

The codifferential defines a sequence of mappings, known as the DeRham complex, which connects $k+1$-forms to k-forms. For $\mathscr{M} \subset \mathbb{R}^n$ we have

$$\emptyset \xleftarrow[d^*]{} \Lambda^0 \xleftarrow[d^*]{} \Lambda^1 \xleftarrow[d^*]{} \cdots \xleftarrow[d^*]{} \Lambda^n \longleftarrow \mathbb{R}$$

It's easy to see that d^* is nilpotent, i.e. $d^*d^* = 0$ (using the $\star\star$ and d^2 properties).

Example 2.9 (Action of codifferential d^* in $\mathbb{R}^3$)**.**
The action of the exterior derivative is similar to the div, curl and grad operators. Using the properties of the wedge product $\wedge$, and the exterior derivative d, we find for $\mathscr{M} \subset \mathbb{R}^3$,

1-form:

$$d^*u^{(1)} = -\left[\frac{\partial u_1}{\partial x_1} + \frac{\partial u_2}{\partial x_2} + \frac{\partial u_3}{\partial x_3}\right]$$

2-form:

$$d^*\omega^{(2)} = (-1)^{n+1}\left[\left(\frac{\partial \omega_3}{\partial x_2} - \frac{\partial \omega_2}{\partial x_3}\right)dx^1 + \left(\frac{\partial \omega_1}{\partial x_3} - \frac{\partial \omega_3}{\partial x_1}\right)dx^2 + \left(\frac{\partial \omega_2}{\partial x_1} - \frac{\partial \omega_1}{\partial x_2}\right)dx^3\right]$$

2-form:

$$d^*\rho^{(3)} = -\left[\frac{\partial \rho}{\partial x_1}dx^2 \wedge dx^3 + \frac{\partial \rho}{\partial x_2}dx^3 \wedge dx^1 + \frac{\partial \rho}{\partial x_3}dx^1 \wedge dx^2\right]$$

Hence $d^*u^{(1)}$ defines a 0-form with components of div operator, $d^*\omega^{(2)}$ defines a 1-form with components of curl operator, and $d^*\rho^{(3)}$ defines a 2-form with component of the grad operator. The codifferential is the adjoint of the exterior derivative.

Theorem 2.3 (Integration-by-parts, (Sec. 14.1 [18]))**.**
For forms $\alpha^{(k-1)} \in \Lambda^{(k-1)}$, and $\beta^{(k)} \in \Lambda^{(k)}$, we have the relation,

$$(\alpha^{(k-1)}, d^*\beta^{(k)})_{\mathscr{M}} = (d\alpha^{(k-1)}, \beta^{(k)})_{\mathscr{M}} - (\alpha^{(k-1)}, \beta^{(k)})_{\partial\mathscr{M}}, \tag{2.26}$$

Now any differential k-form can be decomposed in orthogonal components tangential and normal to the boundary, i.e. $\alpha^{(k)} = \alpha^n dx_n + \alpha^t dx_t$. Hence we can evaluate the boundary integral in terms of tangential and normal components of $\alpha^{(k-1)}, \beta^{(k)}$,

$$(\alpha^{(k-1)}, \beta^{(k)})_{\partial\mathscr{M}} = \int_{\partial\mathscr{M}} \langle \alpha^t, \beta^n \rangle d\Gamma. \tag{2.27}$$

Proof can be found in Appendix B. We will often use Theorem 2.3 to reduce continuity constraint on our solution space, or to get rid of the co-differential.

We combine the exterior derivative and the codifferential operator to define the Laplace-DeRham operator, which is a generalised Laplace operator for k-forms.

Definition 2.17 (Laplace-de-Rham Operator, (Sec. 14.2 [18]))**.**
For any k-form we define the Laplace-de-Rham operator $\Delta : \Lambda^{(k)} \to \Lambda^{(k)}$ as

$$\Delta\alpha^{(k)} := dd^*\alpha^{(k)} + d^*d\alpha^{(k)} = (d+d^*)^2\alpha^{(k)} \tag{2.28}$$

Because $d^*\beta^{(0)} = 0$ for any 0-form $\beta^{(0)}$, the Laplace-DeRham operator acting on a 0-form reduces to $\Delta = d^*d$, which is the equivalence of the scalar Laplacian. The operators reduces to $\Delta = dd^*$ when applied to a volume n-form.

The codifferential governs the a topological structure that mirrors the structure of the exterior derivative. It governs existence of solutions analogue to the Poincaré lemma, Equation 2.12. In Appendix A we combine properties of both operators to derive the *Hodge decomposition*, which states there exists an unique decomposition in orthogonal complements for each k-form.

Theorem 2.4 (Hodge decomposition, (Sec. 14.2 [18]))**.**
For any k-form on a closed manifold $\mathcal{M}$ there exists an unique decomposition

$$\alpha^{(k)} = d\phi^{(k-1)} + d^*\psi^{(k+1)} + h^{(k)}, \tag{2.29}$$

where $h^{(k)}$ is a harmonic form, i.e. $\Delta h^{(k)} = 0$. Note that this doesn't imply uniqueness of $\phi^{(k-1)}$ and $\psi^{(k+1)}$. On a contractable manifold the space of harmonic forms is empty, i.e. $h^{(k)} = 0$.

2.5. POISSON PROBLEMS

There exists one-to-one correspondence between PDE's described using vector calculus and differential geometry. In multivariate calculus we distinguish between physical variables associated with scalars and those associated with vectors. In differential geometry we associate physical variables with points, lines, surfaces, and volumes. Any scalar function can be used to describe a point or volume $(0,3)$-form in $\mathbb{R}^3$, and any vector function can be used to describe a line or surface $(1,2)$-form. The duality between a point and a volume, and that between a surface and a line is encoded in the Hodge $\star$-operator. Let's analyse the example of potential flow, which we introduced in section 2.2.

Example 2.10 (Potential flow in $\mathbb{R}^2$)**.**
The velocity field can be interpreted as a field of lines along which fluid parcels are transported. Hence we can associate a 1-form with velocity, i.e. $v^{(1)}$. Now the quantity $\omega^{(2)} = dv^{(1)}$ is known as vorticity and is a measure of rotation within the flow. In the case of irrotational flow, i.e. $\omega^{(2)} = 0$ in our domain, we would get $dv^{(1)} = 0$. Assuming that the domain is simply connected, there exists a potential function $\phi^{(0)}$ such that $d\phi^{(0)} = v^{(1)}$ (Theorem 2.1).

Consider the quantity given by $q^{(1)} = \star v^{(1)}$. The dual form $q^{(1)}$ is defined through a line like a flux. Mass flux in vector calculus is given by $\vec{q} = -\rho\vec{v}$, where ρ is mass density (which we will assume to be constant). It follows that the 1-form $q^{(1)}$ describes scaled mass flux (note that the minus sign is encoded in the Hodge-$\star$ operator). The quantity $\sigma^{(2)} = dq^{(1)}$ then describes total flux through our two-dimensional volumes. If we don't consider any mass source or sink then we obtain $dq^{(1)} = 0$. Now again there exists a potential function $\psi^{(0)}$ such that $d\psi^{(0)} = q^{(1)}$ (Theorem 2.1). This potential function is called the stream function. Note that in $\mathbb{R}^3$ the stream function is a 1-form with three components.

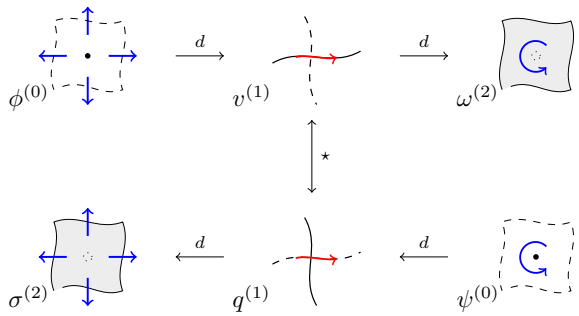

Figure 2.7: Tonti diagram of the relations governed by potential flow theory. On the top row, inner-oriented relation of the potential function $\phi^{(0)}$, velocity $v^{(1)}$, and vorticity $\omega^{(2)}$ is shown. On the bottom row, outer-oriented relation of mass production $\sigma^{(2)}$, mass flux $q^{(1)}$, and the stream function $\psi^{(0)}$ is shown.

The relations are visualised in a *Tonti diagram* Figure 2.7. Horizontal relations described through the exterior derivative d are *conservation equations*. They are independent of metric and describe a relation between change of a quantity within a domain, and the flux through the boundary of the domain. Vertical relations describe *constitutive equations*. They depend on metric and material parameters. Examples include Fourier's law $\vec{q} = -\kappa\nabla u$ in heat conduction problems, or Darcy's law $\vec{q} = -\frac{\kappa}{\mu}\nabla p$ in flow through porous media. We could combine the relations to obtain the Laplace equation for the potential function $\Delta\phi^{(0)} = 0$, or the stream function $\Delta\psi^{(0)} = 0$, which are relatively easy to solve.

Example 2.11 (Stokes' flow in $\mathbb{R}^2$)**.**
Consider a Newtonian (viscosity μ constant and isotropic), incompressible (mass density ρ constant) fluid. Now in the viscous flow regime ($Re \ll 1$, i.e. viscous forces are dominant over advective inertial forces), the flow is governed by equations,

$$\begin{cases} \nu\Delta\vec{v} - \nabla p + \vec{f} &= 0 \\ \nabla\cdot\vec{v} &= 0, \end{cases}$$

where ν is the kinematic viscosity, $\vec{v}$ is the velocity, p the pressure, and $\vec{f}$ any body forces. The first equation describes conservation of momentum, the second equation describes

conservation of mass. We can translate to the language of differential geometry. We obtain,

$$\begin{cases} \nu d^* d v^{(1)} + d p^{(0)} & = f^{(1)} \\ -d^* v^{(1)} & = 0. \end{cases}$$

We can obtain an equivalent dual formulation of these equations by pre-multiplying the equations with the Hodge-$\star$, define dual forms, i.e. $q^{(1)} = \star v^{(1)}$, $p^{(0)} = \star p^{(2)}$, and $f^{(1)} = \star g^{(1)}$, and use the identities of d^*, d and $\star$ to simplify the result. For the Stokes' flow equations one obtains,

$$\begin{cases} \nu d d^* q^{(1)} - d^* p^{(2)} & = g^{(1)} \\ d q^{(1)} & = 0. \end{cases}$$

The advantage of this formulation, is that the mass conservation constraint $d q^{(1)} = 0$ depends on the exterior derivative d. This means that a discretisation based on this formulation can be made such that it satisfies conservation of mass exactly pointwise (using the incidence matrices introduced in section 2.3). Structure preserving spectral element solution methods for the Stokes' flow problem are studied in [21]. Their discretisation satisfies pointwise divergence-free solution.

The last example showed that formulation has consequences in the discrete setting. We can choose the formulation such that certain relations are satisfied strongly pointwise, while others are weakly satisfied. The choice of formulation will also have a consequence on the boundary conditions. Some boundary condition may be enforced strongly (*essential*) in one formulation, while it may be enforced weakly (*natural*) in a different one.

So far we have not considered the possibility of arbitrary physical geometries. Often, the quantity of interest will be defined on a geometry through a mapping. In the finite-element method we will need to *pull-back* differential k-forms to some parent domain on which the numerical integration rules are defined. The pull-back operator commutates with the exterior derivative. In Appendix C we derive appropriate transformations for each k. These relations conserve the topological structure of the exterior derivative on arbitrary domains.

2.6. SUMMARY OF RESULTS

Analysis of PDE's through exterior calculus enables us to distinguish between relations that depend on metric, and those that are topological. Topological relations can be described by algebraic equations, which can be satisfied exactly in the discrete setting. Proper discretisation of these relations guarantees numerical stability, and exact behaviour of simulated physics.

The exterior derivative d is a topological operator, which describes derivatives of differential forms analogous to the grad-, curl-, and div- operators. In the discrete setting it can be satisfied without error by construction of incidence matrices. This construction preserves the kernel structure of the exterior derivative, which governs existence of

PDE solutions. The kernel structure of the exterior derivative is encoded in the DeRham complex.

$$\mathbb{R} \longrightarrow \Lambda^{(0)} \xrightarrow{d} \Lambda^{(1)} \xrightarrow{d} \Lambda^{(2)} \xrightarrow{d} \Lambda^{(3)} \xrightarrow{d} \emptyset$$

The Hodge-$\star$ is a metric-dependent operator, which maps differential forms to their dual representation. It is used together with the exterior derivative d to describe elliptic PDE's. Its action needs to be approximated in the discrete setting. In finite volume techniques its action is approximated through construction of a dual grid, whereas in finite-element techniques is is approximated through inner-product relations. Finally, the Hodge-$\star$ allows us to map PDE's to a favourable configuration, in which certain relations or boundary conditions can be satisfied exactly.

3

STRUCTURE PRESERVING ISOGEOMETRIC ANALYSIS

"Don't worry, everything will B-spline"

We can use powerful tools from functional analysis to prove well-posedness of elliptic PDE problems. In this approach one derives a weak formulation of the PDE problem by taking the inner product with a test function. The weak formulation of the problem can be converted to a discrete problem by introducing a finite-dimensional basis in which the unknowns and test-function can be expanded. In *isogeometric analysis* spline bases from computer aided design are used to discretise the problem. In this chapter we will introduce concepts from functional analysis, and explain the fundamentals of isogeometric analysis. We will construct a discretisation framework using splines that is compatible with the DeRham complex.

Weak formulations of elliptic PDE problems that define a symmetric bilinear operator have been discretised successfully using the *finite element method*. Mixed type formulations however have posed difficulties. Such problems are known for spurious oscillations within the numerical solution. In order to cope with these oscillations penalising techniques were introduced, which in turn have a negative effect on the accuracy, (Sec. 6.3 [2]). Classical is the work by Brezzi on stability requirements for these mixed-type formulations [22]. It was shown that spurious oscillations do not appear when inf-sub stable finite element spaces are used. Using the concepts introduced in chapter 2, we derive appropriate basis functions. The resulting method doesn't require penalising techniques for stability, as shown by [5, 11, 23].

In section 3.1 we introduce fundamentals of functional analysis and introduce a DeRham sequence of *Sobolev spaces*. We will derive symmetric and mixed formulations of the Poisson problem, and prove well-posedness for both problem types. Furthermore we will explain how we can discretise the problem by considering finite-dimensional Sobolev subspaces. *Bézier, B-spline,* and *NURBS*- polynomial bases will be introduced in the context of *isogeometric analaysis* in section 3.2. These basis functions will be used

to construct finite-dimensional Sobolev subspaces that are compatible with the DeRham complex in section 3.3. We will make a link to concepts introduced in chapter 2, and unveil the cochain structure of spline spaces. Finally, in section 3.4, we successfully discretise both Poisson problems using linear combinations of incidence matrices and mass matrices.

3.1. THE SOBOLEV-DERHAM COMPLEX

Finite projection methods, e.g. isogeometric analysis and the finite element method, can be derived from *variational analysis*. In this approach one constructs a *weak formulation* of the PDE problem by taking the inner product with some test function. Well-posedness of these problems can be proven by selecting appropriate trial- and solution spaces. In this section we construct these spaces, such that they satisfy the DeRham sequence. We introduce the Poisson problems that will be studied in this chapter, and derive corresponding weak formulations. We end this section by explaining how we weak formulations can be discretised.

Consider orientable manifold Ω with tangent space $\mathcal{T}\Omega$ and cotangent space $\mathcal{T}^*\Omega$. In section 2.4 we defined an inner product on these spaces. We use the inner product to define inner product spaces $L^2\Lambda^{(k)}$.

Definition 3.1 (Inner product space $L^2\Lambda^{(k)}$, (Sec. 2 [5]))**.**
Let $\Lambda^{(k)}(\Omega)$ denote the space of k-forms on manifold Ω. We define the corresponding space of square integrable forms $L^2\Lambda^{(k)}(\Omega)$ as,

$$L^2\Lambda^{(k)} := \{\alpha^{(k)} \in \Lambda^{(k)} : \|\alpha^{(k)}\|_{L^2\Lambda^{(k)}} < \infty\}, \tag{3.1}$$

where,

$$\|\alpha^{(k)}\|^2_{L^2\Lambda^{(k)}} = \left(\alpha^{(k)}, \alpha^{(k)}\right)_\Omega = \int_\Omega \alpha^{(k)} \wedge \star\alpha^{(k)} \tag{3.2}$$

i.e. the norm defined by the inner product.

Definition 3.2 (Sobolev spaces $W_d\Lambda^{(k)}$, (Sec. 2 [5]))**.**
We define the Sobolev space $W_d\Lambda^{(k)}(\Omega)$ as

$$W_d\Lambda^{(k)} := \{\alpha^{(k)} \in L^2\Lambda^{(k)} : d\alpha^{(k)} \in L^2\Lambda^{(k+1)}\}, \tag{3.3}$$

with corresponding Sobolev norm,

$$\|\alpha^{(k)}\|^2_{W_d\Lambda^{(k)}} = \|\alpha^{(k)}\|^2_{L^2\Lambda^{(k)}} + \|d\alpha^{(k)}\|^2_{L^2\Lambda^{(k+1)}} \tag{3.4}$$

Note that $W_d\Lambda^{(0)}$ is the equivalent of the Sobolov space $H^1(\Omega)$, $W_d\Lambda^{(1)}$ of $H(\text{curl};\Omega)$, and $W_d\Lambda^{(2)}$ of $H(\text{div};\Omega)$, i.e. descriptions of Sobolev spaces generally encountered in literature, e.g. [11]. In $\Omega \subseteq \mathbb{R}^3$ these spaces satisfy the DeRham sequence, i.e. the *DeRham Sobolev complex*,

$$W_d\Lambda^{(0)} \xrightarrow{d} W_d\Lambda^{(1)} \xrightarrow{d} W_d\Lambda^{(2)} \xrightarrow{d} L^2\Lambda^{(3)}$$

This construction can be mirrored to construct Sobolev spaces with respect to the codifferential d^*,

$$W_{d^*}\Lambda^{(k)} := \{\alpha^{(k)} \in L^2\Lambda^{(k)} : d^*\alpha^{(k)} \in L^2\Lambda^{(k-1)}\}, \tag{3.5}$$

with corresponding Sobolev norm,

$$\|\alpha^{(k)}\|_{W_{d^*}\Lambda^{(k)}} = \|\alpha^{(k)}\|_{L^2\Lambda^{(k)}} + \|d^*\alpha^{(k)}\|_{L^2\Lambda^{(k-1)}} \tag{3.6}$$

These spaces incorporates the existence of the DeRham complex given by

$$L^2\Lambda^{(0)} \xleftarrow[d^*]{} W_{d^*}\Lambda^{(1)} \xleftarrow[d^*]{} W_{d^*}\Lambda^{(2)} \xleftarrow[d^*]{} W_{d^*}\Lambda^{(3)}$$

These spaces act as trial- and solution-spaces in variational analysis of PDE problems. In this approach one derives a weak formulation of the PDE problem. In this chapter we will study Poisson problems, e.g. those appearing in potential flow theory, section 2.5.

Problem 3.1 (The 0-form Poisson Problem in $\mathbb{R}^2$)**.**
Consider the domain $\Omega = [0,1]^2 \subset \mathbb{R}^2$ with boundary $\partial\Omega = \Gamma_d \cup \Gamma_n$, where $\Gamma_d \cap \Gamma_n = \emptyset$. Given forcing $f^{(0)} \in \Lambda^{(0)}$, find solution $\psi^{(0)} \in \Lambda^{(0)}$ such that,

$$\begin{cases} \Delta\psi^{(0)} &= f^{(0)}, \\ \psi^{(0)} &= 0, \text{ on } \Gamma_d \\ \partial_n\psi^{(0)} &= 0, \text{ on } \Gamma_n \end{cases} \tag{3.7}$$

A corresponding weak formulation of this problem can be obtained by taking the inner product with some test function $w^{(0)}$. Given forcing $f^{(0)} \in L^2\Lambda^{(0)}$, find solution $\psi^{(0)} \in W_d\Lambda^{(0)}$, such that,

$$\left(dw^{(0)}, d\psi^{(0)}\right)_\Omega = \left(w^{(0)}, f^{(0)}\right)_\Omega, \qquad \forall w^{(0)} \in W_d\Lambda_0^{(0)}, \tag{3.8}$$

where $W_d\Lambda_0^{(0)}$ is the space of compactly supported functions,

$$\Lambda_0^{(0)} := \{\alpha^{(0)} \in \Lambda^{(0)} : \text{with } \alpha^{(0)} = 0 \text{ on } \Gamma_d\}.$$

The derivation of this weak formulation, and a proof of well-posedness of the weak formulation is given in Appendix D. In the derivation of the weak formulation we used integration by parts, Theorem 2.3, for two reasons. In the discrete setting we will use a finite span of basis functions of a given polynomial order. Integration by parts reduces continuity requirements on the span of basis functions. The second reason is that we now have an expression that doesn't contain the codifferential d^*, but only contains the exterior derivative d, which we can discretise using the framework introduced in section 2.3.

Problem 3.2 (The 2-form Poisson Problem in $\mathbb{R}^2$)**.**
Consider the domain $\Omega = [0,1]^2 \subset \mathbb{R}^2$ with boundary $\partial\Omega = \Gamma_d \cup \Gamma_n$, where $\Gamma_d \cap \Gamma_n = \emptyset$. Given forcing $f^{(2)} \in \Lambda^{(0)}$, find solution $\psi^{(2)} \in \Lambda^{(2)}$ such that,

$$\begin{cases} \Delta\psi^{(2)} &= f^{(2)}, \\ \psi^{(2)} &= 0, \text{ on } \Gamma_d \\ \partial_t\psi^{(2)} &= 0, \text{ on } \Gamma_n \end{cases} \tag{3.9}$$

As before, we could multiply with some test-function $w^{(2)}$, and apply integration by parts, to obtain.

$$\left(d^* w^{(2)}, d^*\psi^{(2)}\right)_\Omega = (w^{(2)}, f^{(2)})_\Omega. \tag{3.10}$$

This formulation won't do us any good in the discrete setting, because it contains the codifferential d^*. Alternatively we write Equation 3.9 as an equivalent system of first order differential equations,

$$\begin{cases} d^*\psi^{(2)} &= v^{(1)}, \\ dv^{(1)} &= f^{(2)}, \\ \psi^{(2)} &= 0, \text{ on } \Gamma_d \\ \partial_t\psi^{(2)} &= 0, \text{ on } \Gamma_n \end{cases} \tag{3.11}$$

The corresponding weak formulation of this system can be obtained taking inner products with test functions $q^{(1)}$ and $w^{(2)}$, and apply integration by parts. Given forcing $f^{(2)} \in L^2\Lambda^{(2)}$, find solutions $v^{(1)} \in W_d\Lambda^{(1)}$ and $\psi^{(2)} \in W_d\Lambda^{(2)}$, such that,

$$\begin{cases} \left(dq^{(1)}, \psi^{(2)}\right)_\Omega &= \left(q^{(1)}, v^{(1)}\right)_\Omega, \qquad \forall q^{(1)} \in W_d\Lambda_0^{(1)}, \\ \left(w^{(2)}, dv^{(1)}\right)_\Omega &= \left(w^{(2)}, f^{(2)}\right)_\Omega, \qquad \forall w^{(2)} \in L^2\Lambda^{(2)}. \end{cases} \tag{3.12}$$

The derivation of this weak formulation, and a proof of well-posedness of the weak formulation is given in Appendix D. Well-posedness of this formulation depends explicitly on the kernel structure of the Sobolev DeRham complex,

$$W_d\Lambda^{(0)} \xrightarrow{d} W_d\Lambda^{(1)} \xrightarrow{d} L^2\Lambda^{(2)}$$

To ensure well-posedness of the discretised problem, discrete function spaces need to be constructed that satisfy the same structure. In section 3.3 how we can do so.

In the example of the 0-form Poisson equation, Example D.1, we obtained weak formulation of the form,

$$\text{Find } u \in V, \text{ such that} \quad a(v,u) = F(v), \quad \text{for all } v \in V,$$

where S and V are the solution- and trial function spaces, $a(\cdot,\cdot)$ a bilinear form, and $F(\cdot)$ a functional. In the *Galerkin* discretisation approach we take a finite-dimensional

subspace $V_h \subset V$, and take the solution space equation to the trial $S_h := V_h$. In our case V_h will consist of the space spanned by the isoparametric basis, which we will introduce in the next section, section 3.2. We define the finite-dimensional solution u_h such that it satisfies,

$$\text{Find } u_h \in S_h, \text{ such that} \quad a(v_h, u_h) = F(v_h), \quad \text{for all } v_h \in V_h.$$

Such discretisation approach is known as a *conforming* method. A discrete solution is sought that satisfies the continuous PDE problem. Well-posedness of the problem was proven for any element $v \in V$, and hence for any $v_h \in V_h$. This implies well-posedness of the discrete problem in the case of symmetric operator problems as the Poisson problem. Note that well-posedness of the 2-form problem depends on the kernel structure of the Sobolev DeRham complex, which needs to be mirrored by discrete spaces to prove well-posedness in the discrete setting.

$$\mathbb{R} \longrightarrow W_d\Lambda_h^{(0)} \xrightarrow{d} W_d\Lambda_h^{(1)} \xrightarrow{d} \cdots \xrightarrow{d} L^2\Lambda_h^{(n)} \longrightarrow \emptyset.$$

Now, because,

$$\begin{aligned} a(u, v_h) &= F(v_h), \text{ and} \\ a(u_h, v_h) &= F(v_h), \text{ for all } v_h \in V, \end{aligned}$$

We have that $a(u, v_h) - a(u_h, v_h) = a(u - u_h, v_h) = F(v_h) - F(v_h) = 0$. This is known as the Galerkin orthogonality. The global error $\epsilon = (u - u_h)$ is bounded.

Theorem 3.1 (Cea's Lemma, (Sec. 1.5 [2]))**.**
Consider the finite-dimensional form of variational problem that satisfies the conditions of Theorem D.3 or Theorem D.4. The approximate finite element solution u_h to the analytical solution $u \in V$ of the weak problem under consideration, is bounded by

$$\|u - u_h\| \leq C \min_{v_h \in V_h} \|u - v_h\|.$$

If the finite-dimensional solution space is the span of a piecewise polynomial basis of polynomial order p, then

$$\min_{v_h \in V_h} \|u - v_h\| \leq C(u) h^s,$$

where h is a measure of mesh size, and $C(u)$ a positive constant that depends on smoothness of the solution u. Constant s depends on smoothness of solution and polynomial order of the basis.

The theorem states that the approximate solution converges to the exact solution in the Sobolev norm. We call the order of convergence optimal when $s = p$. In the next section we will introduce isoparametric bases. The span of these bases will be used as our finite-dimensional solution- and trial spaces.

3.2. BASIS FUNCTIONS AND ISOGEOMETRIC ANALYSIS

In the restriction to finite-dimensional function-spaces one approximates physical quantities as a linear combination of basis functions. The challenge is then to find the appropriate coefficients, such that the combination approximates the physical solution. The basis functions are generally defined on a simple regular mesh, which we call *the parameter space*. However, most often the physical problem that we aim to solve, is defined on some kind of geometry, which we call *the physical space*. To solve the problem in the physical space, it is required to map the basis from the parent domain to the physical domain. The mapping can also be approximated as a linear combination of basis function when it is not explicitly known.

In mechanics we often find an intimate relation between geometry and the physics. Accelerations, velocities and displacements affect the geometry on which the equations need to be solved. Take for example a problem where we would solve for the displacements of some kind of structure or material at a given period of time. We would then like to update our geometry using the found displacements. If the displacements and the mapping are defined in a different basis, we would need to interpolate or project our solution from one basis to the other. In many cases solutions sensitive to errors in the geometry, e.g. thin-shell dynamics, boundary layers in fluid dynamics. The interpolation errors can have a significant impact on the approximate solution. To circumvent this problem, one would need to use the same basis for the mapping as the one used for analysis. This is known as the *isoparametric approach*.

In the modern day design process however, geometries are dictated through *CAD* (Computer Aided Design). Many CAD programs use *Bézier curves*, *B-splines* and *NURBS* (Non-uniform rational B-splines) to represent geometries. The concept of using the same basis for analysis as the one used for the mappings is known as the *isogeometric approach*. The isogeometric paradigm was pitched by the Hughes group in 2005 to bridge the gap between CAD design and finite elements analysis [8].

In this section we will introduce the framework of isogeometric analysis. We will first introduce various bases, Béziers, B-splines, and NURBS, that are used to describe geometries in CAD. These basis functions will be the fundamental tool in our analysis. Definitions and formulas that will be introduced shortly can be found in the book by Piegl and Tiller, [24].

Bézier curves are widely used in computer graphics, because they can be manipulated intuitively, and are able to represent smooth geometries. A Bézier curve is a linear combination of *Bernstein polynomials*, which can be efficiently evaluated through the recursive *deCasteljau Algorithm*.

Definition 3.3 (Bézier Curves, (Sec. 1.3 [24]))**.**
A Bézier curve of polynomial order p is the mapping $\boldsymbol{C}(t) : \mathbb{R} \to \mathbb{R}^d$ given by,

$$\boldsymbol{C}(\xi) = \sum_{i=0}^{p} \lambda_{i,p}^{B}(\xi)\boldsymbol{P}_i, \;\; 0 \leq \xi \leq 1, \tag{3.13}$$

where $\lambda_{i,p}$ is the i-th Bernstein polynomial basis function, and coefficients $\{\boldsymbol{P}_i\}$ with

$\boldsymbol{P}_i \in \mathbb{R}^d$ are the *control points*. The i-th Bernstein polynomial is defined through,

$$\lambda_{i,p}(\xi) = \binom{p}{i} (\xi)^i (1-\xi)^{p-i}. \tag{3.14}$$

The polygon that interpolates the control points linearly is known as the *control polygon* or *control net*. The curve lies in the convex hull of its control polygon, and the curves' ends are tangent to the control polygon. Finally, the Bézier curves are variation diminishing, i.e. they preserve the local monotonicity. Note that there exists a change of basis to express a Bézier curves in Lagrange polynomials instead of Bernstein polynomials. Lagrange interpolation polynomials are classically used in FEA.

Success of the Bézier basis is due to these properties, which enable for intuitive design. Classical polynomial interpolation does not satisfy these properties. The disadvantage of Bézier curves is that they cannot be controlled locally, i.e. changing one coefficients will affect the whole curve (Bernstein polynomials have full support over parameter domain $\xi \in [0,1]$). One solution would be to use curves that consist of multiple Bézier segments, so called composite Bézier curves. The drawbacks of these curves are that continuity is difficult to achieve over segments, and that the number of control points increase with the polynomial degree p. These difficulties are overcome by the use of B-spline curves. B-splines carry the same advantageous properties as Bézier curves, and have local support.

Definition 3.4 (B-spline Curves, (Sec. 2.2 - 2.3 [24]))**.**
A B-spline curve of polynomial order p is the mapping $\boldsymbol{C}(\xi) : \mathbb{R} \to \mathbb{R}^d$ such that,

$$\boldsymbol{C}(\xi) = \sum_{i=1}^{n} \lambda_{i,p}(\xi) \boldsymbol{P}_i, \ \ \xi \in \mathbb{R}, \tag{3.15}$$

where $\lambda_{i,p}$ is the i-th B-spline basis function, and $\boldsymbol{P}_i \in \mathbb{R}^d$ the i-th control point. A B-spline is defined by its *knot vector* through the Cox-de-boor recursive formula. A knot vector is a non-decreasing sequence of real numbers $\Xi = \{\xi_1, \cdots, \xi_{n+p+1}\}$, such that the entries ξ_i, known as knots, satisfy $\xi_i \leq \xi_{i+1}$, for $i = 1, \cdots, n+p+1$. Furthermore, we require the first and final entry to be non-equal, and each have multiplicity of $p+1$, i.e. *open* knot vector. The i-th B-spline basis function $\lambda_{i,p}$ is then defined through the recursion,

$$\begin{aligned} p = 0, \qquad & \lambda_{i,0}(\xi) = \begin{cases} 1, & \text{if } \xi_i \leq \xi < \xi_{i+1} \\ 0, & \text{else} \end{cases} \\ p > 0, \qquad & \lambda_{i,p}(\xi) = \frac{\xi - \xi_i}{\xi_{i+p} - \xi_i} \lambda_{i,p-1}(\xi) + \frac{\xi_{i+p+1} - \xi}{\xi_{i+p+1} - \xi_{i+1}} \lambda_{i+1,p-1}(\xi), \end{aligned} \tag{3.16}$$

where we define $\frac{\xi - \xi_i}{\xi_{i+p} - \xi_i} = 0$ if $\xi_{i+p} - \xi_i = 0$, and $\frac{\xi_{i+p+1} - \xi}{\xi_{i+p+1} - \xi_{i+1}} = 0$ if $\xi_{i+p+1} - \xi_{i+1} = 0$. By construction the B-spline basis functions are a partition of unity (i.e. they sum up to 1), and the i-th B-spline basis function is supported on the interval $[\xi_i, \xi_{i+p+1})$. The continuity of a basis function can be reduced by using repeated knot values. The Bernstein

polynomial basis of order p can be obtained through the recursion by taking knot vector $\Xi = \{0, \cdots, 0, 1, \cdots, 1\}$. Hence the space of Bézier curves is contained within the space of B-spline curves, Figure 3.1. The derivative of a B-spline basis function is given by,

$$\frac{d}{d\xi}\lambda_{i,p}(\xi) = \frac{p}{\xi_{i+p} - \xi_i}\lambda_{i,p-1}(\xi) - \frac{p}{\xi_{i+p+1} - \xi_{i+1}}\lambda_{i+1,p-1}(\xi). \tag{3.17}$$

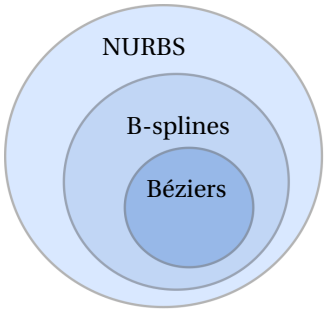

Figure 3.1: Set topology of functions used in computational geometry.

Example 3.1 (Example basis)**.**
Consider knot vector $\{0,0,0,\frac{1}{2},1,1,1\}$. Using Equation 3.16 we find the B-spline basis for $p = \{0,1,2\}$, Figure 3.2.

p = 0

$$\lambda_{1,0}(\xi) = \lambda_{2,0}(\xi) = \lambda_{5,0}(\xi) = \lambda_{6,0}(\xi) = 0$$

$$\lambda_{3,0}(\xi) = \begin{cases} 1, & \text{if } 0 \le \xi < \frac{1}{2} \\ 0, & \text{else} \end{cases}$$

$$\lambda_{4,0}(\xi) = \begin{cases} 1, & \text{if } \frac{1}{2} \le \xi < 1 \\ 0, & \text{else} \end{cases}$$

p = 1

$$\lambda_{1,1}(\xi) = \lambda_{5,1}(\xi) = 0$$

$$\lambda_{2,1}(\xi) = \begin{cases} 1-2\xi, & \text{if } 0 \le \xi < \frac{1}{2} \\ 0, & \text{else} \end{cases}$$

$$\lambda_{3,1}(\xi) = \begin{cases} 2\xi, & \text{if } 0 \le \xi < \frac{1}{2} \\ 2-2\xi, & \text{if } 0 \le \xi < 1 \\ 0, & \text{else} \end{cases}$$

$$\lambda_{4,1}(\xi) = \begin{cases} 2\xi - 1, & \text{if } \frac{1}{2} \le \xi < 1 \\ 0, & \text{else} \end{cases}$$

p = 2

$$\lambda_{1,2}(\xi) = \begin{cases} (1-2\xi)^2, & \text{if } 0 \le \xi < \frac{1}{2} \\ 0, & \text{else} \end{cases}$$

$$\lambda_{2,2}(\xi) = \begin{cases} 2\xi(2-3\xi), & \text{if } 0 \le \xi < \frac{1}{2} \\ (1-\xi)(2-2\xi), & \text{if } 0 \le \xi < 1 \\ 0, & \text{else} \end{cases}$$

$$\lambda_{3,2}(\xi) = \begin{cases} 2\xi^2, & \text{if } 0 \le \xi < \frac{1}{2} \\ (3\xi-1)(2-2\xi), & \text{if } 0 \le \xi < 1 \\ 0, & \text{else} \end{cases}$$

$$\lambda_{4,2}(\xi) = \begin{cases} (2\xi-1)^2, & \text{if } \frac{1}{2} \le \xi < 1 \\ 0, & \text{else} \end{cases}$$

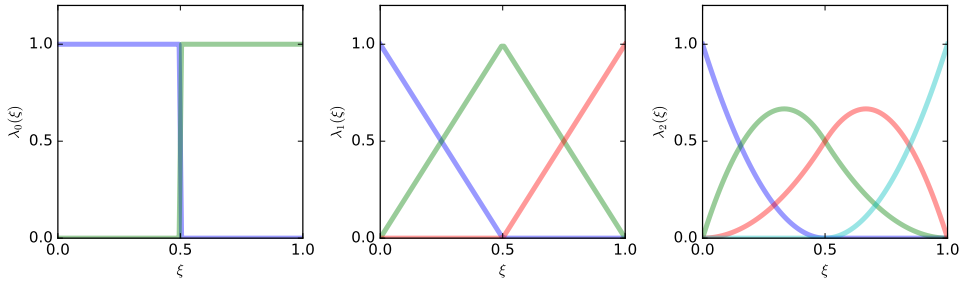

Figure 3.2: Non-zero B-spline basis functions for knot vector $\Xi = \{0,0,0,\frac{1}{2},1,1,1\}$ for polynomial order $p = 0$ (left), $p = 1$ (center), and $p = 2$ (right).

A B-spline basis, which consists of piecewise polynomials, cannot be used to describe conic curves, i.e. hyperbola, parabola, and ellipses. An additional dimension of weighing coefficients can be used to construct these conic sections. These weighed B-splines are NURBS, (Non-uniform rational B-splines).

Definition 3.5 (NURBS Curves, (Sec. 4.2 [24]))**.**
A NURBS curve of polynomial order p is the mapping $\boldsymbol{C} : \mathbb{R} \to \mathbb{R}^d$ such that,

$$\boldsymbol{C}(\xi) = \sum_{i=1}^{n} \rho_{i,p}(\xi)\boldsymbol{P}_i, \ \ \xi \in \mathbb{R}, \tag{3.18}$$

where $\lambda_{i,p}$ is the i-th rational basis function, and $\boldsymbol{P}_i \in \mathbb{R}^d$ the i-th control point. the rational basis functions are defined through their knot vector, and a vector of weights $\boldsymbol{w} \in \mathbb{R}^{n+1}$. The i-th rational basis function $\rho_{i,p}$ is given by,

$$\rho_{i,p}(\xi) = \frac{\lambda_{i,p}(\xi)\, w_i}{\sum_{i=1}^{n} \lambda_{i,p}(\xi)\, w_i}, \tag{3.19}$$

where $\lambda_{i,p}$ is the i-th B-spline basis function of polynomial order p. The coefficients $\boldsymbol{P}_i^w = [\boldsymbol{P}_i, w_i]^T \in \mathbb{R}^{d+1}$ are elements of the $d+1$ projective space. The resulting NURBS curve is then defined in the d model space. For unitary weights, $w_i = 1$, the NURBS curve becomes a B-spline curve. Hence the space of B-spline curves is contained within the space of NURBS curves, Figure 3.1.

Example 3.2 (NURBS Curve - Construction of a Circle)**.**
In this example we show how we can construct a circular curve using a rational spline basis. Let knot vector Ξ, weights w, and coefficients $\boldsymbol{P}$ be

$$\Xi = \left\{0,0,0,\frac{1}{4},\frac{1}{4},\frac{2}{4},\frac{2}{4},\frac{3}{4},\frac{3}{4},1,1,1\right\},$$
$$w = \left\{1,\frac{\sqrt{2}}{2},1,\frac{\sqrt{2}}{2},1,\frac{\sqrt{2}}{2},1,\frac{\sqrt{2}}{2},1\right\},$$
$$\boldsymbol{P} = \begin{bmatrix} 1 & 1 & 0 & -1 & -1 & -1 & 0 & 1 & 1 \\ 0 & 1 & 1 & 1 & 0 & -1 & -1 & -1 & 0 \end{bmatrix},$$

Take B-spline basis polynomial $p = 2$. Now the set of rational basis functions $\rho_{i,p}(\xi)$, Figure 3.3, can be constructed using Equation 3.19 and the Cox-de-Boor algorithm, Equation 3.16. Note that repeated knots in Ξ affect the continuity of the basis functions. The multiplicity of an interior knot m produces a B-spline or rational basis function with continuity $(p - m)$. Furthermore, note that any B-spline or NURBS curve interpolates the control net where the basis functions have C^0 continuity, Figure 3.4.

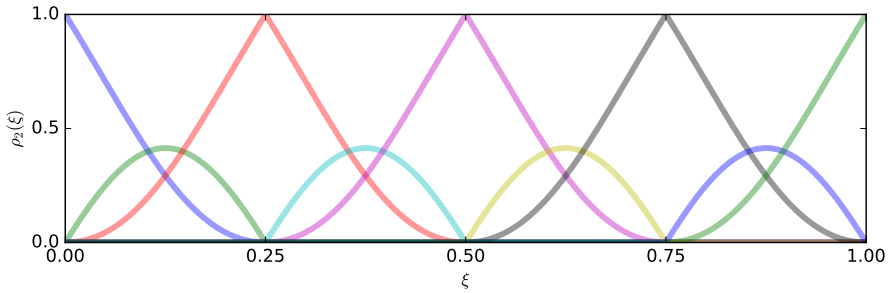

Figure 3.3: Set of rational basis functions for $p = 2$, knot vector $\Xi = \left\{0,0,0,\frac{1}{4},\frac{1}{4},\frac{2}{4},\frac{2}{4},\frac{3}{4},\frac{3}{4},1,1,1\right\}$,and set of weights $w = \left\{1,\frac{\sqrt{2}}{2},1,\frac{\sqrt{2}}{2},1,\frac{\sqrt{2}}{2},1,\frac{\sqrt{2}}{2},1\right\}$.

Now Equation 3.18 can be used to compute the NURBS curve (red), Equation 3.18. In the figure it is shown how the weighting curve $W(\xi) = \sum_{i=1}^{n} \lambda_{i,p}(\xi) w_i$ projects the B-spline curve defined by $\sum_{i=0}^{p} \lambda_{i,p}(\xi) w_i \boldsymbol{P}_i$ onto the circle.

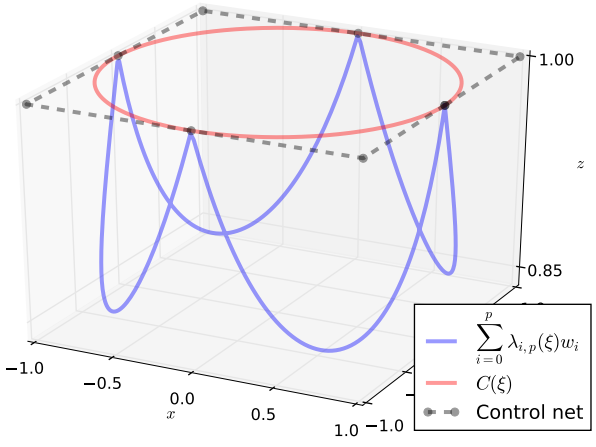

Figure 3.4: NURBS circular curve (red) with corresponding 9-point control net (black). The weighing curve (blue) projects a B-spline curve onto the circle.

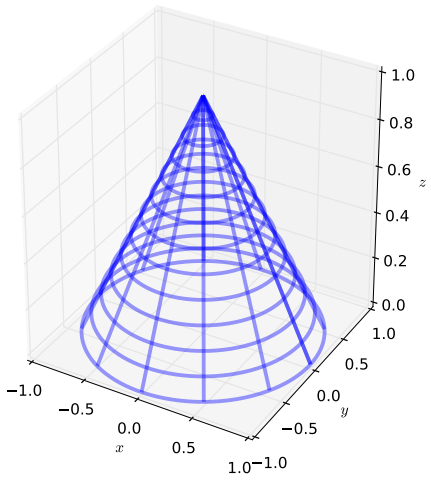

Figure 3.5: Cone surface which is constructed by taking tensor product of circular curve from Example 3.2 and a linear curve.

Higher order geometries, i.e. surfaces and volumes, can be constructed by taking tensor products of these fundamental curves, e.g. Figure 3.5. An alternative way is the use of *T-splines*. The control net of a T-spline surface can have T-shaped joints, while the control net of a NURBS surface must be the topological counterpart of a Cartesian mesh (can only have crossroad intersections). The development of unstructured spline geometries is an active field of research. *Patches* of NURBS geometries can be sewn together to construct complexer objects.

A B-spline basis can be refined without modifying the geometry. In one approach one inserts new knots to the knot vector, which is known as *knot insertion*. Another approach is to increase the multiplicity of the knots, and increasing the degree of basis functions, which is known as *degree elevation*. These refinement strategies are analogous to h- and p- refinement in classical finite elements method. In a third refinement strategy, known as k-refinement, one combines knot and insertion and degree elevation. There does not exist an analogy for this approach in FEA.

Definition 3.6 (Knot Insertion, (Sec. 2.1.4.1 [25]))**.**
Given knot vector $\Xi = \{\xi_1, \xi_2, \cdots, \xi_{n+p+1}\}$, and extended knot vector with m additional knots, $\bar{\Xi} = \{\xi_1 = \bar{\xi}_1, \bar{\xi}_2, \cdots, \bar{\xi}_{n+m+p+1} = \xi_{n+p+1}\}$, such that $\Xi \subset \bar{\Xi}$. The control points of the extended knot vector $\bar{\boldsymbol{P}}$ can be obtained from the original control points $\boldsymbol{P}$ through,

$$\bar{\boldsymbol{P}} = \mathbb{T}^p \boldsymbol{P}, \tag{3.20}$$

where the transformation matrix $\mathbb{T}^p$ is defined through the recursive formula,

$$\mathbb{T}^0_{i,j} = \begin{cases} 1, & \bar{\xi}_i \in [\xi_j, \xi_{j+1}) \\ 0, & \text{otherwise} \end{cases}$$

$$\mathbb{T}^{q+1}_{i,j} = \frac{\bar{\xi}_{i+q} - \xi_j}{\xi_{j+q} - \xi_j} \mathbb{T}^q_{i,j} + \frac{\xi_{j+q+1} - \bar{\xi}_{i+q}}{\xi_{j+q+1} - \xi_{j+1}} \mathbb{T}^q_{i,j+1}, \quad \text{for } q = 0, 1, \cdots, p-1. \tag{3.21}$$

Definition 3.7 (Order Elevation, (Sec. 2.1 [25]))**.**
Given a knot vector $\Xi = \{\xi_1, \xi_2, \cdots, \xi_{n+p+1}\}$. The multiplicity of the knots are increased by one without adding new knot values. The new control points can be determined using the transformation matrix $\mathbb{T}$ defined in Definition 3.6.

This leads to the following framework of isogeometric analysis. Given a geometric mapping defined in NURBS, B-spline, or Bézier expansions, one can refine the geometry using the strategies described above to obtain a mesh suitable for analysis. Note that the geometry is exactly contained in the coarsest mesh and preserved as the mesh is refined. This is different from classical finite-element approaches in which refinement requires interpolation of the CAD geometry (with interpolation errors as the consequence). Furthermore, note that NURBS must be refined in the projective space. Finally, one can link a NURBS geometry to a FEA code through *Bézier extraction.* Bézier extraction is the process of transforming the basis to obtain a basis of composite Bézier bases. These can be transformed element-by-element to a Lagrangian basis, which is exploited in many classical FEA codes.

3.3. DERHAM CONFORMING SPLINE SPACES

In line with the isoparametric paradigm we express quantities of interest in terms of the geometric bases introduced in the previous section. Following various works, [8, 11, 13, 26], we start out with B-splines to set up a framework for $\mathbb{R}^1$. B-splines are chosen because of their use in representing geometries and because of their controllable smoothness. The control net of a linear combination of splines form a cochain structure on which we can differentiate using incidence matrices. We first construct spline spaces in $\mathbb{R}^1$ that satisfy the DeRham sequence. This framework can be extended to arbitrary dimensions by taking tensor products of the spline spaces for the $\mathbb{R}^1$ case.

Definition 3.8 (Spline Space $\mathscr{S}^p_n$)**.**
Let Ξ be an arbitrary knot vector of dimension n, and p some polynomial order that is supported by Ξ. The span of the set of basis functions defined by the set $\{p, \Xi\}$ through Equation 3.16 is denoted by,

$$\mathscr{S}^p_\Xi := \text{span}\{\lambda_{i,p}\}^n_{i=0}. \tag{3.22}$$

In our analysis we will limit ourselves to *uniform* knot vectors. A knot vector is uniform if the knot values are uniformly distributed. Its basis is defined through the combination of its dimension, n, and polynomial order p. We define the span of such basis functions as,

$$\mathscr{S}^p_n := \{\mathscr{S}^p_\Xi : \Xi \text{ open and uniform, with } \dim(\Xi) = n\}. \tag{3.23}$$

These spline spaces will be used as building blocks to define our finite dimensional spaces. First we will define the spaces in $\mathbb{R}^1$ satisfying the sequence,

$$W_d\Lambda_h^{(0)} \xrightarrow{d} L^2\Lambda_h^{(1)}$$

Definition 3.9 (The Space of 0-forms $\Lambda_h^{(0)}$ in $\mathbb{R}^1$)**.**
Consider some scalar function, i.e. some 0-form $f^{(0)} \in W_d\Lambda^{(0)}$ in $\mathbb{R}^1$. An approximation of this function, $f_h^{(0)} \in W_d\Lambda_h^{(0)}$, is a B-spline curve of polynomial order p, i.e. $f_h^{(0)}(\xi) : \mathbb{R} \to \mathbb{R}$ with,

$$\begin{aligned} f_h^{(0)}(\xi) &:= \sum_{i=1}^{n} \lambda_{i,p}(\xi) f_i, \ \ \xi \in \mathbb{R}, \\ \text{or } \ W_d\Lambda_h^{(0)} &:= \mathscr{S}_n^p, \end{aligned} \tag{3.24}$$

where $f_i \in \mathbb{R}$ is the i-th expansion coefficient or control point (notice the similarity with Equation 3.15). Note that a polynomial order of at least $p = 1$ is required to satisfy the Sobolev continuity constraints. We will make use the following notation,

$$f_h^{(0)} = \boldsymbol{f}^T \boldsymbol{\lambda}^p,$$

with $\boldsymbol{f}^T = [f_0, f_1, \cdots, f_n]$ the vector of expansion coefficients, and $\boldsymbol{\lambda}^T = [\lambda_0^p, \lambda_1^p, \cdots, \lambda_n^p]$ the vector of basis functions.

Next consider the 1-form $v_h^{(1)} \in L^2\Lambda_h^{(1)}$ that satisfies $v_h^{(1)} = d f_h^{(0)}$. The question is, how to define its space $L^2\Lambda_h^{(1)}$? Do we let $L^2\Lambda_h^{(1)} := \mathscr{S}_n^p$ as well? We can apply the exterior derivative on the 0-form $f_h^{(0)}$ to obtain the appropriate basis for $v_h^{(1)}$,

$$d f_h^{(0)}(\xi) = \sum_{i=2}^{n} \left(\frac{p}{\xi_{i+p} - \xi_i} \lambda_{i,p-1}(\xi) d\xi \right) (f_i - f_{i-1}).$$

A proof of this result is provided in Appendix E. If we let $v_i = (f_i - f_{i-1})$, and use B-spline basis functions of a polynomial degree lower with scaling $\frac{p}{\xi_{i+p} - \xi_i}$, then the relation $v_h^{(1)} = d f_h^{(0)}$ is exact.

Definition 3.10 (The Space of 1-forms $\Lambda_h^{(1)}$ in $\mathbb{R}^1$)**.**
Consider the 1-form $v^{(1)} \in L^2\Lambda^{(1)}$ in $\mathbb{R}^1$. An approximation of this function, $v_h^{(1)} \in L^2\Lambda_h^{(1)}$, is a B-spline curve of polynomial order $p-1$, i.e. $v_h^{(1)}(\xi) : \mathbb{R} \to \mathbb{R}$ with,

$$\begin{aligned} v_h^{(1)}(\xi) &:= \sum_{i=2}^{n} \frac{p}{\xi_{i+p} - \xi_i} \lambda_{i,p-1}(\xi) v_i d\xi, \\ L^2\Lambda_h^{(1)} &:= \mathscr{S}_n^{p-1}, \end{aligned} \tag{3.25}$$

We distinguish between the basis functions that are used to expand 0-forms and 1-forms, and call them *nodal- and edge type basis functions* in line with the work by Bochev and Gerritsma, [7].

Definition 3.11 (Nodal- & Edge-type basis functions, $\lambda^{(0)}, \lambda^{(1)}$)**.**
The B-spline basis functions that are used to expand 0-forms are nodal-type basis functions, and the basis functions that are used to expand 1-forms are edge-type basis functions, [7]. Consider the relation $v_h^{(1)} = d f_h^{(0)}$, with $f_h^{(0)} \in W_d\Lambda_h^{(0)}$ and $v_h^{(1)} \in L^2\Lambda_h^{(1)}$, such that,

$$f_h^{(0)} = \boldsymbol{f}^T \boldsymbol{\lambda}^{(0)}, \tag{3.26}$$

$$v_h^{(1)} = \boldsymbol{v}^T \boldsymbol{\lambda}^{(1)} d\xi, \tag{3.27}$$

with,

$$\lambda_i^{(0)}(\xi) := \lambda_{i,p}(\xi), \tag{3.28}$$

$$\lambda_i^{(1)}(\xi) := \left(\frac{p}{\xi_{i+p} - \xi_i}\right) \lambda_{i,p-1}(\xi). \tag{3.29}$$

The relation between the expansion coefficients, $v_i = (f_i - f_{i-1})$, is encoded by the incidence matrix $\mathbb{E}^{(1,0)}$, Definition 2.11, such that $\boldsymbol{v} = \mathbb{E}^{(1,0)} \boldsymbol{f}$. The nodal-type basis functions form a partition of unity. The edge-type basis functions have unit mass, proof in Appendix E. This property reduces integration of discrete volume forms to summation of the expansion coefficients, e.g.

$$\int_\Omega v_h^{(1)} = \int_\Omega \left(\sum_{i=2}^{n} \lambda_i^{(1)}(\xi)\, v_i \right) d\xi = \sum_{i=2}^{n} v_i$$

An example pair of nodal- and edge-type basis functions is shown in Figure 3.6. Note that edge-type basis functions cannot be derived for the NURBS basis, as the exterior derivative does not map a NURBS basis onto another NURBS basis. This means we cannot unify the structure-preserving approach completely with isogeometric analysis. In this work we will only consider fixed geometries on which violation of the isoparametric of isogeometric paradigm doesn't induce additional error.

Let us reflect for a moment and compare our framework to the cochain structure introduced in section 2.3. Differentiation of the 0-form is encoded in the same incidence matrix as the action of the coboundary operator δ, indicating that the control net is in fact a cochain structure. Hence, reduction and reconstruction operators, $\mathscr{R}^{(k)}$ and $\mathscr{I}^{(k)}$ can be defined that satisfy commuting properties shown in Figure 3.7. Buffa and Hiemstra, [11, 27], make use of a dual basis to define the action of the reduction operator.

$$\begin{array}{ccc} C^{(0)} & \xrightarrow{\delta} & C^{(1)} \\ \mathscr{I}^{(0)} \downarrow \uparrow \mathscr{R}^{(0)} & & \mathscr{I}^{(1)} \downarrow \uparrow \mathscr{R}^{(1)} \\ W_d\Lambda_h^{(0)} & \xrightarrow{d} & L^2\Lambda_h^{(1)} \end{array}$$

Figure 3.7: Commuting diagram of the reconstruction and reduction operators, cochain spaces $\mathscr{C}^{(k)}$, and the spline spaces $\Lambda_h^{(k)}$.

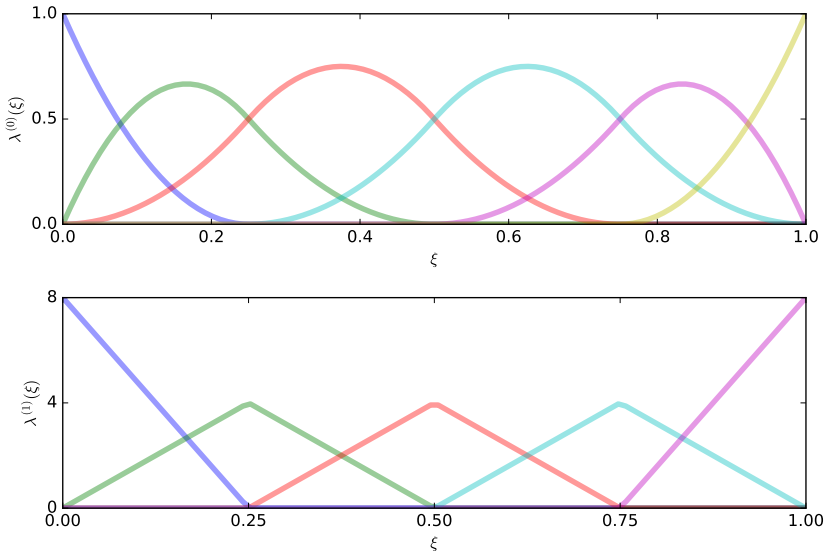

Figure 3.6: Pair of nodal- (top) and edge-type (bottom) basis functions with $p = 2$ and knot vector $\Xi = \left\{0, 0, 0, \frac{1}{4}, \frac{2}{4}, \frac{3}{4}, 1, 1, 1\right\}$. The nodal-type basis form a partition of unity, and the edge-type basis functions have unit mass.

Definition 3.12 (Dual basis $\mu^j_{(k)}$)**.**
A dual basis function function $\mu^j_{(k)}$ is defined such that,

$$\mu^j_{(k)} \lambda^{(k)}_i = \delta^j_i, \tag{3.30}$$

which allows the definition of the reduction and reconstruction operator through application of the basis function or its dual.

$$\mathscr{R}^{(k)}\left(\sum_{i=1}^{n} \alpha_i \lambda^{(k)}_i\right) := \sum_{i=1}^{n} \alpha_i \delta^j_i = \alpha_j = \boldsymbol{\alpha}, \tag{3.31}$$

$$\mathscr{I}^{(k)}(\boldsymbol{\alpha}) := \boldsymbol{\alpha}^T \boldsymbol{\lambda}^{(k)} = \sum_{i=1}^{n} \alpha_i \lambda^{(k)}_i \tag{3.32}$$

The B-spline dual basis however is impractical for various reasons. It is not complete, not integrable using standard quadrature rules, and there is no analytical expression for its basis functions, (Sec. 5.1 [25]). Its existence proves the connection with the cochain structure. We extend this framework to $\mathbb{R}^3$ using tensor products of nodal- and edge-type basis functions.

Definition 3.13 (The Space of k-forms $\Lambda^{(k)}_h$ in $\mathbb{R}^3$)**.**

Let $f_h^{(0)} \in W_d\Lambda^{(0)}$, $v_h^{(1)} \in W_d\Lambda^{(1)}$, and $\omega_h^{(2)} \in W_d\Lambda^{(2)}$. We define,

$$\begin{aligned}
W_d\Lambda_h^{(0)} &:= \mathscr{S}^{p,p,p}_{n,n,n}, \\
W_d\Lambda_h^{(1)} &:= \mathscr{S}^{p-1,p,p} \times \mathscr{S}^{p,p-1,p} \times \mathscr{S}^{p,p,p-1} \\
W_d\Lambda_h^{(2)} &:= \mathscr{S}^{p-1,p-1,p} \times \mathscr{S}^{p,p-1,p-1} \times \mathscr{S}^{p-1,p,p-1} \\
L^2\Lambda_h^{(3)} &:= \mathscr{S}^{p-1,p-1,p-1},
\end{aligned}$$

3

such that,

$$\begin{aligned}
f_h^{(0)} &= \sum \left(\lambda_i^{(0)}(\xi)\lambda_j^{(0)}(\eta)\lambda_k^{(0)}(\zeta)\right) f_{i,j,k} \\
v_h^{(1)} &= \sum \left(\lambda_i^{(1)}(\xi)\lambda_j^{(0)}(\eta)\lambda_k^{(0)}(\zeta)\right) v^{\xi}_{i,j,k} d\xi \\
&\quad + \sum \left(\lambda_i^{(0)}(\xi)\lambda_j^{(1)}(\eta)\lambda_k^{(0)}(\zeta)\right) v^{\eta}_{i,j,k} d\eta \\
&\quad + \sum \left(\lambda_i^{(0)}(\xi)\lambda_j^{(0)}(\eta)\lambda_k^{(1)}(\zeta)\right) v^{\zeta}_{i,j,k} d\zeta \\
\omega_h^{(2)} &= \sum \left(\lambda_i^{(1)}(\xi)\lambda_j^{(1)}(\eta)\lambda_k^{(0)}(\zeta)\right) \omega^{\xi,\eta}_{i,j,k} d\xi \wedge d\eta \\
&\quad + \sum \left(\lambda_i^{(0)}(\xi)\lambda_j^{(1)}(\eta)\lambda_k^{(1)}(\zeta)\right) \omega^{\eta,\zeta}_{i,j,k} d\eta \wedge d\zeta \\
&\quad + \sum \left(\lambda_i^{(1)}(\xi)\lambda_j^{(0)}(\eta)\lambda_k^{(1)}(\zeta)\right) \omega^{\zeta,\xi}_{i,j,k} d\zeta \wedge d\xi.
\end{aligned}$$

Applying the exterior derivative to these forms yields,

$$\begin{aligned}
df_h^{(0)} &= \sum \left(\lambda_i^{(1)}(\xi)\lambda_j^{(0)}(\eta)\lambda_k^{(0)}(\zeta)\right) \left(f_{i,j,k} - f_{i-1,j,k}\right) d\xi \\
&\quad + \sum \left(\lambda_i^{(0)}(\xi)\lambda_j^{(1)}(\eta)\lambda_k^{(0)}(\zeta)\right) \left(f_{i,j,k} - f_{i,j-1,k}\right) d\eta \\
&\quad + \sum \left(\lambda_i^{(0)}(\xi)\lambda_j^{(0)}(\eta)\lambda_k^{(1)}(\zeta)\right) \left(f_{i,j,k} - f_{i,j,k-1}\right) d\zeta, \\
dv_h^{(1)} &= \sum \left(\lambda_i^{(1)}(\xi)\lambda_j^{(1)}(\eta)\lambda_k^{(0)}(\zeta)\right) \left(v^{\xi}_{i,j,k} - v^{\xi}_{i,j-1,k} - v^{\eta}_{i,j,k} + v^{\eta}_{i-1,j,k}\right) d\xi \wedge d\eta \\
&\quad + \sum \left(\lambda_i^{(0)}(\xi)\lambda_j^{(1)}(\eta)\lambda_k^{(1)}(\zeta)\right) \left(v^{\eta}_{i,j,k} - v^{\eta}_{i,j,k-1} - v^{\zeta}_{i,j,k} + v^{\zeta}_{i,j-1,k}\right) d\eta \wedge d\zeta \\
&\quad + \sum \left(\lambda_i^{(1)}(\xi)\lambda_j^{(0)}(\eta)\lambda_k^{(1)}(\zeta)\right) \left(v^{\zeta}_{i,j,k} - v^{\zeta}_{i-1,j,k} - v^{\xi}_{i,j,k} + v^{\xi}_{i,j,k-1}\right) d\zeta \wedge d\xi, \\
d\omega_h^{(2)} &= \sum \left(\lambda_i^{(1)}(\xi)\lambda_j^{(1)}(\eta)\lambda_k^{(1)}(\zeta)\right) \left(\omega^{\xi,\eta}_{i,j,k} - \omega^{\xi,\eta}_{i,j,k-1} + \omega^{\eta,\zeta}_{i,j,k}\right. \\
&\qquad \left. - \omega^{\eta,\zeta}_{i-1,j,k} + \omega^{\zeta,\xi}_{i,j,k} - \omega^{\zeta,\xi}_{i,j-1,k}\right) d\xi \wedge d\eta \wedge d\zeta.
\end{aligned}$$

The coefficients of any derivative $d\alpha_h^{(k)}$ is obtained by applying an incidence matrix to the coefficients of $\alpha_h^{(k)}$. The defined spline spaces satisfy the exact sequence,

$$W_d\Lambda_h^{(0)} \xrightarrow{d} W_d\Lambda_h^{(1)} \xrightarrow{d} W_d\Lambda_h^{(2)} \xrightarrow{d} L^2\Lambda_h^{(3)}$$

We will use a simplified notation, $\phi^{(k)}$, to denote basis functions in $\mathbb{R}^n$. For example, we let,

$$f_h^{(0)} = \boldsymbol{f}^T \boldsymbol{\phi}^{(0)} = \sum f_{i,j,k}\, \phi^{(0)}_{i,j,k}(\xi,\eta,\zeta),$$

with,

$$\phi^{(0)}_{i,j,k} = \lambda^{(0)}_i(\xi)\lambda^{(0)}_j(\eta)\lambda^{(0)}_k(\zeta),$$

and,

$$\begin{aligned} v_h^{(1)} &= (\boldsymbol{v}^\xi)^T \boldsymbol{\phi}^{(1)}_\xi d\xi + (\boldsymbol{v}^\eta)^T \boldsymbol{\phi}^{(1)}_\eta d\eta + (\boldsymbol{v}^\zeta)^T \boldsymbol{\phi}^{(1)}_\zeta d\zeta, \\ &= \begin{bmatrix} (v^\xi)^T & (v^\eta)^T & (v^\zeta)^T \end{bmatrix} \begin{bmatrix} \boldsymbol{\phi}^{(1)}_\xi d\xi \\ \boldsymbol{\phi}^{(1)}_\eta d\eta \\ \boldsymbol{\phi}^{(1)}_\zeta d\zeta \end{bmatrix} \\ &= \boldsymbol{v}^T \boldsymbol{\phi}^{(1)} \end{aligned}$$

with,

$$\phi^{(1)}_{\xi_{i,j,k}} = \lambda^{(1)}_i(\xi)\lambda^{(0)}_j(\eta)\lambda^{(0)}_k(\zeta),$$

Differentiation of a form is then written as,

$$d\omega_h^{(2)} = d\left(\boldsymbol{\omega}^T \boldsymbol{\phi}^{(2)}\right) = (\mathbb{E}^{(3,2)}\boldsymbol{\omega})^T \boldsymbol{\phi}^{(3)}.$$

3.4. DISCRETISATION OF THE POISSON PROBLEMS

The framework of structure-preserving isogeometric analysis enables us to discretise Poisson problems that have been introduced in section 3.1. The resulting linear system consists of a combination of incidence matrices, and mass matrices. In this section we will introduce mass matrices, and show that we can solve both Poisson problems with optimal convergence rates.

Definition 3.14 (Mass Matrices $\mathbb{M}^{(k,k)}$)**.**
The mass matrix, $\mathbb{M}^{(k,k)}$, is the linear mapping $\mathbb{M}^{(k,k)} : C^{(k)} \to C^{(k)}$. It is a Gramian of basis functions, i.e. the Hermitian matrix of inner products with entries $\mathbb{M}^{(k,k)}_{i,j}$ given by,

$$\mathbb{M}^{(k,k)}_{i,j} = \left(\phi^{(k)}_i, \phi^{(k)}_j\right)_\Omega.$$

The mass matrix is symmetric and positive definite. The mass matrix inherits a sparsity pattern by through the local support of the basis functions. Local support can be exploited for element-wise construction of the mass matrix (more details on the element-wise construction of B-spline mass matrices can be found in sec. 3.3.1.4 of the IGA book, [25]). Gauss-Legendre quadrature is used to evaluate the integrals in the assembly routine.

Example 3.3 (Mass matrix of 1-Forms $\mathbb{M}^{(1,1)}$ in $\mathbb{R}^2$)**.**

$$\begin{aligned}
\mathbb{M}^{(1,1)} &= \left(\boldsymbol{\phi}^{(1)}, \boldsymbol{\phi}^{(1)}\right)_\Omega \\
&= \int_\Omega \boldsymbol{\phi}^{(1)} \wedge \star \boldsymbol{\phi}^{(1)} \\
&= \int_\Omega \left(\begin{bmatrix} \boldsymbol{\phi}^{(1)}_\xi d\xi \\ \boldsymbol{\phi}^{(1)}_\eta d\eta \end{bmatrix} \right) \left(\begin{bmatrix} \boldsymbol{\phi}^{(1)}_\xi d\eta \\ -\boldsymbol{\phi}^{(1)}_\eta d\xi \end{bmatrix} \right)^T \\
&= \int_\Omega \left(\begin{bmatrix} \boldsymbol{\phi}^{(1)}_\xi (\boldsymbol{\phi}^{(1)}_\xi)^T & \emptyset \\ \emptyset & \boldsymbol{\phi}^{(1)}_\eta (\boldsymbol{\phi}^{(1)}_\eta)^T \end{bmatrix} \right) d\xi \wedge d\eta
\end{aligned}$$

Example 3.4 (Discretisation of the 0-form Poisson problem)**.**
Consider the problem described in Example D.1 on domain $\Omega = [0,1]^2 \subset \mathbb{R}^2$. We let $\Gamma_n = \emptyset$, and take $f^{(0)} = 2\pi^2 \sin(\pi x)\sin(\pi y)$. The problem is then, given $f^{(0)} \in L^2\Lambda^{(0)}$, find $\psi^{(0)} \in W_d\Lambda^{(0)}$, such that

$$\left(d w^{(0)}, d\psi^{(0)}\right)_\Omega = \left(w^{(0)}, f^{(0)}\right)_\Omega, \qquad \forall\, w^{(0)} \in W_d\Lambda^{(0)}_0.$$

The exact solution of this problem is given by,

$$\psi^{(0)} = \sin(\pi x)\sin(\pi y).$$

We let $W_d\Lambda^{(0)}_h := \mathscr{S}^{p,p}_{n,n}$, such that,

$$\begin{aligned}
w^{(0)}_h &= \boldsymbol{w}^T \boldsymbol{\phi}^{(0)}, \\
\psi^{(0)}_h &= \boldsymbol{\psi}^T \boldsymbol{\phi}^{(0)}.
\end{aligned}$$

The discrete problem consists of finding $\psi^{(0)}_h \in W_d\Lambda^{(0)}_h$ such that,

$$\left(d w^{(0)}_h, d\psi^{(0)}_h\right)_\Omega = \left(w^{(0)}_h, f^{(0)}\right)_\Omega, \qquad \forall\, w^{(0)}_h \in W_d\Lambda^{(0)}_{0_h}.$$

Well-posedness for the discrete problem follows from well-posedness of the continuous problem, proven in Example D.1.

$$\boldsymbol{w}^T (\mathbb{E}^{(1,0)})^T \mathbb{M}^{(1,1)} \mathbb{E}^{(1,0)} \boldsymbol{\psi} = \boldsymbol{w}^T (\boldsymbol{\phi}^{(0)}, f^{(0)})_\Omega.$$

The Dirichlett boundary conditions are essential boundary conditions and need to be enforced strongly. Numerical solution for $W_d\Lambda^{(0)} = \mathscr{S}^{2,2}_{6,6}$ is shown in Figure 3.8a. Convergence for various refinement levels are shown in Figure 3.9a. Observed convergence rates are optimal with respect to chosen spline polynomial order.

Example 3.5 (Discretisation of the 2-form Poisson problem)**.**
Now consider the problem described inExample D.2 on domain $\Omega = [0,1]^2 \subset \mathbb{R}^2$. We let

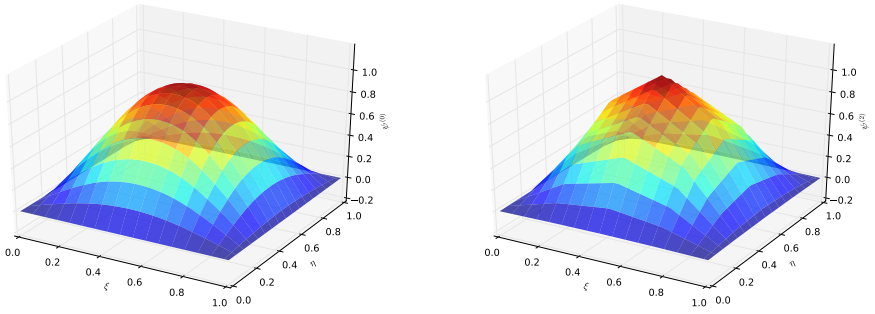

(a) $\psi^{(0)} \in W_d\Lambda^{(0)}$ (b) $\psi^{(2)} \in L^2\Lambda^{(2)}$

Figure 3.8: Reconstructed solution of the 0-form (left) and 2-form (right) Poisson problem, Example 3.4 and Example 3.5. DeRham conforming spline space were taken with $W_d\Lambda^{(0)} := \mathcal{S}^{p,p}_{n,n}$, with polynomial order $p = 2$ and dimension $n = 6$.

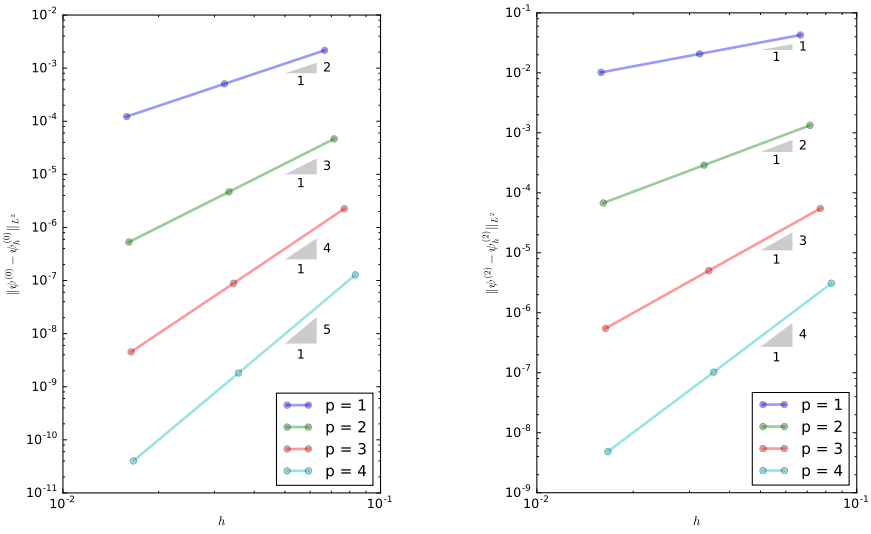

(a) $\|\psi^{(0)} - \psi^{(0)}_h\|_{L^2}$ (b) $\|\psi^{(2)} - \psi^{(2)}_h\|_{L^2}$

Figure 3.9: L^2-Error convergence results for the 0-form (left)- and 2-form (right) Poisson problem, Example 3.4 and Example 3.5, for various h-and p-refinement levels. Measured convergence rates are optimal with respect to spline polynomial order. Note that the space of $\psi^{(0)}$ is equipped with the Sobolev norm, although the weaker convergence in the L^2 norm is shown (left).

$\Gamma_n = \emptyset$, and take $f^{(2)} = 2\pi^2 \sin(\pi x)\sin(\pi y)dx \wedge dy$. The problem then consists of finding the set $(v^{(1)}, \psi^{(2)}) \in (W_d\Lambda^{(1)}, L^2\Lambda^{(2)})$, such that

$$\begin{cases} \left(dq^{(1)}, \psi^{(2)}\right)_\Omega - \left(q^{(1)}, v^{(1)}\right)_\Omega &= 0, & \forall q^{(1)} \in W_d\Lambda_0^{(1)}, \\ \left(w^{(2)}, dv^{(1)}\right)_\Omega &= \left(w^{(2)}, f^{(2)}\right)_\Omega, & \forall w^{(2)} \in L^2\Lambda_0^{(2)}, \end{cases}$$

for a given $f^{(2)} \in L^2\Lambda^{(2)}$. The exact solution of $\psi^{(2)}$ is given by,

$$\psi^{(2)} = \sin(\pi x)\sin(\pi y)dx \wedge dy.$$

3

We let $W_d\Lambda_h^{(1)} := \mathscr{S}_{n-1,n}^{p-1,p} \times \mathscr{S}_{n,n-1}^{p,p-1}$, and $L^2\Lambda_h^{(2)} := \mathscr{S}_{n-1,n-1}^{p-1,p-1}$ such that,

$$\begin{aligned} q_h^{(1)} &= \boldsymbol{q}^T\boldsymbol{\phi}^{(1)}, & w_h^{(2)} &= \boldsymbol{w}^T\boldsymbol{\phi}^{(2)} \\ v_h^{(1)} &= \boldsymbol{v}^T\boldsymbol{\phi}^{(1)}, & \psi_h^{(2)} &= \boldsymbol{\psi}^T\boldsymbol{\phi}^{(2)}. \end{aligned}$$

The discrete problem then consists of finding $(v_h^{(1)}, \psi_h^{(2)}) \in (W_d\Lambda_h^{(1)}, L^2\Lambda_h^{(2)})$, such that

$$\begin{cases} \left(dq_h^{(1)}, \psi_h^{(2)}\right)_\Omega - \left(q_h^{(1)}, v_h^{(1)}\right)_\Omega &= 0, & \forall q_h^{(1)} \in W_d\Lambda_{0_h}^{(1)}, \\ \left(w_h^{(2)}, dv_h^{(1)}\right)_\Omega &= \left(w_h^{(2)}, f^{(2)}\right)_\Omega, & \forall w_h^{(2)} \in L^2\Lambda_{0_h}^{(2)}. \end{cases}$$

Well-posedness of the discrete problem depends on the exactness of the DeRham complex which is satisfied by the discrete (cochain) spaces. The resulting system is given by,

$$\begin{bmatrix} \boldsymbol{q}^T & \boldsymbol{w}^T \end{bmatrix} \begin{bmatrix} -\mathbb{M}^{(1,1)} & (\mathbb{E}^{(2,1)})^T\mathbb{M}^{(2,2)} \\ \mathbb{M}^{(2,2)}\mathbb{E}^{(2,1)} & \emptyset \end{bmatrix} \begin{bmatrix} \boldsymbol{v} \\ \boldsymbol{\psi} \end{bmatrix} = \begin{bmatrix} \boldsymbol{0} \\ \boldsymbol{w}^T(\boldsymbol{\phi}^{(2)}, f^{(2)})_\Omega \end{bmatrix}$$

Note that the resulting system is symmetric. The Dirichlett boundary conditions are natural boundary conditions and are weakly enforced. A numerical solution corresponding to the choice of $W_d\Lambda_h^{(0)} = \mathscr{S}_{6,6}^{2,2}$, (which lets $L^2\Lambda_h^{(2)} = \mathscr{S}_{1,1}^{5,5}$), is shown in Figure 3.8b. Observed convergence rates are optimal with respect to chosen spline polynomial order, Figure 3.9b.

3.5. SUMMARY OF RESULTS

Well-posedness of variational formulations of mixed-type elliptic PDE problems depend on the topological structure of the DeRham complex. One guarantees existence and uniqueness of the solution in both the continuous and the discrete setting by selecting an appropriate set of function spaces, i.e. Sobolev spaces that satisfy the DeRham complex. Finite-dimensional polynomial subspaces are taken to discretise quantities of interest.

In isogeometric analysis spans of finite numbers of B-spline basis functions are taken to define the function spaces in the discrete setting. One distinguishes between nodal- and edge-type B-spline basis functions to discretise 0-forms and 1-forms in $\mathbb{R}^1$. In $\mathbb{R}^n$ tensor products of combinations of these basis functions are taken to construct k-forms.

Derivatives of discrete forms can be obtained by applying an incidence matrix to its vector of coefficients.

The Hodge-$\star$ is discretised through the inner product matrices, known as mass matrices. The resulting linear system consists of a combination of incidence matrices $\mathbb{E}$ and mass matrices $\mathbb{M}$. The system can be inverted to obtain the coefficients of the discrete solution.

4

SCALAR TRANSPORT

Hyperbolic PDE's involve transport of quantities with finite transport velocities. In this chapter we aim to expand the framework derived for elliptic PDE problems to be able to construct structure-preserving discretisation techniques for hyperbolic PDE's. We build towards discretisation of the non-linear convective term of the Euler equations by studying scalar transport problems.

In section 4.1 we expand our toolbox of exterior calculus to be able to formulate and analyse coordinate invariant representations of hyperbolic problems. We introduce the *Lie derivative* $\mathcal{L}_{\boldsymbol{v}}$ and *interior product* $i_{\boldsymbol{v}}$, which describe how differential forms evolve as they are transported along some flow with the velocity vector field $\boldsymbol{v}$. The scalar transport PDE's that will be studied in this chapter are presented in section 4.2. In section 4.3 we discuss various strategies for the discretisation of the interior product. We choose to discretise transport problems on a static (*Eulerian*) mesh using a space-time discretisation approach.

4.1. THE INTERIOR PRODUCT AND THE LIE DERIVATIVE

We introduce additional concepts from exterior calculus to describe transport phenomena. For theorems and notation we rely again on Frankel's geometry of physics, [18]. Consider some initial concentration at a point p, a 0-form $\rho_0^{(0)}(p) := \rho^{(0)}(p, t_0)$, that is subjected to some flow. The problems described in this chapter consist of finding the distribution, $\rho^{(0)}(p, t)$, as it advected along with the flow. We can find the velocity of the the concentration at p by differentiating its coordinate mapping with respect to time. Moreover, given its velocity, we can find its pathway, the *integral curve*, through integration. Existence of these relations is stated in Theorem 4.1.

Theorem 4.1 (Fundamental Theorem on Vector Fields, (Sec. 1.4 [18]))**.**
Let $\boldsymbol{v} : U \to \mathbb{R}^n$ be a differentiable vector field on some manifold $U \subset \mathcal{M}$. For each point

$p \in U$ there is the integral curve $\gamma : (-\epsilon, \epsilon) \to U$, such that,

$$\begin{cases} \frac{d\gamma(t)}{dt} &= v(\gamma(t)), \\ \gamma(0) &= p. \end{cases} \tag{4.1}$$

Furthermore, there is a set U_p, the neighbourhood of p, and a differentiable mapping $\Phi : U_p \times (-\epsilon, \epsilon) \to \mathbb{R}^n$, such that the curve $\phi_t(q) := \Phi(q, t)$ satisfies the differential equation,

$$\frac{\partial}{\partial t}\phi_t(q) = \boldsymbol{v}(\phi_t(q)), \tag{4.2}$$

for all time $t \in (-\epsilon, \epsilon)$ and points $q \in U_p$. The family of mappings $\{\phi_t\}$ is known as local flow. The integral and differential flow-vector field relations are illustrated in Figure 4.1. Note that the velocity-vector $\boldsymbol{v}$ at q is an element of the tangent space $\mathcal{T}\mathcal{M}_q$.

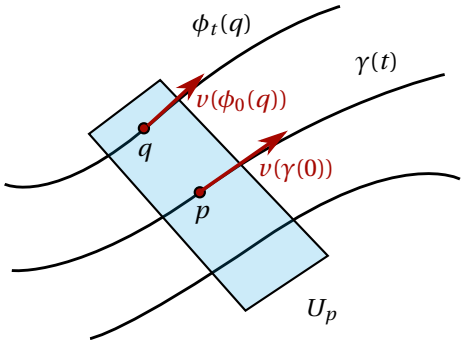

Figure 4.1: Local flow in U_p. The velocity field defines an integral curve $\gamma(t)$ in p with $\boldsymbol{v}(p) = \frac{d\gamma(t)}{dt}\Big|_{t=0}$. Moreover, the local flow $\{\phi_t\}$ in U_p defines a velocity field $\boldsymbol{v}$ through differentiation, e.g. $\frac{\partial}{\partial t}\phi_0(q) = \boldsymbol{v}(\phi_0(q))$.

We can describe the change of a differential form along the flow of a vector field through the action of the differential operator, known as the *Lie-derivative*.

Definition 4.1 (Lie-derivative $\mathcal{L}_{\boldsymbol{v}}$, (Sec. 4.2 [18]))**.**
Let $\boldsymbol{v} \in \mathcal{T}\mathcal{M}$ be the velocity vector field with flow $\{\phi_t\}$. Let $\alpha^{(k)} \in \Lambda^{(k)}(\mathcal{M})$ be a differentiable k-form. The Lie-derivative is the mapping $\mathcal{L}_{\boldsymbol{v}} : \Lambda^{(k)} \to \Lambda^{(k)}$, for which,

$$\mathcal{L}_{\boldsymbol{v}}\alpha^{(k)} := \frac{d}{dt}[\phi_t^*\alpha^{(k)}]_{t=0}, \tag{4.3}$$

where ϕ_t^* denotes the pull-back mapping, Definition C.1. The Lie-derivative satisfies the following relation,

$$\mathcal{L}_{\boldsymbol{v}}(\alpha^{(k)} \wedge \beta^{(l)}) = \mathcal{L}_{\boldsymbol{v}}\alpha^{(k)} \wedge \beta^{(l)} + \alpha^{(k)} \wedge \mathcal{L}_{\boldsymbol{v}}\beta^{(l)}. \tag{4.4}$$

The Lie-derivative and the exterior derivative measure the derivative of some differential k-form. They are related through *Cartan's formula*,

$$\mathcal{L}_{\boldsymbol{v}}\alpha^{(k)} = (d\, i_{\boldsymbol{v}} + i_{\boldsymbol{v}} d)\alpha^{(k)}, \tag{4.5}$$

where $i_{\boldsymbol{v}}$ is the *interior product* . The interior product defines a contraction of a differentiable form with a vector field.

Definition 4.2 (Interior product $i_{\boldsymbol{v}}$, (Sec. 2.9 [18]))**.**
The interior product is the mapping $i_{\boldsymbol{v}} : \Lambda^{(k)} \to \Lambda^{(k-1)}$ defined by,

$$
\begin{aligned}
i_{\boldsymbol{v}} f^{(0)} &= 0, \\
i_{\boldsymbol{v}} \alpha^{(1)} &= \alpha^{(1)}(\boldsymbol{v}),
\end{aligned}
$$

with properties,

$$
\begin{aligned}
i_{\boldsymbol{v}}(\alpha^{(k)} \wedge \beta^{(l)}) &= i_{\boldsymbol{v}}\alpha^{(k)} \wedge \beta^{(l)} + (-1)^k \alpha^{(k)} \wedge i_{\boldsymbol{v}}\beta^{(l)}, \\
i_{\boldsymbol{v}} i_{\boldsymbol{w}} \alpha^{(k)} &= -i_{\boldsymbol{w}} i_{\boldsymbol{v}} \alpha^{(k)},
\end{aligned}
$$

for vector fields $\boldsymbol{v}, \boldsymbol{w}$. Nilpotency follows from the skew-symmetry, i.e. $i_{\boldsymbol{v}}^2 := i_{\boldsymbol{v}} \circ i_{\boldsymbol{v}} = 0$. Note that the Lie-derivative commutes with both the interior product $i_{\boldsymbol{v}}$ and the exterior derivative d, which can easily be derived from Cartan's formula, Equation 4.5, and nilpotency of both operators.

Example 4.1 (Action of the interior product $i_{\boldsymbol{v}}$)**.**
Consider vector field $\boldsymbol{v}$ on $\mathscr{M} \subset \mathbb{R}^3$,

$$
\boldsymbol{v} = \sum_i^n v^i \frac{\partial}{\partial x^i},
$$

and differential forms $u^{(1)} \in \Lambda^{(1)}$, $\omega^{(2)} \in \Lambda^{(2)}$, and $\sigma^{(3)} \in \Lambda^{(3)}$. The action of the interior

product on these forms is given by,

1-form:

$$\begin{aligned} i_{\boldsymbol{v}} u^{(1)} &= \left(\sum_i^n v^i \frac{\partial}{\partial x^i}\right)\left(\sum_j^n u_j dx^j\right) \\ &= \sum_{i,j} v^i u_j \partial^i_j = \sum_i v^i u_i \end{aligned}$$

2-form:

$$\begin{aligned} i_{\boldsymbol{v}} \omega^{(2)} &= \left(\sum_i^n v^i \frac{\partial}{\partial x^i}\right)\left(\sum_{\substack{j,k \\ j<k}}^n \omega_{jk} dx^j \wedge dx^k\right) \\ &= \sum_{\substack{j,k \\ j<k}}^n v^j \omega_{jk} dx_k - \sum_{\substack{j,k \\ j<k}}^n v^k \omega_{jk} dx_j \\ &= \det \begin{vmatrix} dx_1 & dx_2 & dx_3 \\ \omega_{23} & \omega_{13} & \omega_{12} \\ v^1 & v^2 & v^3 \end{vmatrix} \end{aligned}$$

3-form:

$$\begin{aligned} i_{\boldsymbol{v}} \sigma^{(3)} &= \left(\sum_i^n v^i \frac{\partial}{\partial x^i}\right) \sigma dx_1 \wedge dx_2 \wedge dx_3 \\ &= \sigma v^1 dx_2 \wedge dx_3 - \sigma v^2 dx_1 \wedge dx_3 + \sigma v^3 dx_1 \wedge dx_2 \end{aligned}$$

We observe that the action of the interior product with vector field $\boldsymbol{v}$ is similar to the wedge product with some differential form related to $\boldsymbol{v}$ (we recognize components of the vector dot-, cross-, and scalar product). In fact we will be able to relate vector fields to differential forms of the same dimension, and re-express the action of the interior product as a wedge product on forms.

The dimension of a vector field $\boldsymbol{v}$ defined on $\mathscr{M} \subset \mathbb{R}^n$ equals n. We can formulate *isomorphisms* to transform the vector field to differential forms. Differential 1-forms, and $(n-1)$-forms have the same dimension as $\boldsymbol{v}$ which makes them suitable candidates for the proposed relations. To map to the vector field to a 1-form we will make use of the metric tensor, and to go to a $(n-1)$-form, we will make use the interior product acting on the n-form basis.

Definition 4.3 (Metric tensors g_{ij}, and g^{ij}, (Sec. 2.1 [18]))**.** Consider the basis ∂x_j and its dual basis dx^i on $\mathscr{M} \subset \mathbb{R}^n$. The metric tensors g_{ij}, and g^{ij} are the symmetric differentiable matrices,

$$g_{ij} = \langle \partial x_i, \partial x_j \rangle, \tag{4.6}$$

$$g^{ij} = \langle dx^i, dx^j \rangle, \tag{4.7}$$

where the bilinear operation $\langle\cdot,\cdot\rangle$ denotes the pairing. It's easy to see that $g_{ij}g^{ij} = \delta_i^j$, from which it follows that $g^{ij} = g_{ij}^{-1}$. The metric tensors relate the basis to its dual basis,

$$\partial x_i = \partial x_j \delta_i^j = \partial x_j \langle \partial x_i, dx^j \rangle = \langle \partial x_i, \partial x_j \rangle dx^j = g_{ij} dx^j \tag{4.8}$$

$$dx^i = dx^j \delta_i^j = dx^j \langle dx^i, \partial x_j \rangle = \langle dx^i, dx^j \rangle \partial x_j = g^{ij} \partial x_j \tag{4.9}$$

Note that the metric tensor equals a diagonal matrix on orthogonal grids.

Definition 4.4 (Vector - Form isomorphisms)**.** Given vector field $\boldsymbol{v}$ on $\mathcal{M} \subset \mathbb{R}^n$, we can relate $\boldsymbol{v}$ to an inner-oriented 1-form $v^{(1)}$ through the metric tensor,

$$\boldsymbol{v} = \sum_j v^j \partial x_j = \sum_j v^j \left(\sum_i g_{ji} dx^i \right) = \sum_i \left(\sum_j g_{ij} v^j \right) dx^j = v^{(1)}, \tag{4.10}$$

where the components of $v^{(1)}$ are given by $\sum_j g_{ij} v^j$. We can relate $\boldsymbol{v}$ to an outer oriented $(n-1)$-form by applying the interior product to the n-form basis,

$$v^{(n-1)} = i_{\boldsymbol{v}} \text{vol}^{(n)}, \tag{4.11}$$

where $\text{vol}^{(n)} := dx^1 \wedge \cdots \wedge dx^n$ is the volume-form basis. Components of the $(n-1)$-form are as shown in Example 4.1. In literature the vector-form isomorphisms are often referred to as musical isomorphisms, defining the $\flat$ operator to map the vector to a form, and the $\sharp$ operator to map the form to a vector.

Finally, we can rewrite the action of the interior product with vector $\boldsymbol{v}$ on a k-form $\alpha^{(k)}$ as,

$$i_{\boldsymbol{v}} \alpha^{(k)} = (-1)^{k(n-k)} \star (\star \alpha^{(k)} \wedge v^{(1)}), \tag{4.12}$$

where $v^{(1)}$ is the 1-form related to $\boldsymbol{v}$ through Equation 4.10, (proof of this relation can be found in Hirani's work on discrete exterior calculus, [28]). We can combine this relation with Equation 4.11 to find the relation between the 1-form $v^{(1)}$ and the $(n-1)$-form $v^{(n-1)}$,

$$v^{(n-1)} = i_{\boldsymbol{v}} \text{vol}^{(n)} \overset{4.12}{=} \star(\star \text{vol}^{(n)} \wedge v^{(1)}) = \star(1 \wedge v^{(1)}) = \star v^{(1)}, \tag{4.13}$$

from which it follows that,

$$i_{\boldsymbol{v}} \alpha^{(k)} = (-1)^{k(n-k)} \star (\star \alpha^{(k)} \wedge \star v^{(n-1)}), \tag{4.14}$$

We introduce the isomorphisms because they can be used to express the action of the interior product in terms of differential forms, for which we have developed the discretisation approach in chapter 3. We are left with a choice, will we use the 1-form $v^{(1)}$ or the $(n-1)$-form $v^{(n-1)}$? In the problems that we will study we will assume incompressible flow, which implies that conservation of mass is governed by $\text{div}\boldsymbol{v} = 0$. We can relate $\text{div}\boldsymbol{v}$ to $v^{(n-1)}$ by taking the exterior derivative of Equation 4.11,

$$d v^{(n-1)} = d i_{\boldsymbol{v}} \text{vol}^{(n)} = (\text{div}\boldsymbol{v}) \text{vol}^{(n)}. \tag{4.15}$$

It follows that the incompressibility constraint $\operatorname{div}\boldsymbol{v} = 0$ equals $d\,v^{(n-1)} = 0$ and $d^*\,v^{(1)} = 0$. In the discrete setting we are able to preserve the exactness of the exterior derivative d, which makes the isomorphism to $v^{(n-1)}$ the favourable option. However, as we will see, the 1-form isomorphism can be used to derive a slightly simplified representation of the interior product's adjoint. Next we introduce adjoints of the interior product and the Lie derivative, which will be used to manipulate weak formulations later on.

Definition 4.5 (Cointerior product, $i_{\boldsymbol{v}}^*$)**.**
The cointerior product is the mapping $i_{\boldsymbol{v}^*} : \Lambda^{(k)} \to \Lambda^{(k+1)}$ defined by,

$$i_{\boldsymbol{v}}^* := (-1)^{n(k+1)-1} \star i_{\boldsymbol{v}} \star . \tag{4.16}$$

The action of the cointerior product $i_{\boldsymbol{v}}^*$ on differential form $\alpha^{(k)}$ can be written as the action of a wedge product,

$$i_{\boldsymbol{v}}^* \alpha^{(k)} = (-1)^k (\alpha^{(k)} \wedge v^{(1)}), \tag{4.17}$$

where $v^{(1)}$ is the 1-form related to the vector field $\boldsymbol{v}$. The Cointerior product is the adjoint of the interior product,

$$\left(\beta^{(k-1)}, i_{\boldsymbol{v}} \alpha^{(k)}\right)_{\mathcal{M}} = \left(i_{\boldsymbol{v}}^* \beta^{(k-1)}, \alpha^{(k)}\right)_{\mathcal{M}} \tag{4.18}$$

Proofs of these relations are provided in Appendix B.

Definition 4.6 (Co-Lie derivative $\mathcal{L}_{\boldsymbol{v}}^*$)**.**
The Co-Lie derivative is the mapping $\mathcal{L}_{\boldsymbol{v}}^* : \Lambda^{(k)} \to \Lambda^{(k)}$ defined by,

$$\mathcal{L}_{\boldsymbol{v}}^* := (-1)^{k(n+1)+1} \star \mathcal{L}_{\boldsymbol{v}} \star . \tag{4.19}$$

The co-Lie derivative is related to the codifferential and the cointerior product through a relation mirroring Cartan's formula, Equation 4.5,

$$\mathcal{L}_{\boldsymbol{v}}^* \alpha^{(k)} = (d^* i_{\boldsymbol{v}}^* + i_{\boldsymbol{v}}^* d^*) \alpha^{(k)}. \tag{4.20}$$

The co-Lie derivative is the adjoint of the Lie-derivative,

$$\left(\beta^{(k)}, \mathcal{L}_{\boldsymbol{v}}^* \alpha^{(k)}\right)_{\mathcal{M}} = \left(\mathcal{L}_{\boldsymbol{v}} \beta^{(k)}, \alpha^{(k)}\right)_{\mathcal{M}} - \left(\beta^{(k)}, i_{\boldsymbol{v}}^* \alpha^{(k)}\right)_{\partial\mathcal{M}} - \left(i_{\boldsymbol{v}} \beta^{(k)}, \alpha^{(k)}\right)_{\partial\mathcal{M}}. \tag{4.21}$$

In the upcoming section we will use the interior product and Lie-derivative to formulate the equations governing advection problems. We will present the model problems on periodic domains that will be studied in this chapter.

4.2. TRANSPORT PROBLEMS

In this section we derive the governing equations for scalar transport problems. We present some test problems, which will be analysed in the sections to come. Scalar transport is governed by the conservation of mass. Let $\rho^{(n)}$ denote the density of a given quantity. The total mass M is given by,

$$M = \int_{V(t)} \rho^{(n)}, \tag{4.22}$$

where $V(t) \subset \mathscr{M}$ is some volume. Application of the transport theorem leads to the governing equations describing scalar transport. A formal derivation of the governing equations can be found in Appendix G.

Theorem 4.2 (Transport Theorem)**.**
The time-rate of change of a k-form $\alpha^{(k)} \in \Lambda^{(k)}$ paired to a k-dimensional sub-manifold $V \subset \mathscr{M}$ at some time-instant $t \in \mathbb{R}$ is given by,

$$\frac{d}{dt}\int_{V(t)} \alpha^{(k)} = \int_{V(t)} \left(\frac{\partial \alpha^{(k)}}{\partial t} + \mathscr{L}_{\boldsymbol{v}} \alpha^{(k)} \right). \tag{4.23}$$

Theorem 4.3 (Scalar Transport Equations)**.** *The equation for conservation of mass of some quantity with density distribution $\rho^{(n)}$ that is advected along with some incompressible fluid with velocity vector field $\boldsymbol{v}$ is given by,*

$$\int_{V(t)} \left(\frac{\partial \rho^{(n)}}{\partial t} + \mathscr{L}_{\boldsymbol{v}} \rho^{(n)} \right) = 0, \tag{4.24}$$

for some volume $V(t) \subset \mathscr{M}$. The velocity vector field satisfies the incompressibility constraint, $div\boldsymbol{v} = 0$ or $d v^{(n-1)} = 0$, where $v^{(n-1)}$ is the $(n-1)$-form associated with $\boldsymbol{v}$.

We can derive alternative formulations of the governing transport equation, Equation 4.24, by considering dual formulation or incorporating the incompressibility constraint, i.e. the non-conservative form. All four formulations are derived in Appendix G. Consider the dual formulation of the non-conservative formulation,

$$\frac{\partial \rho^{(0)}}{\partial t} + \mathscr{L}_{\boldsymbol{v}} \rho^{(0)} = 0. \tag{4.25}$$

We choose to define the problems on *periodic domains*. A solution leaving one part of the domain, enters the domain on the other side. We denote periodic domains with reverse brackets, $]\cdot,\cdot[$. Note that a periodic domain in $\mathbb{R}^1$ has the topology of a circle, whereas a periodic domain in $\mathbb{R}^2$ has the topology of a torus, Figure 4.2. The benchmark problems that we consider, were introduced in the book by Donea and Huerta (Sec 3.11 [2]).

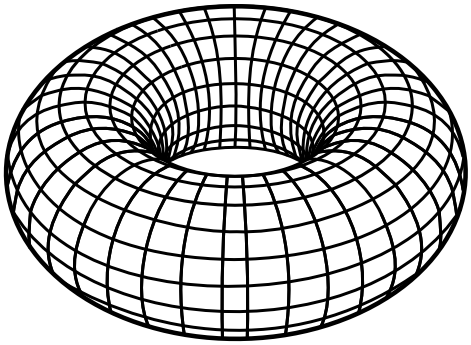

Figure 4.2: Periodic domain in $\mathbb{R}^2$ has the topology of a torus.

Problem 4.1 (Scalar advection-diffusion in $\mathbb{R}^1$)**.**
Consider the space-time manifold $\mathscr{Q} = \Omega \times \mathbb{R}_+$, where $\Omega :=]0,1[$ is the periodic unit-interval. The incompressibility condition in $\mathbb{R}^1$ is satisfied if the velocity field is constant, i.e $\boldsymbol{v} = U\partial_x$, with $U \in \mathbb{R}$. Given some diffusion coefficient $\epsilon \in \mathbb{R}_+$, and as initial solution $\rho^{(0)}(x,0) := \rho_0(x)$ at $t = 0$ the sinusoid,

$$\rho_0(x) = \begin{cases} \frac{1}{2}\left(1 + \cos\left(\frac{\pi}{\sigma}(x - x_0)\right)\right), & \text{if } \|x - x_0\| \leq \sigma, \\ 0, & \text{elsewhere} \end{cases} \tag{4.26}$$

The initial solution is compactly supported on $[x_0 - \sigma, x_0 + \sigma]$, has maximum equal to 1 at x_0, and is continuously differentiable. It has mass $\int \rho_0 dx = \sigma$, and moment $\int \rho_0^2 dx = \frac{3\sigma}{4}$. We take $x_0 = \frac{1}{2}$ and $\sigma = 0.2$, Figure 4.3a. The problem then consists of finding $\rho^{(0)}(x,t) \in \Lambda^{(0)}(\mathscr{Q})$ such that,

$$\begin{cases} \partial_t \rho^{(0)} + i_{\boldsymbol{v}} d\rho^{(0)} - \epsilon d^* d\rho^{(0)} = 0 \\ \rho^{(0)}(x,0) = \rho_0(x) \end{cases}. \tag{4.27}$$

We will mainly focus on the case of pure advection, $\epsilon = 0$, for which the exact solution is given by $\rho^{(0)}(x,t) = \rho_0(x - Ut)$, i.e. the solution traverses the domain with velocity U. We will show that diffusion has a stabilizing effect on the numerical solution.

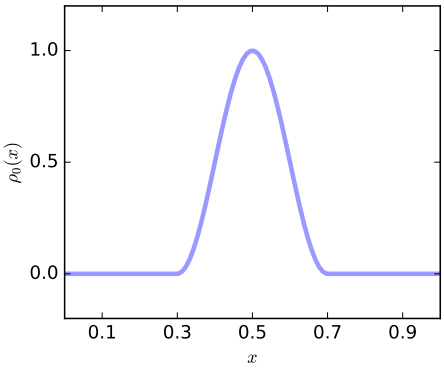

(a) Equation 4.26 with $x_0 = 0.5$ and $\sigma = 0.2$.

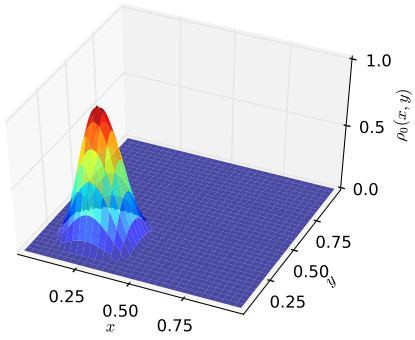

(b) Equation 4.28 with $(x_0, y_0) = (0.3, 0.3$, and $\sigma = 0.2$.

Figure 4.3: Initial condition for the advection problems in $\mathbb{R}^1$ (top) and $\mathbb{R}^2$ (bottom). The initial condition is continuously differentiable, is compactly supported, and has unit maximum at its center location.

Problem 4.2 (Scalar advection in $\mathbb{R}^2$)**.**
Consider the space-time manifold $\mathcal{Q} = \Omega \times \mathbb{R}_+$, where $\Omega =]0,1[^2$ is the periodic unit-square. As an initial condition we take the tensor product of the sinusoids, Equation 4.26,

$$\rho^{(0)}(x, y, 0) = \rho_0(x)\rho_0(y). \tag{4.28}$$

The initial solution is compactly supported on $[(x_0, y_0) \pm (\sigma, \sigma)]$, has its maximum equal to 1 located at (x_0, y_0), and is continuously differentiable. It has mass $\int \rho_0 dx \wedge dy = \sigma^2$, and moment $\int \rho_0^2 dx \wedge dy = \frac{9}{16}\sigma^2$. We take initial position $(x_0, y_0) = (0.3, 0.3)$, and $\sigma = 0.2$. The problem then consists of finding $\rho^{(0)}(x,t) \in \Lambda^{(0)}(\mathcal{Q})$ such that,

$$\begin{cases} \partial_t \rho^{(0)} + i_{\boldsymbol{v}} d\rho^{(0)} = 0 \\ \rho^{(0)}(x, y, 0) = \rho_0(x, y) \end{cases},$$

for a given velocity field $\boldsymbol{v}$. We will consider two different incompressible flow fields, the *circular velocity-field*, and the *Rudman vortex*. We define the circular velocity field,

$$\boldsymbol{v} = -2\left(y - \frac{1}{2}\right)\frac{\partial}{\partial x} + 2\left(x - \frac{1}{2}\right)\frac{\partial}{\partial y}. \tag{4.29}$$

One can verify that div $\boldsymbol{v} = 0$. By using the polar coordinate transformation $(x-\frac{1}{2}, y-\frac{1}{2}) = (r\cos\theta, r\sin\theta)$, one can show the radial component of the flow equals zero. Furthermore we find that $\|\boldsymbol{v}\| = 2r$. Hence, the fluid parcel with initial position on r traverses the orbit $\gamma = r$, with period $T = \frac{2\pi r}{2r} = \pi[s]$. Iso-contours of the stream function are shown in Figure 4.4a, indicating the circular paths, and the increase in velocity with r. Note that the circular velocity field is discontinuous on a periodic domain.

The second test case that we introduce is the Rudman vortex velocity field, [29]. The Rudman vortex is defined as,

$$\boldsymbol{v} = A\sin(\pi x)\cos(\pi y)\frac{\partial}{\partial x} - A\cos(\pi x)\sin(\pi y)\frac{\partial}{\partial y}, \tag{4.30}$$

for some constant $A \in \mathbb{R}$. The Rudman vortex is a continuously differentiable incompressible flow-field that deforms volumes, making it a more difficult test case in the discrete setting. Iso-contours of the Rudman vortex are shown in Figure 4.4b. The distance between 2 iso-contours varies, hence any parcel that is advected in the stream-tube bound by these iso-contours will alternatively accelerate and decelerate along the way.

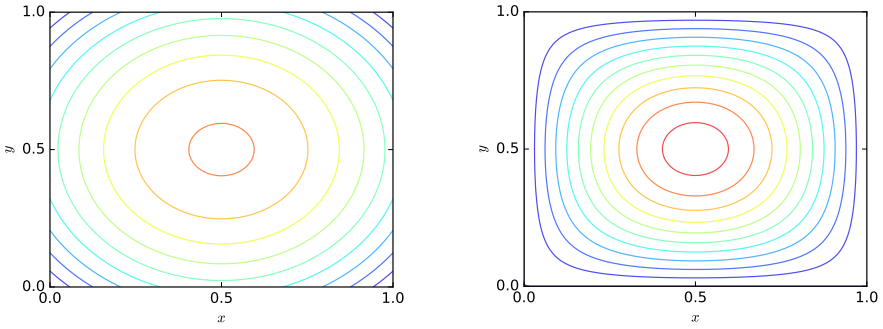

(a) $\psi^{(0)} = -[(x^2 - x) + (y^2 - y)]$ (b) $\psi^{(0)} = \frac{A}{\pi}\sin(\pi x)\sin(\pi y)$

Figure 4.4: Iso-contours of the stream function $\psi^{(0)}$ corresponding to (left) the circular velocity field, Equation 4.29, and (right) the Rudman vortex, Equation 4.30.

In the next sections we will discretise these problems using a *space-time* method. Most classical methods first discretise the spatial dependencies to obtain a semi-discrete system of differential algebraic equations. Often these equations are solved using an explicit, implicit, or combined multi-stepping algorithm. In a space-time finite element method one expands variables in both space- and time-dependent basis functions. One

advantage of this approach is that implementation of time dependencies of the considered problem become trivial. Together with the advantages of isogeometric analysis, space-time discretisations would be highly advantageous for moving-boundary problems, or fluid structure interactions. Another advantage is the possibility to (locally) refine in both space and time, e.g. as shown in the work by Abedi et al. [30]. The advantages of space-time methods come at a cost however. The additional temporal dimension have a huge impact on both assembly cost and solve cost.

Our motivation to choose for space-time approach is that it is consistent with our framework, and because it is convenient for rigorous stability analysis. It motivates us to introduce the following notation.

Definition 4.7 (Space-time Lie-derivative $\mathscr{L}_{\boldsymbol{X}}$, (Sec 4.3 [18]))**.**
Consider the space-time domain $Q = \Omega \times T$, with spatial domain $\Omega \subset \mathbb{R}^{(n)}$, and $T = [0, t]$ the considered time-interval. The space-time Lie-derivative is the mapping $\mathscr{L}_{\boldsymbol{X}} : \Lambda^{(k)}(\Omega) \rightarrow (\Omega)$ that satisfies,

$$\mathscr{L}_{\boldsymbol{X}} \alpha^{(k)} = (\boldsymbol{d} i_{\boldsymbol{X}} + i_{\boldsymbol{X}} \boldsymbol{d}) \alpha^{(k)} \tag{4.31}$$

$$= c \frac{\partial \alpha^{(k)}}{\partial t} + \mathscr{L}_{\boldsymbol{v}} \alpha^{(k)}, \tag{4.32}$$

where constant c is the velocity of the time-frame (usually we take $c = 1$), $\boldsymbol{X}$ the space-time velocity-vector $\boldsymbol{X} := c \frac{\partial}{\partial t} + \boldsymbol{v}$, and $\boldsymbol{d}$ the space-time exterior derivative,

$$\boldsymbol{d} \alpha^{(k)} = dt \wedge \frac{\partial \alpha^{(k)}}{\partial t} + d\alpha^{(k)}. \tag{4.33}$$

4.3. DISCRETISATION OF TRANSPORT PROBLEMS

Solutions on periodic domains will need to be reconstructed using a *periodic spline basis*. A set of periodic node- and edge-type basis is shown in Figure 4.5. Such basis can be obtain from on ordinary B-spline basis through knot insertion, Appendix H. In this approach, we obtain transformation matrices that maps a standard set of B-spline basis functions to a set of periodic B-spline basis functions.

Note that the dimension of the node-type basis corresponding to a periodic basis is equal to the dimension of its corresponding edge-type basis, i.e. a circular grid has an equal amount of nodes and edges. In Appendix H we show how a periodic basis can be constructed.

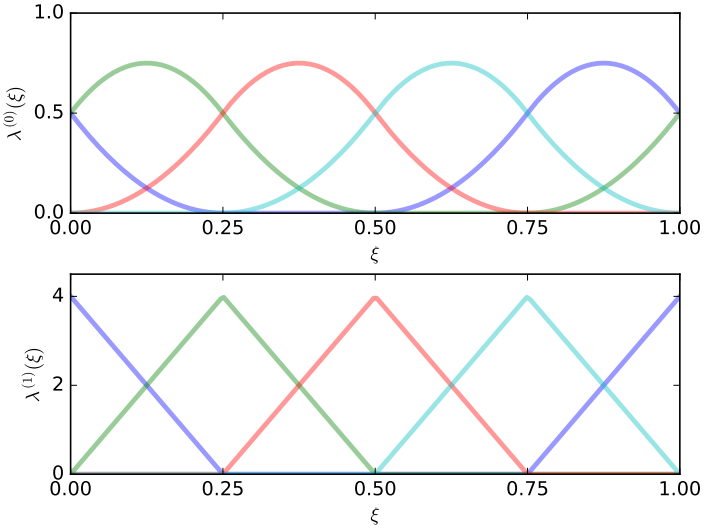

Figure 4.5: The set of (top) nodal- and (bottom) edge-type periodic B-splines, $\lambda_i^{(0)}(\xi)$ and $\lambda_i^{(1)}(\xi)$, corresponding to $W_d\Lambda^{(0)} := \mathscr{P}_4^2$.

Proposed strategies to discretise the Lie-derivative can roughly be divided into 3 categories, *static*, *dynamic*, and *mixed* approaches. In the static approach (Eulerian), the mesh is fixed, and fluxes are approximated using interpolation- or projection methods. In the dynamic approach (Lagrangian), the flow is approximated, and the mesh is advected with the flow. Dynamic approaches require periodical re-meshing to cope with accumulated deformations. In the mixed approach (Semi-Lagrangian), the mesh is advected to approximate fluxes.

Most dynamic- and mixed approaches rely on the idea of *extrusion* , e.g. Bossavit, [31], Heumann & Hiptmair, [32], and Mullen et al. [33]. In these approaches one approximates the extruded volume $E_{\boldsymbol{v}}(V,t)$,

$$E_{\boldsymbol{v}}(V,t) = \bigcup_{\tau\in[0,t]} V(\tau), \tag{4.34}$$

and use an upwind/downwind approach to approximate integral fluxes, Figure 4.6. Another approach was explored in the thesis works by Palha and Rebelo, [34, 35]. They approximated fluxes by pulling back quadrature points over some time-step. The dynamic- and mixed approaches rely on the quality of the mapping. The development of volume-preserving mappings, corresponding to an incompressible flow-field, would be of great benefit for these approaches. Although these approaches are equally valid strategies to discretise transport phenomena, we will pursuit a static strategy.

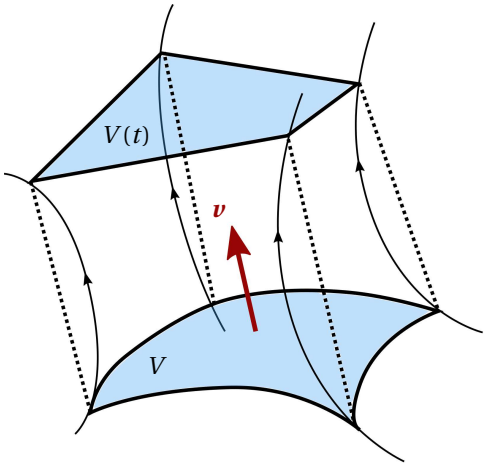

Figure 4.6: Approximation of the extruded volume $E_{\boldsymbol{v}}(V,t)$.

To discretise the action of the interior product in a static approach, we need to find a suitable vector-basis that mimics the pairing of a vector and a differential form. Gerritsma et al. try to define the Lie-derivative on cochain structures using pointwise contractions, [36]. This requires point-wise storage of both function-values and derivatives, e.g. using hermite polynomials. However, we wish to expand the framework introduced in chapter 3 using nodal- and edge-type B-splines to discretise differential forms. Instead of trying to find a proper basis for vectors to discretise the interior product, we look at its adjoint, the wedge product between differential forms.

Example 4.2 (Discrete Wedge Product)**.**
Consider the discretisation of $i_{\boldsymbol{v}}\rho^{(2)}$ on $\Omega \subset \mathbb{R}^2$. We can derive a weak formulation by taking the inner product with test function $w^{(1)}$,

$$\left(w^{(1)}, i_{\boldsymbol{v}}\rho^{(2)}\right)_\Omega \overset{4.18}{=} \left(w^{(1)} \wedge v^{(1)}, \rho^{(2)}\right)_\Omega = \left(\sigma^{(2)}\rho^{(2)}\right)_\Omega,$$

where $v^{(1)}$ is the 1-form associated with $\boldsymbol{v}$, and $\sigma^{(2)} = w^{(1)} \wedge v^{(1)}$. In the discrete setting we take,

$$w_h^{(1)} = \sum_{ij} w_{i,j}^x \lambda_i^{(1)}(x)\lambda_j^{(0)}(y)dx + \sum_{ij} w_{i,j}^y \lambda_i^{(0)}(x)\lambda_j^{(1)}(y)dy$$
$$v_h^{(1)} = \sum_{kl} v_{k,l}^x \lambda_k^{(1)}(x)\lambda_l^{(0)}(y)dx + \sum_{kl} v_{k,l}^y \lambda_k^{(0)}(x)\lambda_l^{(1)}(y)dy$$

The 2-form $\sigma_h^{(2)} := w_h^{(1)} \wedge v_h^{(1)}$ is then given by,

$$\begin{aligned}
\sigma_h^{(2)} = w_h^{(1)} \wedge v_h^{(1)} &= \sum_{ijkl} w_{i,j}^x v_{k,l}^y \lambda_k^{(0)}(x)\lambda_j^{(0)}(y)\lambda_i^{(1)}(x)\lambda_l^{(1)}(y)\,dx\wedge dy \\
&\quad - \sum_{ijkl} w_{i,j}^y v_{k,l}^x \lambda_i^{(0)}(x)\lambda_l^{(0)}(y)\lambda_k^{(1)}(x)\lambda_j^{(1)}(y)\,dx\wedge dy \\
&= \sum_{ijkl} w_{i,j}^x v_{k,l}^y \phi_{k,j}^{(0)}\phi_{i,l}^{(2)}\,dx\wedge dy - w_{i,j}^y v_{k,l}^x \phi_{i,l}^{(0)}\phi_{k,j}^{(2)}\,dx\wedge dy \\
&= \sum_{ijkl} \left(w_{i,l}^x v_{k,j}^y - w_{k,j}^y v_{i,l}^x\right)\phi_{k,l}^{(0)}\phi_{i,j}^{(2)}\,dx\wedge dy \\
&= \sum_{ij}\left[\sum_{kl}\left(w_{i,l}^x v_{k,j}^y - w_{k,j}^y v_{i,l}^x\right)\phi_{k,l}^{(0)}\right]\phi_{i,j}^{(2)}\,dx\wedge dy \\
&= \sum_{ij}\sigma_{i,j}(x,y)\phi_{i,j}^{(2)}\,dx\wedge dy.
\end{aligned}$$

The result is different from the 2-forms that we defined in chapter 3. From the example we see that the wedge product $\wedge$ does not send the discrete forms to the right space, and does not satisfy the desired commutativity shown in the diagram, Figure 4.7. To map the wedge product to the right space we can use projection or interpolation techniques.

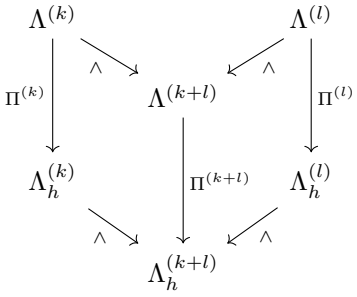

Figure 4.7: desired commutativity of the wedge product

Definition 4.8 (Contraction Matrices $\mathbb{C}_{\boldsymbol{v}_h}^{(k-1,k)}$)**.**
The contraction matrix, $\mathbb{C}_{\boldsymbol{v}_h}^{(k-1,k)}$, is the linear mapping $\mathbb{C}_{\boldsymbol{v}_h}^{(k-1,k)} : C^{(k)} \to C^{(k-1)}$. Its entries $\left(\mathbb{C}_{\boldsymbol{v}_h}^{(k-1,k)}\right)_{i,j}$ are given by,

$$\left(\mathbb{C}_{\boldsymbol{v}_h}^{(k-1,k)}\right)_{i,j} = \left(\phi_i^{(k-1)}, i_{\boldsymbol{v}_h}\phi_j^{(k)}\right)_\Omega = \left(\phi_i^{(k-1)} \wedge v_h^{(1)}, \phi_j^{(k)}\right)_\Omega, \tag{4.35}$$

where $v_h^{(1)} = \Pi^{(1)} v^{(1)}$ with $v^{(1)}$ is the 1-form associated with the vector $\boldsymbol{v}$. The continuous velocity-field $\boldsymbol{v}$ can also be used if it is known. The contraction matrix approximates the interior product. Contraction matrices only approximate the interior product's nilpotency, whereas the incidence matrices satisfy the nilpotency of the exterior derivative exactly.

Example 4.3 (Computation of $\mathbb{C}_{\boldsymbol{v}}^{(0,1)}$ and $\mathbb{C}_{\boldsymbol{v}}^{(1,2)}$)**.**
Let $\boldsymbol{v} = u_x(x,y)\partial_x + u_y(x,y)\partial_y$ be the velocity vector field on $\Omega \subset \mathbb{R}^2$. The 1-form contraction matrix $\mathbb{C}_{\boldsymbol{v}}^{(0,1)}$ is given by,

$$\begin{aligned}
\mathbb{C}_{\boldsymbol{v}}^{(0,1)} &= \left(\boldsymbol{\phi}^{(0)}, i_{\boldsymbol{v}}\phi^{(1)}\right)_\Omega \\
&= \int_\Omega \boldsymbol{\phi}^{(0)} \wedge \star i_{\boldsymbol{v}} \boldsymbol{\phi}^{(1)} \\
&= \int_\Omega \left(\boldsymbol{\phi}^{(0)}\right) \left(\begin{bmatrix} u_x \boldsymbol{\phi}_x^{(1)} \\ u_y \boldsymbol{\phi}_y^{(1)} \end{bmatrix} \right)^T dx \wedge dy \\
&= \int_\Omega \left(\begin{bmatrix} \boldsymbol{\phi}^{(0)} u_x (\boldsymbol{\phi}_x^{(1)})^T & \boldsymbol{\phi}^{(0)} u_y (\boldsymbol{\phi}_y^{(1)})^T \end{bmatrix} \right) dx \wedge dy
\end{aligned}$$

The 2-form contraction matrix $\mathbb{C}_{\boldsymbol{v}}^{(1,2)}$ is given by,

$$\begin{aligned}
\mathbb{C}_{\boldsymbol{v}}^{(1,2)} &= \left(\boldsymbol{\phi}^{(1)}, i_{\boldsymbol{v}}\phi^{(2)}\right)_\Omega \\
&= \int_\Omega \boldsymbol{\phi}^{(1)} \wedge \star i_{\boldsymbol{v}} \boldsymbol{\phi}^{(2)} \\
&= \int_\Omega \left(\begin{bmatrix} \boldsymbol{\phi}_x^{(1)} dx \\ \boldsymbol{\phi}_y^{(1)} dy \end{bmatrix} \right) \left(\begin{bmatrix} -u_x \boldsymbol{\phi}^{(2)} dx \\ -u_y \boldsymbol{\phi}^{(2)} dy \end{bmatrix} \right)^T \\
&= \int_\Omega \left(\begin{bmatrix} -\boldsymbol{\phi}_x^{(1)} u_y (\boldsymbol{\phi}^{(2)})^T \\ \boldsymbol{\phi}_y^{(1)} u_x (\boldsymbol{\phi}^{(2)})^T \end{bmatrix} \right) dx \wedge dy
\end{aligned}$$

We can use a combination of incidence matrices $\mathbb{E}^{(k,k-1)}$ and contraction matrices $\mathbb{C}_{\boldsymbol{v}_h}^{(k-1,k)}$, to differentiate the Lie-derivative as shown in the following example.

Example 4.4 (Discretisation of the scalar advection-diffusion equation)**.**
Consider the scalar advection-diffusion problem on the space-time domain $\mathcal{Q} = \Omega \times T$, where $\Omega =]0,1[$ is the unit-interval periodic domain, Problem 4.1, and $T = [0,t]$ the considered time-interval. Note that the space-time domain Q has the topology of a cylinder. We obtain a weak formulation of Equation 4.27 by taking the inner product with test-function $w^{(0)} \in W_d\Lambda_0^{(0)}(Q)$, with $w^{(0)} = 0$ at $t = 0$, and integrate-by-parts the diffusive term,

$$\left(w^{(0)}, \mathscr{L}_{\boldsymbol{X}} \rho^{(0)}\right)_Q = \epsilon \left(dw^{(0)}, d\rho^{(0)}\right)_Q,$$

with $\mathscr{L}_{\boldsymbol{X}}$ the space-time Lie-derivative, and $\boldsymbol{X} = c\partial_t + u\partial_x$. To discretise the system we take $W_d\Lambda_h^{(0)} := \mathscr{S}_{n,n}^{p,p}$. The 0-form basis is the product of periodic splines in the spatial dimension and ordinary splines in the temporal dimension, $\phi_{i,j}^{(0)}(x,t) = \lambda_i(x)\lambda_j(t)$. We let,

$$w_h^{(0)} = \boldsymbol{w}^T \boldsymbol{\phi}^{(0)}, \qquad \rho_h^{(0)} = \boldsymbol{\rho}^T \boldsymbol{\phi}^{(0)},$$

and find,

$$\begin{aligned}
\left(w_h^{(0)}, i_{\boldsymbol{X}} \boldsymbol{d} \rho_h^{(0)}\right)_Q &= \boldsymbol{w}^T \mathbb{C}_{\boldsymbol{X}}^{(0,1)} \mathbb{E}^{(10)} \boldsymbol{\rho} \\
\left(dw_h^{(0)}, d\rho_h^{(0)}\right)_Q &= \boldsymbol{w}^T \left(\mathbb{E}_\Omega^{(1,0)}\right)^T \mathbb{M}^{(1,1)} \mathbb{E}_\Omega^{(1,0)} \boldsymbol{\rho},
\end{aligned}$$

where $\mathbb{E}^{(1,0)}_{\Omega}$ is the incidence matrix acting on spatial edges only. Note that $\mathbb{E}^{(1,0))} = \left[\mathbb{E}^{(1,0)}_{\Omega}, \mathbb{E}^{(1,0)}_{T}\right]^T$, with $\mathbb{E}^{(1,0)}_{T}$ acting on temporal edges. The resulting system can be written as,

$$\mathbb{C}^{(0,1)}_{\boldsymbol{X}}\mathbb{E}^{(1,0))}\boldsymbol{\rho} = \epsilon\left(\mathbb{E}^{(1,0)}_{\Omega}\right)^T \mathbb{M}^{(1,1)}\mathbb{E}^{(1,0)}_{\Omega}\boldsymbol{\rho}$$

Note that the initial condition is an essential boundary condition which needs to be enforced. For a few example runs we take spline spaces with dimension $n = 24$, and polynomial order $p = 2$. We consider the following 3 cases,

1. Pure advection with $U = 1$, $c = 1$, and $\epsilon = 0$
2. Advection-diffusion with $U = 1$, $c = 1$, and $\epsilon = 0.001$
3. Slowed time-frame with $U = 1$, $c = \frac{1}{2}$, and $\epsilon = 0.001$

The results are shown in Figure 4.8. In every case mass was conserved with machine precision. In the first case solution traversed the domain once. Spurious oscillations are observed at various locations through space and time. These oscillations or *wiggles* are characteristic in higher-order approximations of advective problems. These wiggles accumulate over time destabilizing the numerical solution. The next section is devoted to the analysis and control of these oscillations.

In the second problem diffusion was added, causing the distribution to smear out as it travels through space and time. The action of diffusion is, unlike convection, governed by symmetric operations causing the smearing to take place in both spatial directions. Spurious oscillations will smear out for this case. Some classical solution methods add artificial diffusion, or exploit the dissipative behaviour of a scheme to control oscillations. The disadvantage of these approaches is that they also smear out the desired solution.

In the final case we halved the velocity of the time frame. This has the consequence that it takes twice as long to reach the end-state. We observed that the distribution traverses the domain two times, and that the smearing reduces the distribution to the near constant value of $\sigma = 0.2$.

To reduce the cost of assembly and solving we take a partition of the domain in temporal direction. Consider space-time domain $Q = [\Omega, T]$ with $T = [0, t]$. We take a uniformly distributed sequence of time-instants, $\{0 = t_0, t_1, t_2, \ldots, t_N = t\}$, such that $T = \bigcup_{k=0}[t_k, t_{k+1}]$, and $\Delta t = [t_{k+1} - t_k]$. The domain is now divided into $N-1$ space-time *slabs*. The system can be assembled- and solved in a sequence, one slab at a time. The initial condition of a new slab equals the outflow solution of the previous slab, which gives C^0 continuity in-between slabs. Alternatively, a discontinuous-galerkin method can be used to enforce continuity over slabs.

Example 4.5 (Circular Transport using Space-Time Slabs)**.**
Consider the circular transport problem on a periodic domain introduced in Problem 4.2. We let $T = [0, \pi]$, i.e. 1 period, and divide Q in $N = 8$ space-time slabs $\Delta Q = \Omega \times \Delta T$ with

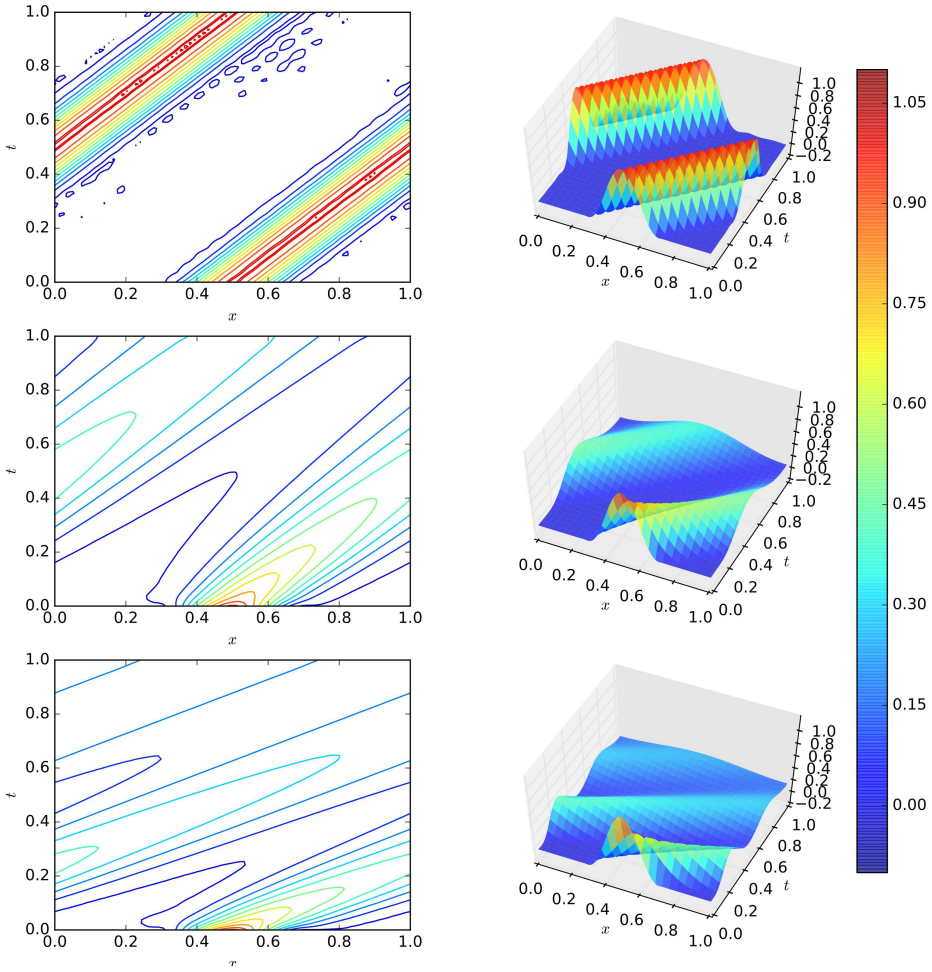

Figure 4.8: Solutions for scalar advection diffusion equation on space-time manifold $Q = \Omega \times [0,1]$ for $n = 24, p = 2$. Three cases were considered. Upper figures correspond to $\{u, c, \epsilon\} = \{1, 1, 0\}$, center figures to $\{u, c, \epsilon\} = \{1, 1, 0.001\}$, and lower figures to $\{u, c, \epsilon\} = \{1, \frac{1}{2}, 0.001\}$. Left column shows iscontours of the distribution as it travels through space-time. The right column shows surface plots. Colors/height indicate the value of the density $\rho^{(0)})_h$.

temporal length $\Delta T = \pi/8$. We obtain the weak formulation of the space-time problem on a slab by multiplying with some test-function $w^{(0)} \in \Lambda_0^{(0)}(\Delta Q)$,

$$\left(w^{(0)}, \mathscr{L}_{\boldsymbol{X}} \rho^{(0)}\right)_{\Delta Q} = 0, \qquad \forall w^{(0)} \in \Lambda_0^{(0)}(\Delta Q),$$

where the boundary condition at $t = t_k$ is enforced strongly at each slab. We define the discrete problem by taking $\Lambda_h^{(0)} = \mathscr{S}^{2,2,2}_{24,24,8} \times \mathscr{S}^2_8$, such that $w_h^{(0)} = \boldsymbol{w}^T \boldsymbol{\phi}^{(0)}$ and $\rho^{(0)} =$

$\boldsymbol{\rho}^T \boldsymbol{\phi}^{(0)}$. We find system of equations,

$$\mathbb{C}^{(0,1)}_{\boldsymbol{X}} \mathbb{E}^{(1,0)} \boldsymbol{\rho} = 0.$$

The system needs to be solved slab-by-slab using the final solution at ΔQ^k as initial solution for ΔQ^{k+1}. Results are shown Figure 4.9a.

The shape and the height of the sinusoid are reasonably well preserved with some error at its outer contour, and some deformation at its lower- and left side. Again, erroneous wiggles are observed over the domain. These wiggles form a circular pattern along the sinusoids pathway. These oscillations generally have a large amplitude at the outer region where the transport velocity is the highest. In the next section we aim to get a better understanding of these oscillations, and try to control them.

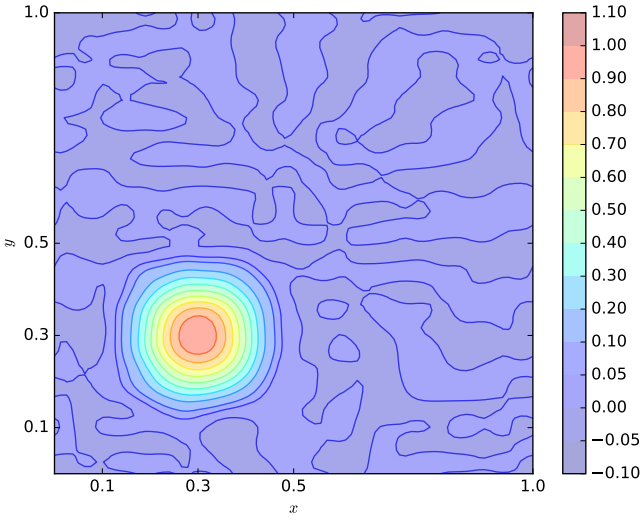

(a) Reconstructed solution, $\rho_h^{(0)}$

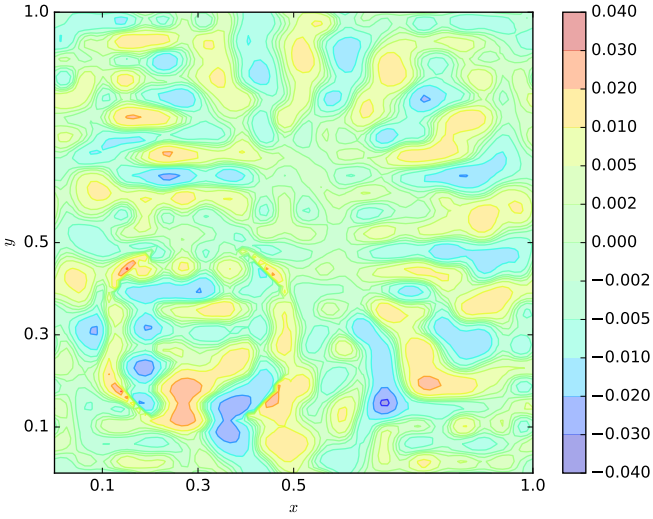

(b) Error, $e_\rho^{(0)}$

Figure 4.9: Contour plots of approximate solution $\rho_h^{(0)}$ and corresponding error $e_\rho^{(0)}$ using a standard Galerkin approach to solve the circular advection problem after one period, $T = \pi$. Spatial × temporal spline spaces $\Lambda_h^{(0)} := \mathscr{P}^{2,2}_{24,24} \times \mathscr{S}^2_8$, number of slabs $k = 8$.

4.4. SUMMARY OF RESULTS

The Lie-derivative $\mathscr{L}_{\boldsymbol{v}}$ describes variations of a k-form along the flow of some vector field $\boldsymbol{v}$. It is related to the exterior derivative d and the interior product $i_{\boldsymbol{v}}$ through Cartan's formula. The interior product $i_{\boldsymbol{v}}$ describes the contraction of some k-form with a vector field $\boldsymbol{v}$, and it is a topological operator. These operators are used to construct a coordinate invariant representation of hyperbolic PDE's.

The vector field $\boldsymbol{v}$ can be related to a 1-form $v^{(1)}$, which can be discretised in the existing framework using nodal- and edge-type B-spline basis functions. This construction introduces Hodge-$\star$ dependencies, inducing error in the discretisation, i.e. the exact structure of the interior product is not conserved. The contraction matrix $\mathbb{C}_{\boldsymbol{v}}$ is the resulting inner product matrix of the interior product. The resulting system consists of a linear combination of incidence, mass, and contraction matrices, $\mathbb{E}$, $\mathbb{M}$, and $\mathbb{C}_{\boldsymbol{v}}$. The discrete solution suffers from spurious oscillations, which grow over time.

5

EULER EQUATIONS

The incompressible Euler equations in fluid dynamics describe balance of mass, momentum, and energy in absence of viscosity and thermal conductivity when variations of density are small, i.e. incompressible fluids. Solutions of these equations describe the pressure, velocity, thermal fields in a region of interest. The incompressible Euler equations have a rich geometric structure, which studied in the classical work by Arnold, [15]. The Euler equations contain various symmetries and invariants. In our discretisation we aim to preserve this structure, and conserve invariants in our simulations.

In section 5.1 we present an coordinate invariant representation of the Euler equations, and discuss various formulations. The discretisation approach is discussed in section 5.2. The spatial discretisation can be constructed, such that the invariants are conserved at the semi-discrete level. The time integrator must be carefully selected to satisfy this conservation at each discrete time level. In section 5.3 we verify our results by running various simulations.

5.1. THE EULER EQUATIONS

The *Euler equations* govern conservation of mass, momentum, and energy under the assumptions of *incompressible* and *inviscid* flow. Solutions of these equations describe the motion of idealised fluids. Under the assumption of incompressible flow, variations in mass density $\rho^{(n)}$ are assumed to be small. For this case the mass and momentum equations can be solved independently from the energy equation. The assumption is generally used to model liquids and subsonic gas flows (i.e. low Mach number flows). Under the assumption of inviscid flow, viscous effects and shear stresses are assumed to be zero. For this case, boundary layers and turbulent effects are neglected. This assumption is used to model convection-dominates flow (i.e. high Reynolds number flows) outside boundary layers.

The conservation of momentum of an incompressible and inviscid fluid flow in $\mathbb{R}^n$ is

given by,

$$\frac{\partial v_j}{\partial t} + v_i \left(\frac{\partial v_j}{\partial x^i} \right) = -\frac{1}{\rho} \frac{\partial p}{\partial x^j} + b_j, \tag{5.1}$$

with v_i the components of the velocity field with $j = \{1, \cdots, n\}$, p the pressure, ρ the mass density, and b_i components of body force. In Appendix I we derive a coordinate invariant form of the Euler equations expressed.

Theorem 5.1 (Euler Equations for Incompressible Flow, (Sec. 4.3c [18]))**.** *The equations for conservation of mass and momentum for an ideal incompressible fluid on manifold $\mathcal{M} \subset \mathbb{R}^n$ are given by,*

$$d^* v^{(1)} = 0 \tag{5.2}$$

$$\frac{\partial v^{(1)}}{\partial t} + \mathcal{L}_{\boldsymbol{v}} v^{(1)} = -d f^{(0)}, \tag{5.3}$$

where $\boldsymbol{v}$ is the velocity-vector field, $v^{(1)}$ the velocity 1-form associated with $\boldsymbol{v}$, and $f^{(0)}$ given by,

$$f^{(0)} = \int \frac{dp}{\rho} - \frac{1}{2} \| v^{(1)} \|^2 + \phi^{(0)},$$

with pressure p, mass density ρ, and potential $\phi^{(0)}$. We can solve for $f^{(0)}$ using the pressure Poisson equation, which can be obtained by taking the codifferetial d^* of Equation I.3, and substitute the incompressibility constraint, Equation I.2,

$$d^* \mathcal{L}_{\boldsymbol{v}} v^{(1)} = -\Delta f^{(0)}. \tag{5.4}$$

An equivalent system of equations can be derived by taking the exterior derivative d of these equations.

Theorem 5.2 (Vorticity Formulation of the Euler Equations)**.** *The equations for conservation of mass and momentum for an ideal incompressible fluid on manifold $\mathcal{M} \subset \mathbb{R}^n$ are given by,*

$$\Delta \psi^{(2)} = \omega^{(2)} \tag{5.5}$$

$$\frac{\partial \omega^{(2)}}{\partial t} + \mathcal{L}_{\boldsymbol{v}} \omega^{(2)} = 0, \tag{5.6}$$

where $\psi^{(2)}$ is the stream function with $d^* \psi^{(2)} = v^{(1)}$, and vorticity $\omega^{(2)} = d v^{(1)}$.

The Euler equations have a Hamiltonian structure, which was studied in the classical work by Vladimir Arnold [15]. The equations govern various symmetries and invariants. In the discrete setting we aim to preserve these structures and conserve the mentioned quantities over time. The Euler equations satisfy conservation of integral *circulation* Γ,

vorticity Ω, and *helicity* H,

$$\frac{d}{dt}\Gamma = \frac{d}{dt}\oint_{\gamma(t)} v^{(1)} = 0, \tag{5.7}$$

$$\frac{d}{dt}\Omega = \frac{d}{dt}\int_{A(t)} \omega^{(2)} = 0, \tag{5.8}$$

$$\frac{d}{dt}H = \frac{d}{dt}\int_{V(t)} h^{(3)} = 0, \tag{5.9}$$

where $h^{(3)} = v^{(1)} \wedge \omega^{(2)}$ is the helicity 3-form. Formal derivation of these results is given in Appendix I. Note that conservation of circulation and vorticity express an equal result, one can derive one from another by applying the generalised Stokes' theorem, Equation 2.13. Helicity is not the only quadratic invariant conserved by the Euler equations. The equations also govern conservation of *kinetic-energy* K,

$$\frac{d}{dt}K = \frac{d}{dt}\frac{1}{2}\left(v^{(1)}, v^{(1)}\right)_{V(t)} = 0, \tag{5.10}$$

and in $\mathbb{R}^2$ the conservation of *enstrophy* S,

$$\frac{d}{dt}S = \frac{d}{dt}\frac{1}{2}\left(\omega^{(2)}, \omega^{(2)}\right)_{V(t)} = 0. \tag{5.11}$$

Proof of these relations is given in Appendix I.

The exact part of the Lie derivative, i.e. $d i_{\boldsymbol{v}} v^{(1)}$, can be included in the right-hand-side term to minimize the amount of terms that need to be discretised. We define the *energy head* ,

$$g^{(0)} := f^{(0)} + i_{\boldsymbol{v}} v^{(1)}, \tag{5.12}$$

such that the momentum equation, Equation I.3, can be written as,

$$\frac{\partial v^{(1)}}{\partial t} + i_{\boldsymbol{v}} d v^{(1)} = -d g^{(0)}, \tag{5.13}$$

which is known as Gromeka-Lamb's formulation (sec. 4.4.10. [37]).

We can obtain dual formulations of the Euler equations by applying the Hodge $\star$-operator, and substituting the adjoint co-differential d^* and co-Lie-derivative $\mathscr{L}^*_{\boldsymbol{v}}$, which have been introduced in section 2.4 and section 4.1. In order to avoid confusion with $v^{(1)}$ in $\mathbb{R}^2$ we denote $q^{(1)} = i_{\boldsymbol{v}}\text{vol}^{(n)}$ as the $(n-1)$-form associated with the velocity vector field $\boldsymbol{v}$.

Theorem 5.3 (Dual Formulations of the Euler equations)**.** *The dual equations for the conservation of mass and momentum for an ideal incompressible fluid on manifold* $\mathcal{M} \subset \mathbb{R}^n$ *are given by,*

$$d q^{(n-1)} = 0 \tag{5.14}$$

$$\frac{\partial q^{(n-1)}}{\partial t} - i^*_{\boldsymbol{v}} \omega^{(n-2)} = d^* g^{(n)}, \tag{5.15}$$

where $\boldsymbol{v}$ is the velocity-vector field, $q^{(n-1)} = \star v^{(1)}$ the forms associated with $\boldsymbol{v}$, $\omega^{(n-2)} = (-1)^{n-1} d^* q^{(n-1)}$ is the dual vorticity form, and $g^{(n)} = \star g^{(0)}$ the energy head, Equation 5.12. The dual pressure Poisson equation is given by,

$$-d i^*_{\boldsymbol{v}} \omega^{(n-2)} = \Delta g^{(n)}. \tag{5.16}$$

The stream function is given by $\psi^{(n-2)}$, such that $d\psi^{(n-2)} = q^{(n-1)}$. The dual vorticity formulation is given by,

$$(-1)^{n-1} \Delta \psi^{(n-2)} = \omega^{(n-2)} \tag{5.17}$$

$$\frac{\partial \omega^{(n-2)}}{\partial t} - d^* i^*_{\boldsymbol{v}} \omega^{(n-2)} = 0. \tag{5.18}$$

Note that $d^* i^*_{\boldsymbol{v}} \omega^{(n-2)} = i^*_{\boldsymbol{\omega}} \star q^{(1)}$.

In the continuous setting primal and dual formulation are equivalent. In the discrete setting, however, as we have learned in the previous chapters, the choice of formulation has an impact on the conservative properties. The exactness of the exterior derivative d can be conserved. The primal formulation enables exactness of the vorticity constraint $dd v^{(1)} = d\omega^{(2)} = 0$ in the discrete setting, whereas the dual formulation enables exactness of the incompressibility constraint $dd\psi^{(n-2)} = dq^{(n-1)} = 0$.

Note that the equations introduced need to be solved in pairs in order to solve for all unknowns. The pressure Poisson equation, Equation 5.16, needs to be solved together with the momentum equations, Equation 5.15, to solve for unknowns $q^{(1)}$ and $g^{(n)}$. Similarly the stream function Poisson equation, Equation 5.17, needs to be solved with the vorticity equation, Equation 5.18, to solve for unknowns $\omega^{(n-2)}$ and $\psi^{(n-2)}$. We will refer to these as the *momentum-pressure* equations, and the *vorticity-stream* equations.

5.2. DISCRETISATION OF THE EULER EQUATIONS

Exactness of conservation of mass, i.e. the incompressibility constraint, is required in the discrete setting in order to satisfy conservation of some other quantities as we will show later on. This motivates us to discretise the dual formulations, where the incompressibility is governed by the exterior derivative d, rather than the codifferential d^*. In this section we will derive discretisations of the momentum and vorticity formulation. The semi-discrete system conserves integral mass, vorticity, kinetic energy and enstrophy (proof in Appendix J). The time discretisation technique must carefully be selected to conserve these quantities over time.

Definition 5.1 (discretisation of the Momentum-Pressure Formulation)**.** Consider the periodic unit square domain, $\Omega =]0,1[^2$. We obtain a weak-formulation of the pressure Poisson equation and the velocity equation, Equation 5.16 and Equation 5.15, by taking the inner product with test functions $r^{(2)} \in \Lambda^{(2)}_0(\Omega)$ and $s^{(1)} \in \Lambda^{(1)}_0(\Omega)$,

$$\begin{cases} \left(r^{(2)}, d i^*_{\boldsymbol{\omega}} \star q^{(1)}\right)_\Omega & = \left(r^{(2)}, dd^* g^{(2)}\right)_\Omega, \\ \left(s^{(1)}, \partial_t q^{(1)}\right)_\Omega - \left(s^{(1)}, i^*_{\boldsymbol{\omega}} \star q^{(1)}\right)_\Omega & = \left(ds^{(1)}, g^{(2)}\right)_\Omega \end{cases}.$$

Note that the pressure-Poisson equations needs to be solved by taking a system of first order equations as was done for the 2-form Poisson equation, Example 3.5. We define the discrete solution by taking,

$$\begin{aligned} r_h^{(2)} &= \boldsymbol{r}^T \boldsymbol{\phi}^{(2)}, & s_h^{(1)} &= \boldsymbol{s}^T \boldsymbol{\phi}^{(1)}, \\ g_h^{(2)} &= \boldsymbol{g}^T \boldsymbol{\phi}^{(2)}, & q_h^{(1)} &= \boldsymbol{q}^T \boldsymbol{\phi}^{(1)}, \end{aligned}$$

which leads to the non-linear time-dependent system of equations,

$$\begin{bmatrix} -\mathbb{M}^{(1,1)} & \left(\mathbb{E}^{(2,1)}\right)^T \mathbb{M}^{(2,2)} \\ \mathbb{E}^{(2,1)} & \varnothing \end{bmatrix} \begin{bmatrix} \boldsymbol{h} \\ \boldsymbol{g} \end{bmatrix} = \begin{bmatrix} \mathbf{0} \\ -\mathbb{E}^{(2,1)} \left(\mathbb{M}^{(1,1)}\right)^{-1} \mathbb{C}^{(1,1)}_{\boldsymbol{\omega}_h} \boldsymbol{q} \end{bmatrix} \tag{5.19}$$

$$\mathbb{M}^{(1,1)} \frac{\partial \boldsymbol{q}}{\partial t} - \mathbb{C}^{(1,1)}_{\boldsymbol{\omega}_h} \boldsymbol{q} = \left(\mathbb{E}^{(2,1)}\right)^T \mathbb{M}^{(2,2)} \boldsymbol{g}. \tag{5.20}$$

The semi-discrete system of non-linear equations satisfies conservation of mass, vorticity, kinetic energy, and enstrophy. Proof is presented in Appendix J. However, not every time discretisation preserves the invariance of these quantities over time. Numerical schemes that preserve structures of Hamiltonian systems are *symplectic integrators* and *energy-conserving integrators*. Palha and Gerritsma studied and derived these integrators for Hamiltonian ODE systems from a structure-preserving discretisation framework, [38]. The simplest of these methods is the *implicit midpoint method*.

Definition 5.2 (Implicit Midpoint Method)**.** Given time-dependent system of non-linear equations,

$$\begin{cases} \frac{d\boldsymbol{y}(t)}{dt} = \mathbb{A}(\boldsymbol{y})\boldsymbol{y}(t) \\ \text{with,} \quad \boldsymbol{y}(t_k) = \boldsymbol{y}_k, \end{cases} \tag{5.21}$$

where $\boldsymbol{y}_k$ denotes the solution at time-instant t_k. The implicit midpoint method is given by,

$$\frac{\boldsymbol{y}_{k+1} - \boldsymbol{y}_k}{\Delta t} = \mathbb{A}(\tilde{\boldsymbol{y}})\tilde{\boldsymbol{y}}, \tag{5.22}$$

with $\tilde{\boldsymbol{y}} = \frac{1}{2}\left(\boldsymbol{y}_{k+1} + \boldsymbol{y}_k\right)$, and time-step $\Delta t = t_{k+1} - t_k$. The implicit midpoint method is second order accurate in time.

Application of the implicit midpoint method to the discrete momentum equation, Equation J.2, yields the system of non-linear equations,

$$\mathbb{M}^{(1,1)} \frac{\boldsymbol{q}_{k+1} - \boldsymbol{q}_k}{\Delta t} - \frac{1}{2}\mathbb{C}^{(1,1)}_{\tilde{\boldsymbol{\omega}}_h}\left(\boldsymbol{q}_{k+1} + \boldsymbol{q}_k\right) = \frac{1}{2}\left(\mathbb{E}^{(2,1)}\right)^T \mathbb{M}^{(2,2)}\left(\boldsymbol{g}_{k+1} + \boldsymbol{g}_k\right). \tag{5.23}$$

We define the following algorithm,

1. **Initialise:**
   Given solution $\boldsymbol{q}_k$, $\boldsymbol{\omega}_k$, $\boldsymbol{g}_k$ at time level t_k. Let initially $\tilde{\boldsymbol{\omega}} := \boldsymbol{\omega}_k$.

2. **Iterate:**
   Assemble contraction matrix $\mathbb{C}^{(1,1)}_{\tilde{\boldsymbol{\omega}}_h}$. Simultaneously solve the discrete momentum equation and the pressure-Poisson equation, Equation 5.23 and Equation J.1, to obtain solutions q_{k+1} and g_{k+1}. Evaluate $\boldsymbol{\omega}_{k+1}$, let $\tilde{\boldsymbol{\omega}} := \frac{1}{2}(\boldsymbol{\omega}_{k+1} + \boldsymbol{\omega}_k)$. Iterate this step until set convergence criterion is met.

Conservation of mass depends on pairing of $\mathbb{C}^{(1,1)}_{\tilde{\boldsymbol{\omega}}_h}\boldsymbol{q}$ and $\boldsymbol{g}$, which can be achieved by simultaneously solving for q_{k+1} and g_{k+1}. Conservation of integral vorticity is independent of the choice on time-integrator. It depends on the exactness of the exterior derivative, which, by construction, is satisfied by $\mathbb{E}^{(1,0)}$. Conservation of kinetic energy and enstrophy are preserved using the implicit midpoint method (can be checked using the relations in Appendix J). However, enstrophy conservation depends on correct matching of $\tilde{\boldsymbol{\omega}}$ and $\tilde{\boldsymbol{q}}$, which requires convergence of the linearisation technique. We let our convergence criterion depend on the enstrophy error, i.e. we iterate until

$$\frac{S_h(t_{k+1}) - S_h(t_0)}{S_h(t_0)} \leq \tau, \tag{5.24}$$

where τ is the desired tolerance, e.g. $\tau = 10^{-6}$, and S_h the discrete enstrophy,

$$S_h = \boldsymbol{\omega}^T \left(\mathbb{E}^{(1,0)}\right)^T \mathbb{M}^{(1,1)} \boldsymbol{q}. \tag{5.25}$$

Definition 5.3 (discretisation of the Vorticity-Stream Formulation)**.** Consider the periodic unit-square domain, $\Omega =]0,1[^2$. We obtain weak-formulations of the stream-function Poisson equation and the vorticity equation, Equation 5.17 and Equation 5.18, by taking the inner product with test functions $r^{(0)}, s^{(0)} \in \Lambda^{(0)}_0(\Omega)$,

$$\begin{cases} -\left(dr^{(0)}, d\psi^{(0)}\right)_\Omega & = \left(r^{(0)}, \omega^{(0)}\right)_\Omega \\ \left(s^{(0)}, \partial_t \omega^{(0)}\right)_\Omega - \left(i_{\boldsymbol{v}} ds^{(0)}, \omega^{(0)}\right)_\Omega & = 0 \end{cases} \tag{5.26}$$

We define the discrete solution by taking,

$$\begin{aligned} r^{(0)}_h &= \boldsymbol{r}^T \boldsymbol{\phi}^{(0)}, & s^{(0)}_h &= \boldsymbol{s}^T \boldsymbol{\phi}^{(0)}, \\ \psi^{(0)}_h &= \boldsymbol{\psi}^T \boldsymbol{\phi}^{(0)}, & \omega^{(0)}_h &= \boldsymbol{\omega}^T \boldsymbol{\phi}^{(0)}, \end{aligned}$$

which leads to the non-linear time-dependent system of equations,

$$\mathbb{M}^{(0,0)} \boldsymbol{\omega} + \left(\mathbb{E}^{(1,0)}\right)^T \mathbb{M}^{(1,1)} \mathbb{E}^{(1,0)} \boldsymbol{\psi} = \boldsymbol{0} \tag{5.27}$$

$$\mathbb{M}^{(0,0)} \frac{\partial \boldsymbol{\omega}}{\partial t} - \left(\mathbb{C}^{(0,1)}_{\boldsymbol{v}_h} \mathbb{E}^{(1,0)}\right)^T \boldsymbol{\omega} = \boldsymbol{0} \tag{5.28}$$

We will prove that the discrete equations satisfy the relevant conservation laws that we derived in the previous section, section 5.1.

Application of the implicit midpoint method to the discrete vorticity equation, Equation J.5, yields the system of non-linear equations,

$$\mathbb{M}^{(0,0)} \frac{\boldsymbol{\omega}_{k+1} - \boldsymbol{\omega}_k}{\Delta t} - \frac{1}{2} \left(\mathbb{C}^{(0,1)}_{\tilde{\boldsymbol{v}}_h} \mathbb{E}^{(1,0)} \right)^T (\boldsymbol{\omega}_{k+1} + \boldsymbol{\omega}_k) = \mathbf{0}. \tag{5.29}$$

We define the following algorithm.

1. **Initialise:**
   Given solution $\boldsymbol{q}_k$, $\boldsymbol{\omega}_k$, $\boldsymbol{g}_k$ at time level t_k. Let initially $\tilde{\boldsymbol{q}} := \boldsymbol{q}_k$.

2. **Iterate:**
   Assemble contraction matrix $\mathbb{C}^{(0,1)}_{\tilde{\boldsymbol{v}}_h}$. Solve the discrete vorticity equation, Equation 5.29, to obtain $\boldsymbol{\omega}_{k+1}$. Then solve the discrete stream-function Poisson equation, Equation 5.27, to obtain solution stream-function $\boldsymbol{\psi}_{k+1}$. Evaluate $\boldsymbol{q}_{k+1}$, and let $\tilde{\boldsymbol{q}} := \frac{1}{2}(\boldsymbol{q}_{k+1} + \boldsymbol{q}_k)$. Iterate this step until set convergence criterion is met.

The advantage of this formulation is that conservation of mass is satisfied by construction of the stream-function. Therefore, it is not required to solve the vorticity- and Poisson equations simultaneously. Again, conservation of integral vorticity is independent on the choice of time integrator. Conservation of kinetic-energy and enstrophy are preserved using the implicit midpoint method. However, conservation of kinetic-energy depends on the non-linear solution, and requires convergence of the linearisations technique. We let the convergence criterion depend on the kinetic-energy error, i.e. we set,

$$\frac{K_h(t_{k+1}) - K_h(t_0)}{K_h(t_0)} \leq \tau, \tag{5.30}$$

where τ is the desired tolerance, and K_h the discrete kinetic-energy,

$$K_h = \boldsymbol{\psi}^T \mathbb{M}^{(0,0)} \boldsymbol{\omega}. \tag{5.31}$$

It was shown by Palha and Gerritsma that the non-linear systems ,Equation 5.23 and Equation 5.29, can be combined into two systems of quasi-linear equations which can be solved staggered at time [17]. This approach combines the mass, vorticity, and enstrophy conserving properties of the vorticity formulation with the vorticity, and kinetic-energy conserving properties of the momentum formulation, and conserves all quantities without costly iterative techniques. In the next section we validate our results by introducing some test problems.

5.3. RESULTS, AND ANALYSIS

The problem of two co-rotating *Taylor vortices* was introduced by Mullen et al. to analyze the performance of structure-preserving discretisations. Two equipotent vortices will split apart above some critical distance. Non-conserving methods fail to reproduce this behaviour after which the vortices merge together into one big vortex, [33]. We will look at the problem of

Example 5.1 (Taylor Vortices)**.** Consider the Euler equations on $\Omega =]0,1[^2$. As initial condition we consider a distribution of $N = 2$ Taylor vortices of equal strength, which induce vorticity,

$$\omega(\boldsymbol{x}) = \sum_{i=1}^{2} \frac{U\sigma_i}{a}\left(2 - \frac{(\boldsymbol{r}-\boldsymbol{r_i})^2}{a^2}\right)\exp\frac{1}{2}\left(1 - \frac{(\boldsymbol{r}(\boldsymbol{x})-\boldsymbol{r}_i)^2}{a^2}\right), \tag{5.32}$$

where $U = 1$ is the maximal tangential velocity, $a = 0.075$ the vortex strength, $\sigma_i = \pm 1$, the direction of rotation (positive for counter-clockwise), and $(\boldsymbol{r}(\boldsymbol{x}) - \boldsymbol{r}_i)^2$ the squared distance to the i-th core. We place initial cores near the center of the domain, $(x_i, y_i) = \{(0.4, 0.5), (0.6, 0.5)\}$, Equation 5.32. The cores will start to circle around the center. The vortices deform in a stretching motion, which causes a tail to be formed at each vortex. The cores briefly touch, but the cores have gained too much momentum to merge. Instead they drift apart. Note that stabilized numerical techniques would induce momentum loss, which could fail in capturing this behaviour.

We considered two configurations to show that the conservative properties are independent of discretisation parameters. In the first configuration we used a spline basis of polynomial order $p = 1$ with dimension $n = 48$, and used a time-step $\Delta t = 1/16$. In the second configuration we let $p = 2$ and $n = 64$, and let $\Delta t = 1/32$. The solutions at $t = 1.5$ are shown in Figure 5.1. Both configurations were able to capture the non-merging motion. The resulting distributions are roughly the same. However, the cores corresponding to the first configuration are less compact. We also observe more local extrema in the centre region and in the tail regions. Finally, there is a difference in the core locations.

The vortex-stream formulation governs static conservation of mass, and dynamic conservation of vorticity, kinetic energy, and enstrophy. We compare the dynamically conserved quantities to their initial value, whereas the static quantity is evaluated at each instant. Results of both configurations are shown in Figure 5.1. Both configurations conserve enstrophy, vorticity, and mass with great precision. Kinetic energy is bounded with relative error less than 1 percent. The quadratic quantities, i.e. kinetic energy and enstrophy, are better conserved by the second configuration.

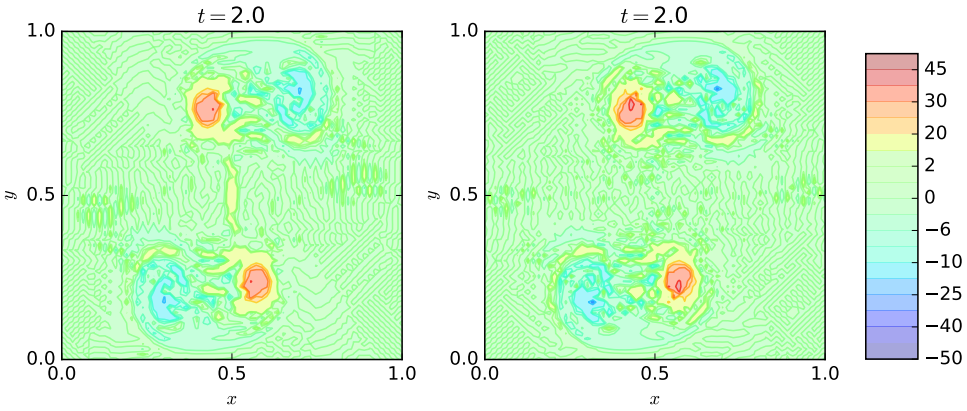

Figure 5.1: Vorticity $\omega^{(0)}$ at $t = 1.5$ of Taylor vortices on a periodic domain. Spline basis $n = 48$, $p = 1$, and time-step $\Delta t = 1/32$ (left), and $n = 64$, $p = 2$, $\Delta t = 1/64$ (right).

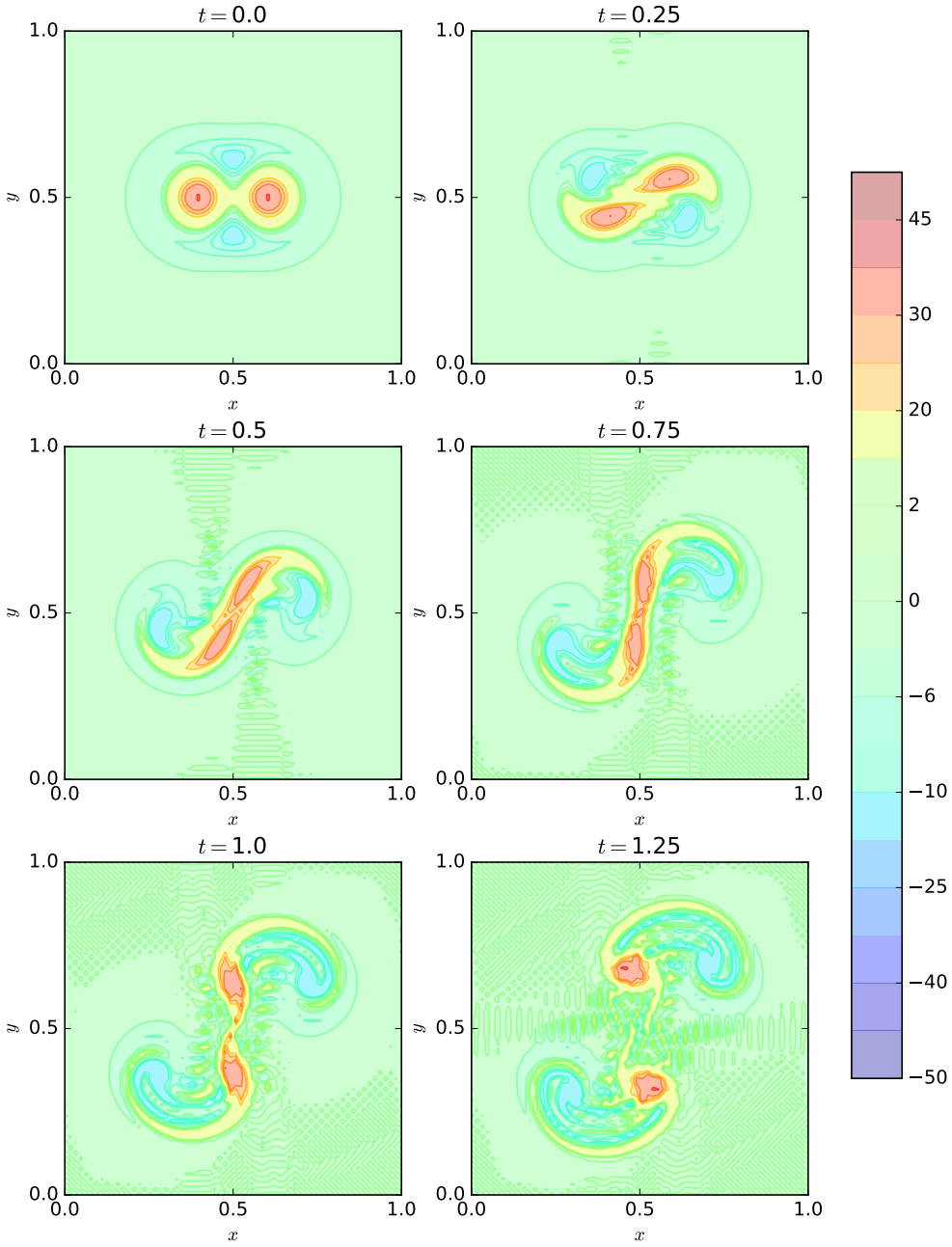

Figure 5.2: Vorticity $\omega^{(0)}$ at various time-instants of simulated motion of an initial distribution of co-rotating Taylor vortices on a periodic domain. Results were obtained using spline basis of polynomial order $p = 2$ and dimension $n = 64$, and time-step size $\Delta t = 1/64$.

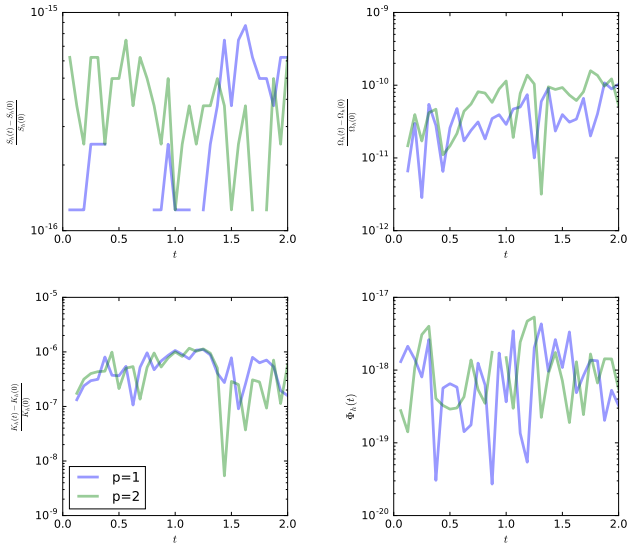

Figure 5.3: Enstrophy error (upper left), vorticity error (upper right), kinetic energy error (lower left), and total mass flux (lower right) over time for the co-rotating Taylor vortices on a periodic domain. Spline basis $n = 48$, $p = 1$, and time-step $\Delta t = 1/32$ (blue), and $n = 64$, $p = 2$, $\Delta t = 1/16$ (green).

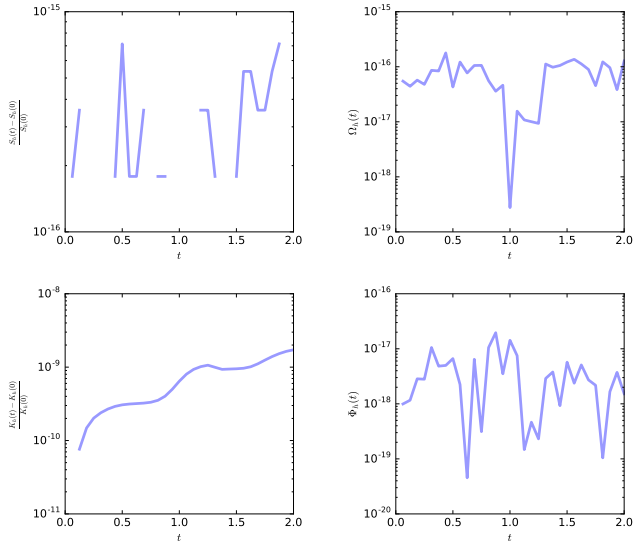

Figure 5.4: Enstrophy error error (upper left), vorticity (upper right), kinetic energy error (lower left), and total mass flux (lower right) over time for the counter-rotating Taylor vortices on a semi-periodic domain. Spline basis $n = 64$, $p = 2$, and time-step $\Delta t = 1/16$ were used.

Example 5.2 (Solid Wall Boundary)**.** So far we have only considered periodic domains. In this example we introduce solid wall boundaries. Consider cylindrical domain $\Omega =]0,1[\times[0,1]$, which is periodic in x and non-periodic in y. Boundaries $\partial\Omega = \{(x,y) \in \Omega,\ y \in \{0,1\}\}$ are impenetrable walls, which requires normal velocity components to be equal to zero, i.e. $q_x^{(1)} = -v\,dx = 0$ at $\partial\Omega$.

The weak formulation of the vorticity-stream formulation including boundary terms is given by,

$$\begin{cases} -\left(dr^{(0)}, d\psi^{(0)}\right)_\Omega + \left(r^{(0)}, d\psi^{(0)}\right)_{\partial\Omega} & = \left(r^{(0)}, \omega^{(0)}\right)_\Omega \\ \left(s^{(0)}, \partial_t \omega^{(0)}\right)_\Omega - \left(i_{\boldsymbol{v}} ds^{(0)}, \omega^{(0)}\right)_\Omega + \left(s^{(0)}, i_{\boldsymbol{v}}^* \omega^{(0)}\right)_{\partial\Omega} & = 0 \end{cases}$$

The boundary terms that appear in the stream function Poisson equation can be used to satisfy tangential flow conditions. The bounder terms in the vorticity equation can be used to describe the in- and outflow of vorticity. In the case of the mentioned solid-wall boundary conditions, evaluation of these natural boundary conditions yields,

$$\left(r^{(0)}, d\psi^{(0)}\right)_{\partial\Omega} = \int_{\partial\Omega} r^{(0)} \wedge \star\, d\psi^{(0)} = \cancel{\int_{\partial\Omega} r \frac{\partial\psi}{\partial x} dy} - \int_{\partial\Omega} r \frac{\partial\psi}{\partial y} dx$$

$$\left(s^{(0)}, i_{\boldsymbol{v}}^* \omega^{(0)}\right)_{\partial\Omega} = \int_{\partial\Omega} s^{(0)} \wedge \star\, i_{\boldsymbol{v}}^* \omega^{(0)} = -\cancel{\int_{\partial\Omega} s\omega u\, dy} + \cancel{\int_{\partial\Omega} s\omega v\, dx}$$

In- and outflow boundary conditions are essential boundary conditions. The impenetrable wall condition corresponds to zero inflow. It follows that the stream function ψ needs to be constant at the boundaries,

$$\left.\frac{\partial\psi}{\partial x}\right|_{\partial\Omega} = q_x^{(1)}(\partial\Omega) = 0$$
$$\Rightarrow \psi(\partial\Omega) = C,$$

where we take $C = 0$. As an initial condition we consider a distribution of two counter-rotating Taylor vortices, i.e. $\sigma_i = \{+1, -1\}$ with cores locations, $(x_i, y_i) = \{(0.4, 0.75), (0.6, 0.75)\}$. Other parameters are taken as introduced in Equation 5.32. To discretise the system we take a spline basis with $p = 2$ and $n = 64$, and let time-step $\Delta t = 1/32$. Results are shown in Figure 5.5.

The counter-rotating cores induce an upward velocity, which transports the cores to the upper wall. Note that the outer regions of the vortices are rotating in opposite direction, which induces a downward velocity transporting the outer regions to the lower wall. Near the wall the cores start travelling parallel to the wall in opposite direction until they meet again, where they induce a downward velocity which transports the cores downward. Note that the solid wall acts as a counter-rotating core.

The integral quantities kinetic energy, vorticity, enstrophy, and mass flux were measured over time, Figure 5.4. Again we observe that enstrophy, vorticity and mass flux are conserved with machine precision.

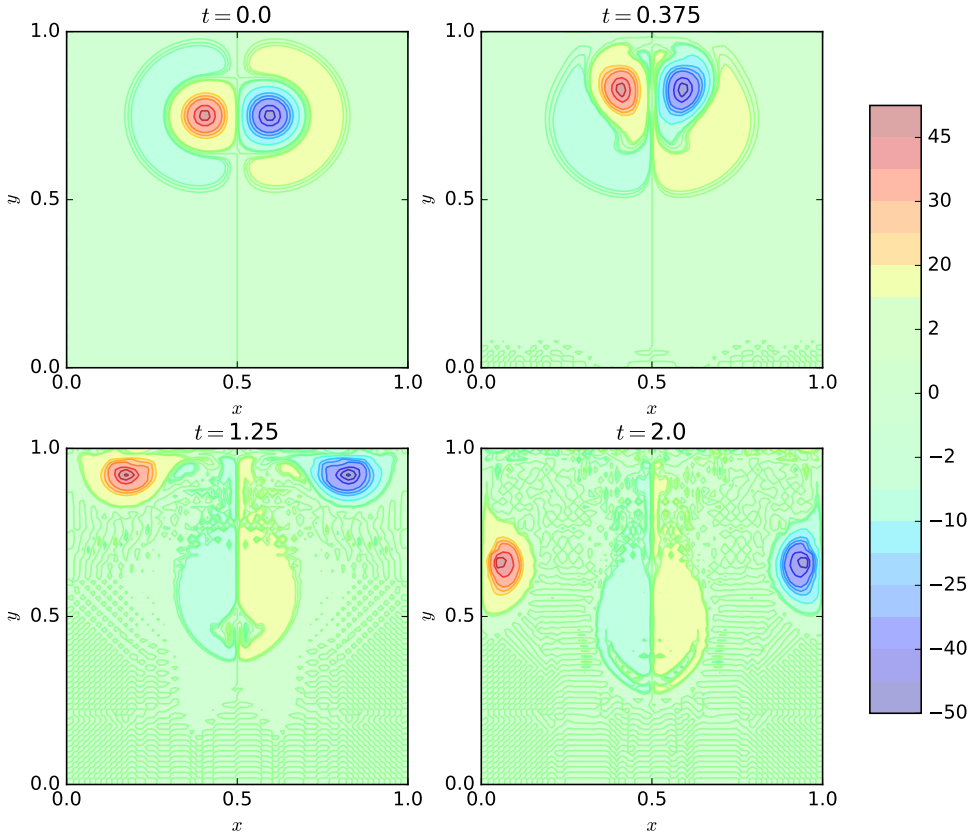

Figure 5.5: Vorticity $\omega^{(0)}$ at various time-instants of simulated motion of an initial distribution of counter-rotating Taylor vortices on a semi-periodic domain with upper- and lower solid wall boundaries.

5.4. SUMMARY OF RESULTS

The incompressible Euler govern conservation of mass, and momentum. The equations have a rich geometric structure, governing various symmetries and invariants. In $\mathbb{R}^2$ the integral quantities mass, vorticity, kinetic-energy, and enstrophy are conserved over time. The equivalent vorticity formulation can be derived by taking the exterior derivative of the momentum equations. The dual formulation must be taken, such that the equation for the conservation of mass depends on the exterior derivative, which can be satisfied without error in the discrete setting.

Conservation of the integral quantities hinges on the exactness of the exterior derivative d and the interior product $i_{\boldsymbol{v}}$. The introduced framework ensures that this structure is preserved in the semi-discrete system of equations. A symplectic or energy conserving time integrator must be chosen to conserve the integral quantities over time.

6

CONCLUSION & FUTURE DIRECTIONS

This thesis is the result of a research project on discretisation techniques for CFD. The project was divided in three objectives. The first objective was to study the existing existing structure-preserving IGA framework for elliptic PDE's. The second objective was to expand this theoretical framework to discretise hyperbolic PDE's, and the third objective was to construct a structure-preserving IGA discretisation for the incompressible Euler equations, chapter 5.

Recently, some attention has been focused on structure-preserving discretisation techniques within the scientific community. In these techniques special care is taken in the preservation of fundamental mathematical structures, symmetries, and invariants in the discretisation process. Exterior calculus proves to be insightful in identifying relevant topological dependencies. In exterior calculus we describe elliptic PDE's with the topological derivative operator d and the metric dual Hodge-$\star$ operator. Conservation of the important topological structure of the derivative operator d lies at the heart of the structure-preserving framework. The framework is of theoretical relevance. It explains the correctness of using dual grids in finite-volume methods, and allows derivation of inf-sub stable basis functions in finite-element methods.

The extension to hyperbolic PDE's is not trivial. A superior theory to discretise the convective terms and the vector fields is unavailable at this moment. However, by carefully selecting the geometric formulation of the PDE, it is possible to conserve the nilpotency property of the interior product. This proved to be the key ingredient in the construction of an energy-conserving discretisation for the incompressible Euler equations in $\mathbb{R}^2$. These discrete Euler equations behave as the continuous Euler equations when the mesh has sufficient resolution to represent relevant vortical structures, and when spurious oscillations are within bounds. It needs to be verified if this construction is valid for arbitrary geometries.

The next step is to develop a structure-preserving discretisation for the incompressible Euler equations in $\mathbb{R}^3$. It will be challenging to conserve integral helicity. Another

step might be the discretisation of the compressible Euler equations, for which there exists a wide range of formulations and discretisaions. I wonder if it is possible to identify an optimal formulation, or some fundamental construction, that needs to be satisfied at the discrete level. These directions will improve our understanding of discretisations and improve accuracy of simulations.

A

DeRham Cohomology

The *DeRham* sequence has important topological relations that governs existence of differential forms on manifolds. In *cohomology* we reduce these relations to topological structures, i.e. *chains* and *cochains*. In section 2.3 we have shown that the *codifferential* δ is the topological analogue of the exterior derivative d. In this chapter we introduce the structures corresponding to the exterior derivative d, the coboundary operator δ, and the codifferential d^*. We will present the Poincaré lemma and the Hodge decomposition.

Definition A.1 (Closed Forms, (Sec. 5.2 [18]))**.**
A k-form $\alpha^{(k)}$ is *closed* if $d\alpha^{(k)} = 0$. The space of closed k-forms $\mathcal{Z}_d\Lambda^{(k)}$ is the kernel of the exterior derivative, i.e.

$$\mathcal{Z}_d\Lambda^{(k)} := \{\alpha^{(k)} \in \Lambda^{(k)} : d\alpha^{(k)} = 0\} \subset \Lambda^{(k)}.$$

Definition A.2 (Exact Forms, (Sec. 5.2 [18]))**.**
A k form $\alpha^{(k)}$ is *exact* if there exists a $\beta^{(k-1)}$ s.t. $\alpha^{(k)} = d\beta^{(k-1)}$. The space of exact k-forms $\mathcal{B}_d\Lambda^{(k-1)}$ is the range of the exterior derivative, i.e.

$$\mathcal{B}_d\Lambda^{(k-1)} := d\Lambda^{(k-1)} \subset \Lambda^{(k)}.$$

It follows that every exact form is closed, i.e. if,

$$\beta^{(k-1)} \text{ s.t. } \alpha^{(k)} = d\beta^{(k-1)} \text{ then } d\alpha^{(k)} = dd\beta^{(k-1)} = 0.$$

The topological structure is depicted in Figure A.1. The converse is true on *contractible manifolds*. Contractible spaces can be continuously reduced to a point. Examples include any (star) domain in Euclidean space.

Theorem A.1 (Poincaré Lemma, (Sec. 5.4 [18]))**.**
On a contractible manifold $\mathcal{M}$ every closed k-form is exact, i.e.

$$\forall\, \alpha^{(k)} \in \mathcal{Z}_d\Lambda^{(k)}(\mathcal{M}), \text{ there exists } \beta^{(k-1)} \in \Lambda^{(k-1)}(\mathcal{M}) \text{ s.t. } \alpha^{(k)} = d\beta^{(k-1)}.$$

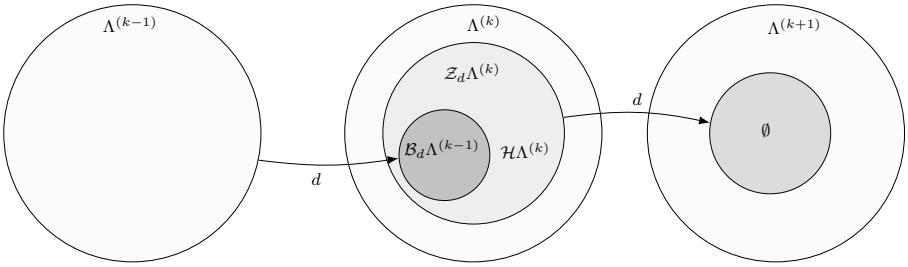

Figure A.1: Poincaré Lemma, The range of the exterior derivative $\mathscr{B}_d\Lambda^{(k-1)}$ is contained in the kernel $\mathscr{Z}_d\Lambda^{(k)}$. On contractible domains the converse is also true, for which then $\mathscr{B}_d\Lambda^{(k-1)} = \mathscr{Z}_d\Lambda^{(k)}$.

The theorem proofs existence of solutions for balancing relations is physics. These relations, often of the form $\text{grad}(\phi) = f$, $\text{curl}(\vec{\omega}) = \vec{g}$, and $\text{div}(\vec{v}) = h$, are fundamental in physics. From the theorem it also follows that for any volume form $\alpha^{(n)}$, there exist a potential function. Since $d\Lambda^{(n)} = 0$, we have that $\Lambda^{(n)} = \mathscr{Z}_d\Lambda^{(n)}$, hence

$$\forall \alpha^{(n)} \in \Lambda^{(n)} = \mathscr{Z}_d\Lambda^{(n)}, \exists \beta^{(n-1)} \in \mathscr{B}_d\Lambda^{(k-1)} \text{ s.t. } d\beta^{(n-1)} = \alpha^{(n)}. \tag{A.1}$$

Thus the exterior derivative acting on $\Lambda^{(n-1)}$ is surjective on contractible domains (surjectivity of the $\nabla\cdot$ operator). Note that this is only true if and only if the boundary conditions satisfy the compatibility condition. Finally, the theorem implies that the kernel of $\Lambda^{(k)}$ is equal to $d\Lambda^{(k-1)}$ on contractible manifolds, i.e. $\mathscr{B}_d\Lambda^{(k-1)} = \mathscr{Z}_d\Lambda^{(k)}$. Hence we can decompose the space of k-forms $\Lambda^{(k)}$ into

$$\Lambda^{(k)}(\mathscr{M}) = \mathscr{Z}_d\Lambda^{(k)} \oplus \mathscr{Z}_d^C\Lambda^{(k)}, \tag{A.2}$$

where $\mathscr{Z}_d^C$ denotes the complement of $\mathscr{Z}_d\Lambda^{(k)}$ in $\Lambda^{(k)}$. On non-contractible domains we can define the space of k-forms which are closed but not exact. We call such forms Harmonic forms.

Definition A.3 (Harmonic forms, (Sec. 14.2 [18]))**.** The space of harmonic k-forms $\mathscr{H}\Lambda^{(k)}$ is defines as

$$\mathscr{H}\Lambda^{(k)} := \{\alpha^{(k)} \in \mathscr{Z}_d\Lambda^{(k)} : \alpha^{(k)} \notin \mathscr{B}_d\Lambda^{(k-1)}\}.$$

On contractible domains $\mathscr{H}\Lambda^{(k)} = \emptyset$. The space of closed k-forms can be written as the sum of exact k-forms united with the space of harmonic k-forms,

$$\mathscr{Z}_d\Lambda^{(k)} = \mathscr{B}_d\Lambda^{(k-1)} \oplus \mathscr{H}\Lambda^{(k)}.$$

If we combine this expression with Equation A.2 we obtain,

$$\Lambda^{(k)}(\mathscr{M}) = \mathscr{B}_d\Lambda^{(k-1)} \oplus \mathscr{H}\Lambda^{(k)} \oplus \mathscr{Z}_d^{\mathscr{C}}\Lambda^{(k)}.$$

This result is known as the *Hodge decomposition.* The Hodge decomposition enables us to decompose differential forms in algebraic complements.

Definition A.4 (Co-closed Forms, (Sec. 14.2 [18]))**.**
A k-form $\alpha^{(k)}$ is co-closed if $d^*\alpha^{(k)} = 0$. The space of co-closed k-forms $\mathcal{Z}_{d^*}\Lambda^{(k)}$ is the kernel of the codifferential, i.e.

$$\mathcal{Z}_{d^*}\Lambda^{(k)} := \{\alpha^{(k)} \in \Lambda^{(k)} : d^*\alpha^{(k)} = 0\} \subset \Lambda^{(k)}.$$

Definition A.5 (Co-exact Forms, (Sec. 14.2 [18]))**.**
A k form $\alpha^{(k)}$ is co-exact if $\exists\beta^{(k+1)}$ s.t. $\alpha^{(k)} = d^*\beta^{(k+1)}$. The space of co-closed k-forms $\mathcal{B}_{d^*}\Lambda^{(k+1)}$ is the range of the codifferential, i.e.

$$\mathcal{B}_{d^*}\Lambda^{(k+1)} := d^*\Lambda^{(k+1)} \subset \Lambda^{(k)}$$

Definition A.6 (Harmonic Form, (Sec. 14.2 [18]))**.**
In line with our previous definition, section 2.2, we can define the space of harmonic forms as follows,

$$\mathcal{H}\Lambda^{(k)} := \{\alpha^{(k)} \in \mathcal{Z}_d\Lambda^{(k)} : \alpha^{(k)} \notin \mathcal{B}_d\Lambda^{(k-1)}\}$$
$$\mathcal{H}\Lambda^{(k)} := \{\alpha^{(k)} \in \mathcal{Z}_{d^*}\Lambda^{(k)} : \alpha^{(k)} \notin \mathcal{B}_{d^*}\Lambda^{(k+1)}\}.$$

These definitions can be united as follows. A k-form $\alpha^{(k)}$ is *harmonic* if $\Delta\alpha^{(k)} = 0$. The space of harmonic k-forms is defined as,

$$\mathcal{H}\Lambda^{(k)} := \{\alpha^{(k)} \in \Lambda^{(k)} : d\alpha^{(k)} = d^*\alpha^{(k)} = 0\}.$$

As in section 2.2 we can decompose the space of k-forms in orthogonal components,

$$\Lambda^{(k)}(\mathcal{M}) = \mathcal{B}_d\Lambda^{(k-1)} \oplus \mathcal{H}\Lambda^{(k)} \oplus \mathcal{Z}_d^{\mathscr{C}}\Lambda^{(k)}$$
$$\Lambda^{(k)}(\mathcal{M}) = \mathcal{B}_{d^*}\Lambda^{(k+1)} \oplus \mathcal{H}\Lambda^{(k)} \oplus \mathcal{Z}_{d^*}^{\mathscr{C}}\Lambda^{(k)}.$$

The decompositions can be unified by taking $\mathcal{Z}_d^{\mathscr{C}}\Lambda^{(k)} = \mathcal{B}_{d^*}\Lambda^{(k+1)}$ and $\mathcal{Z}_{d^*}^{\mathscr{C}}\Lambda^{(k)} = \mathcal{B}_d\Lambda^{(k-1)}$. This leads to a more useful definition of the Hodge decomposition.

Theorem A.2 (Hodge decomposition, (Sec. 14.2 [18]))**.**
For any k-form on a closed manifold $\mathcal{M}$ there exists an unique decomposition

$$\alpha^{(k)} = d\phi^{(k-1)} + d^*\psi^{(k+1)} + h^{(k)},$$

where $h^{(k)}$ is a harmonic form. Note that this doesn't imply uniqueness of $\phi^{(k-1)}$ and $\psi^{(k+1)}$. On a contractable manifold the space of harmonic forms is empty, i.e. $h^{(k)} = 0$.

The coboundary operator δ induces the same topological structure on cochain complexes. We can define cochain spaces analogue to the spaces of closed-, exact-, and harmonic form.

$$B_\delta C^{(k-1)} := \delta C^{(k-1)},$$
$$Z_\delta C^{(k)} := \{\boldsymbol{c}^{(k)} \in C^{(k)} : \delta\boldsymbol{c}^{(k)} = \emptyset\},$$
$$HC^{(k)} := \{\boldsymbol{c}^{(k)} \in Z_\delta C^{(k)} : \boldsymbol{c}^{(k)} \notin B_\delta C^{(k-1)}\},$$

The topological structure of these spaces is shown in equivalent to the one shown in Figure A.1. The topology of the exterior derivative is preserved in discrete cochain structures. This structure governs discrete counterparts of the Poincaré lemma, that depends on the exactness of the coboundary operator.

B

DERIVATION OF ADJOINT RELATIONS

In section 2.4 we introduced the L^2-inner product through the action of the Hodge-$\star$ operator. In this chapter we derive the various *adjoint* relations that have been used throughout the work. Let $\mathscr{L} : \Lambda^{(k)}(\mathscr{M}) \to \Lambda^{(l)}(\mathscr{M})$ be a linear operator. The adjoint operator is the liner operator $\mathscr{L}^* : \Lambda^{(l)}(\mathscr{M}) \to \Lambda^{(k)}(\mathscr{M})$ that satisfies,

$$\left(\alpha^{(k)}, \mathscr{L}^* \beta^{(l)}\right)_{\mathscr{M}} = \left(\mathscr{L}\alpha^{(k)}, \beta^{(l)}\right)_{\mathscr{M}}, \tag{B.1}$$

for some $\alpha^{(k)} \in \Lambda^{(k)}(\mathscr{M})$ and $\beta^{(l)} \in \Lambda^{(l)}(\mathscr{M})$. The exterior derivative d, the interior product $i_{\boldsymbol{v}}$, and the Lie derivative $\mathscr{L}_{\boldsymbol{v}}$ do not depend on metric. Their respective adjoints, the codifferential d^*, the cointerior product $i^*_{\boldsymbol{v}}$, and the co-Lie derivative $\mathscr{L}^*_{\boldsymbol{v}}$ do explicitly depend on the metric-dependent Hodge-$\star$ operator. The adjoint relations can be used to obtain a more favourable weak formulation. Note that in many derivations we use the following property of the Hodge-$\star$ operator, $\star\star\alpha^{(k)} = (-1)^{k(n-k)}$.

1. **The codifferential:**

$$d^*\alpha^{(k)} = (-1)^{n(k-1)+1} \star d \star \alpha^{(k)} \tag{B.2}$$

Let $\alpha^{(k-1)} \in \Lambda^{(k-1)}$, and $\beta^{(k)} \in \Lambda^{(k)}$, now

$$\begin{aligned}
d(\alpha^{(k-1)} \wedge \star\beta^{(k)}) =& d\alpha^{(k-1)} \wedge \star\beta^{(k)} + (-1)^{k-1}\alpha^{(k-1)} \wedge d \star \beta^{(k)} \\
=& d\alpha^{(k-1)} \wedge \star\beta^{(k)} + (-1)^{k-1}\alpha^{(k-1)} \wedge \left((-1)^{(n-k+1)(k-1)} \star\star\right) d \star \beta^{(k)} \\
=& d\alpha^{(k-1)} \wedge \star\beta^{(k)} + (-1)^{(n-k)(k-1)}\alpha^{(k-1)} \wedge \star\star d \star \beta^{(k)} \\
=& d\alpha^{(k-1)} \wedge \star\beta^{(k)} + (-1)^{(n-k)(k-1)}\alpha^{(k-1)} \wedge \star\left((-1)^{n(k-1)-1} d^*\right)\beta^{(k)} \\
=& d\alpha^{(k-1)} \wedge \star\beta^{(k)} + (-1)^{-k(k-1)-1}\alpha^{(k-1)} \wedge \star d^*\beta^{(k)} \\
=& d\alpha^{(k-1)} \wedge \star\beta^{(k)} - \alpha^{(k-1)} \wedge \star d^*\beta^{(k)}.
\end{aligned}$$

In the last line we used that $k(k-1)$ is even for all k. By rearranging the terms, integrating over manifold $\mathcal{M}$, and using Theorem 2.2 and Definition 2.15, we find,

$$\begin{aligned}
&\int_{\mathcal{M}} \alpha^{(k-1)} \wedge \star d^* \beta^{(k)} = \int_{\mathcal{M}} d\alpha^{(k-1)} \wedge \star \beta^{(k)} - \int_{\partial\mathcal{M}} \alpha^{(k-1)} \wedge \star \beta^{(k)} \\
\Leftrightarrow \quad &\left(\alpha^{(k-1)}, d^* \beta^{(k)}\right)_{\mathcal{M}} = \quad \left(d\alpha^{(k-1)}, \beta^{(k)}\right)_{\mathcal{M}} - \int_{\partial\mathcal{M}} \alpha^{(k-1)} \wedge \star \beta^{(k)}. \qquad \text{(B.3)}
\end{aligned}$$

The adjoint relation is obtained when the boundary term reduces to zero.

2. **The cointerior product:**

$$i_{\boldsymbol{v}}^* := (-1)^{n(k+1)-1} \star i_{\boldsymbol{v}} \star \qquad \text{(B.4)}$$

Let $\alpha^{(k)} \in \Lambda^{(k)}$, $\beta^{(k-1)} \in \Lambda^{(k-1)}$, and $\boldsymbol{v}$ be a vector field, and $v^{(1)}$ the 1-form associated with $\boldsymbol{v}$. Substitution the 1-form isomorphism, Equation 4.10, in the definition of $i_{\boldsymbol{v}}^*$ yields,

$$\begin{aligned}
i_{\boldsymbol{v}}^* \beta^{(k-1)} =& (-1)^{nk-1+(k-1)(n-k+1)} \star\star(\star\star \beta^{(k-1)} \wedge v^{(1)}) \\
=& (-1)^{nk-1+(k-1)(n-k+1)+(k-1)(n-k+1)+k(n-k)} (\beta^{(k-1)} \wedge v^{(1)}) \\
=& (-1)^{k^2-1} (\beta^{(k-1)} \wedge v^{(1)}) \\
=& (-1)^{k-1} (\beta^{(k-1)} \wedge v^{(1)}),
\end{aligned}$$

Taking the inner product of $\beta^{(k-1)}$ and $i_{\boldsymbol{v}} \alpha^{(k)}$ yields,

$$\begin{aligned}
\left(\beta^{(k-1)}, i_{\boldsymbol{v}} \alpha^{(k)}\right)_{\mathcal{M}} =& \int_{\mathcal{M}} \beta^{(k-1)} \wedge \star i_{\boldsymbol{v}} \alpha^{(k)} \\
\overset{4.10}{=}& (-1)^{k(n-k)} \int_{\mathcal{M}} \beta^{(k-1)} \wedge \star\star \left(\star \alpha^{(k)} \wedge v^{(1)}\right) \\
=& (-1)^{k(n-k)+(n-k+1)(k-1)} \int_{\mathcal{M}} \beta^{(k-1)} \wedge \star \alpha^{(k)} \wedge v^{(1)} \\
=& (-1)^{k(n-k)+(n-k+1)(k-1)+(n-k)} \int_{\mathcal{M}} \beta^{(k-1)} \wedge v^{(1)} \wedge \star \alpha^{(k)} \\
=& (-1)^{k-1} \left(\beta^{(k-1)} \wedge v^{(1)}, \alpha^{(k)}\right)_{\mathcal{M}} \\
=& \left(i_{\boldsymbol{v}}^* \beta^{(k-1)}, \alpha^{(k)}\right)_{\mathcal{M}}
\end{aligned}$$

The cointerior product $i_{\boldsymbol{v}}^*$ is the adjoint of the interior product $i_{\boldsymbol{v}}$.

$$\left(\beta^{(k-1)}, i_{\boldsymbol{v}} \alpha^{(k)}\right)_{\mathcal{M}} = \left(i_{\boldsymbol{v}}^* \beta^{(k-1)}, \alpha^{(k)}\right)_{\mathcal{M}} \qquad \text{(B.5)}$$

3. **The co-Lie derivative:**

$$\mathcal{L}_{\boldsymbol{v}}^* := (-1)^{k(n+1)+1} \star \mathcal{L}_{\boldsymbol{v}} \star. \qquad \text{(B.6)}$$

The co-Lie derivative is related to the codifferential and cointerior product that is similar Cartan's formula, Equation 4.5. Let $\alpha^{(k)} \in \Lambda^{(k)}$ and $\boldsymbol{v}$ some vector field. We find,

$$\begin{aligned}
\mathscr{L}_{\boldsymbol{v}}^{*}\alpha^{(k)} &\overset{4.5}{=} (-1)^{k(n+1)+1} \star (d i_{\boldsymbol{v}} \star + \star i_{\boldsymbol{v}} d) \star \alpha^{(k)} \\
&= (-1)^{k(n+1)+1} \star \left((-1)^{(n-k-1)(k+1)} d \star \star i_{\boldsymbol{v}} + (-1)^{(n-k+1)(k-1)} \star i_{\boldsymbol{v}} \star \star d \right) \star \alpha^{(k)} \\
&= (-1)^{k(n+1)+1} \left((-1)^{(n-k-1)(k+1)+n} d^{*} i_{\boldsymbol{v}}^{*} + (-1)^{(n-k+1)(k-1)+n} i_{\boldsymbol{v}}^{*} d^{*} \right) \alpha^{(k)} \\
&= (d^{*} i_{\boldsymbol{v}}^{*} + i_{\boldsymbol{v}}^{*} d^{*}) \alpha^{(k)}. \qquad \text{(B.7)}
\end{aligned}$$

Using adjoint relations Equation B.3 and Equation B.5 we find,

$$\begin{aligned}
\left(\beta^{(k)}, \mathscr{L}_{\boldsymbol{v}}^{*} \alpha^{(k)} \right)_{\mathscr{M}} &\overset{B.7}{=} \left(\beta^{(k)}, d^{*} i_{\boldsymbol{v}}^{*} \alpha^{(k)} \right)_{\mathscr{M}} + \left(\beta^{(k)}, i_{\boldsymbol{v}}^{*} d^{*} \alpha^{(k)} \right)_{\mathscr{M}} \\
&= \left(d\beta^{(k)}, i_{\boldsymbol{v}}^{*} \alpha^{(k)} \right)_{\mathscr{M}} - \left(\beta^{(k)}, i_{\boldsymbol{v}}^{*} \alpha^{(k)} \right)_{\partial\mathscr{M}} + \left(i_{\boldsymbol{v}} \beta^{(k)}, d^{*} \alpha^{(k)} \right)_{\mathscr{M}} \\
&= \left(i_{\boldsymbol{v}} d\beta^{(k)}, \alpha^{(k)} \right)_{\mathscr{M}} - \left(\beta^{(k)}, i_{\boldsymbol{v}}^{*} \alpha^{(k)} \right)_{\partial\mathscr{M}} \qquad \text{(B.8)} \\
&\quad + \left(d i_{\boldsymbol{v}} \beta^{(k)}, \alpha^{(k)} \right)_{\mathscr{M}} - \left(i_{\boldsymbol{v}} \beta^{(k)}, \alpha^{(k)} \right)_{\partial\mathscr{M}} \\
&\overset{4.5}{=} \left(\mathscr{L}_{\boldsymbol{v}} \beta^{(k)}, \alpha^{(k)} \right)_{\mathscr{M}} - \left(\beta^{(k)}, i_{\boldsymbol{v}}^{*} \alpha^{(k)} \right)_{\partial\mathscr{M}} - \left(i_{\boldsymbol{v}} \beta^{(k)}, \alpha^{(k)} \right)_{\partial\mathscr{M}}. \qquad \text{(B.9)}
\end{aligned}$$

The adjoint relation is obtained when the boundary terms reduce to zero.

C

GENERALISED PIOLA TRANSFORMATIONS

In this chapter we derive the pull-back operators for k-forms in $\mathbb{R}^3$. These transformations commutate with the exterior derivative, such that the DeRham structure is preserved on arbitrary geometries. Note that these transformations are also useful when determining integrals on some parent domain.

Definition C.1 (Pull-back operator ϕ^*, (Sec. 2.7 [18]))**.**
Consider smooth bijective coordinate mapping $\phi : \mathcal{N} \to \mathcal{M}$. Consider local coordinates x^i for manifold $\mathcal{M}$ and ξ^j for manifold $\mathcal{N}$, such that $x = \phi(\xi) = x(\xi)$. Let $\alpha^{(0)} \in \Lambda^{(0)}(\mathcal{M})$ be some 0-form. We define pull-back operator ϕ^* to be equal to $(\phi^* \alpha^{(0)})(\xi) := \alpha(x(\xi))$. The pull-back operator satisfies the following properties,

$$\begin{aligned}
\phi^*(d\alpha^{(0)}) &= d(\phi^* \alpha^{(0)}) \\
\phi^*(\alpha^{(k)} \wedge \beta^{(l)}) &= (\phi^* \alpha^{(k)}) \wedge (\phi^* \beta^{(l)})
\end{aligned}$$

We can use these properties to derive pull-back operators for arbitrary k-forms in $\mathbb{R}^3$. Let $\beta^{(1)}$ be some 1-form.

$$\begin{aligned}
\phi^* \beta^{(1)} &= \phi^*(\beta_i \, dx_i) = \beta_i(x(\xi)) d\phi^*(x_i) \\
&= \beta_i(x(\xi)) \frac{\partial x^i}{\partial \xi^j} d\xi_j \\
&= \tilde{\beta} d\xi_j = \tilde{\beta}^{(1)}.
\end{aligned}$$

or $\tilde{\beta} = \beta F$, where $F = F_{ij} = \frac{\partial x^i}{\partial \xi^j}$ is the *deformation gradient.* Now for some 2-form $\omega^{(2)}$ we

find,

$$\begin{aligned}\phi^*\omega^{(2)} &= \phi^*\omega_{ij}dx_i\wedge dx_j = \omega_{ij}(x(\xi))(\phi^*dx_i)\wedge(\phi^*dx_j)\\ &= \omega_{ij}(x(\xi))\frac{\partial x^i}{\partial\xi^k}\frac{\partial x^j}{\partial\xi^l}d\xi_k\wedge d\xi_l\\ &= \tilde{\omega}^{(2)},\end{aligned}$$

with $i\neq j$, and $k\neq l$. We find that $\frac{\partial x^i}{\partial\xi^k}\frac{\partial x^j}{\xi^l}d\xi_k\wedge d\xi_l$ defines the adjugate of the deformation gradient matrix, i.e.

$$\tilde{\omega} = \omega\text{Adj}(F) = \omega(\det F)(F^{-1}).$$

Note that this relations is famous as the Piola (stress) transformation. Finally, for some 3-form $\rho^{(3)}$ we find,

$$\phi^*\rho^{(3)} = \rho(x(\xi))\frac{\partial x^i}{\partial\xi^l}\frac{\partial x^j}{\partial\xi^m}\frac{\partial x^k}{\partial\xi^n}d\xi_l\wedge d\xi_m\wedge d\xi_n,$$

where we obtain $\tilde{\rho} = \rho(\det F)$. These transformations for the components of k-forms commute with the exterior derivative, such that any DeRham complex in some physical space is also satisfied in some pull-backed parameter space. The transformations are known as the generalized Piola transformations. We can pull-back integrals using the general pull-back formula.

Theorem C.1 (General pull-back formula, (Sec. 3.1 [18]))**.**
Consider again the smooth bijective coordinate mapping $\phi:\mathcal{N}\to\mathcal{M}$. Let $U\subset\mathcal{N}$, such that $\phi(U)\subset\mathcal{M}$. Let $\alpha^{(k)}\in\Lambda^{(k)}(\mathcal{M})$ be a k-form. The integral of $\alpha(k)$ on $\phi(U)$ can be pulled-back to U,

$$\int_{\phi(U)}\alpha^{(k)} = \int_U\phi^*\alpha^{(k)}. \tag{C.1}$$

D

WELL-POSEDNESS OF THE POISSON PROBLEM

Well-posedness of elliptic PDE problems can be analysed in the powerful Hilbert space setting. In this setting, weak formulations of the PDE problems are analysed. We will introduce some fundamental properties and theorems that enable us to prove existence and uniqueness to the PDE problems. Furthermore we prove well-posedness for the Poisson problems that were introduced in chapter 3.

Lemma D.1 (Cauchy-Schwarz inequality)**.**
Any two k-forms $\alpha^{(k)}, \beta^{(k)} \in L^2\Lambda^{(k)}$ satisfy the inequality

$$|(\alpha^{(k)}, \beta^{(k)})| \leq \|\alpha^{(k)}\|_{L^2\Lambda^{(k)}} \|\beta^{(k)}\|_{L^2\Lambda^{(k)}} \tag{D.1}$$

Lemma D.2 (Generalised Poincaré inequality, (proof in [39]))**.**
Consider a k-form $\alpha^{(k)} \in W_d\Lambda^{(k)}(\Omega)$ on contractible manifold Ω, i.e. the space of harmonic k-forms is empty. Then $\alpha^{(k)}$ satisfies,

$$\|\alpha^{(k)}\|_{L^2\Lambda^{(k)}} \leq C\|d\alpha^{(k)}\|_{L^2\Lambda^{(k+1)}}, \tag{D.2}$$

for some constant C. The Poincaré inequality allows us to define an equivalent Sobolev norm $\|\alpha^{(k)}\|_{W_d\Lambda^k} := \|d\alpha^k\|_{L^2\Lambda^{(k+1)}}$.

Definition D.1 (Weakly coercive)**.**
Let H_1, H_2 denote Hilbert spaces. A bilinear form $B(\cdot,\cdot) : H_1 \times H_2 \to \mathbb{R}$ is *weakly coercive* if

$$\sup_{v\in H_2} \frac{B(u,v)}{\|v\|_{H_2}} \geq \alpha\|u\|_{H_1}, \ \forall u \in H_1,$$
$$\text{and } \sup_{u\in H_1} \frac{B(u,v)}{\|u\|_{H_1}} \geq \alpha\|v\|_{H_2}, \ \forall v \in H_2,$$

where $\alpha \in \mathbb{R}$.

Definition D.2 (Coercive)**.**
A bilinear form $B(\cdot,\cdot) : H \times H \to \mathbb{R}$ is *coercive* if

$$B(u,u) \geq \alpha \|u\|_H^2, \ \forall u \in H.$$

Definition D.3 (Continuous)**.**
A bilinear form $B(\cdot,\cdot) : H_1 \times H_2 \to \mathbb{R}$ is *continuous* if

$$|B(u,v)| \leq c \|u\|_{H_1} \|v\|_{H_2},$$

where $c \in \mathbb{R}$.

The Lax-Milgram theorem is a powerful theorem to prove existence and uniqueness of solution to coercive PDE problems. We will also consider indefinite variational problems for which well-posedness can be proved using Brezzi's theorem, Theorem D.4.

Theorem D.3 (Lax-Milgram)**.**
Let $u, v \in H$, and let $F : H \to \mathbb{R}$ define a bounded linear functional, and let $a(\cdot,\cdot) : H \times H \to \mathbb{R}$ be a continuous, coercive, bilinear form. Then

$$\exists! u \in H \quad s.t. \quad a(u,v) = F(v), \qquad \forall v \in H.$$

Problem D.1 (Mixed Variational Problem)**.**
Given a pair of Hilbert spaces H_1, H_2, bilinear forms $a(\cdot,\cdot) : H_1 \times H_1 \to \mathbb{R}$, $b(\cdot,\cdot) : H_1 \times H_2 \to \mathbb{R}$, and bounded linear functionals $F(\cdot) : H_1 \to \mathbb{R}$, and $G(\cdot) : H_2 \to \mathbb{R}$. We then seek $u \in H_1$, $p \in H_2$ s.t.

$$\begin{cases} a(u,v) - b(v,p) &= F(v), \\ b(u,q) &= G(q), \end{cases} \tag{D.3}$$

$\forall v \in H_1$, $\forall q \in H_2$.

Theorem D.4 (Inf-Sup Condition - Brezzi's Theorem (Sec. 2.1 [22]))**.**
Let $Z = \{v \in H_1 : b(v,q) = 0, \ \forall q \in H_2\}$, let bilinear form $a(\cdot,\cdot)$ be continuous on $H_1 \times H_1$ and coercive on $Z \times Z$. There exists an unique solution $(u,p) \in H_1 \times H_2$ for Problem D.1 if and only if bilinear form $b(\cdot,\cdot)$ is continuous on $H_1 \times H_2$ and if

$$\sup_{v \in H_1} \frac{b(v,p)}{\|v\|_{H_1}} \geq C \|p\|_{H_2}.$$

We will apply these theorems to two example problems in the framework of exterior calculus using the DeRham Sobolev Complex. The first problem, the 0-form Poisson problem, is associated with unconstrained optimization of a quadratic functional. This type of problem has classically been solved successfully using Rayleigh-Ritz approach. In this approach the problem is converted to a set of discrete minimization problems with resulting linear problem $\mathbb{A}\boldsymbol{u} = \boldsymbol{f}$, where $\mathbb{A}$ is a *symmetric positive definite (SPD)* matrix.

Example D.1 (0-form Poisson problem)**.**
Consider the domain $\Omega = [0,1]^2 \subset \mathbb{R}^2$ with boundary $\partial\Omega = \Gamma_d \cup \Gamma_n$, where $\Gamma_d \cap \Gamma_n = \emptyset$. Given $f^{(0)} \in \Lambda^{(0)}$, find $\psi^{(0)} \in \Lambda^{(0)}$ such that,

$$\begin{cases} \Delta\psi^{(0)} & = f^{(0)}, \\ \psi^{(0)} & = 0, \text{ on } \Gamma_d \\ \partial_n \psi^{(0)} & = 0, \text{ on } \Gamma_n \end{cases}$$

We obtain a weak formulation of this problem by taking the inner product with some test function $w^{(0)} \in \Lambda_0^{(0)}$. Where $\Lambda_0^{(0)}$ is the space of compactly supported 0-forms according,

$$\Lambda_0^{(0)} := \{\alpha^{(0)} \in \Lambda^{(0)} : \operatorname{tr} \alpha^{(0)} = 0 \text{ on } \Gamma_d\}.$$

We use integration by parts for two reasons. First, we would like to reduced the continuity constraints on the considered trial space. Secondly, we would like to get rid of the codifferential d^*. We find,

$$\begin{aligned} & \left(w^{(0)}, d^* d\psi^{(0)}\right)_\Omega = \left(w^{(0)}, f^{(0)}\right)_\Omega \\ \Leftrightarrow\ & \left(dw^{(0)}, d\psi^{(0)}\right)_\Omega = \left(w^{(0)}, f^{(0)}\right)_\Omega + (w^{(0)}, d\psi^{(0)})_{\partial\Omega}. \end{aligned}$$

For this case the boundary integral reduces to zero. We hence obtain the following weak formulation. Given $f^{(0)} \in L^2\Lambda^{(0)}$, find $\psi^{(0)} \in W_d\Lambda^{(0)}$ s.t.

$$\left(dw^{(0)}, d\psi^{(0)}\right)_\Omega = \left(w^{(0)}, f^{(0)}\right)_\Omega, \qquad \forall w^{(0)} \in W_d\Lambda_0^{(0)}.$$

We can rewrite this problem in variational formulation, defining bilinear form $a(\cdot,\cdot)$ and functional $F(\cdot)$,

$$\begin{aligned} & a(\cdot,\cdot) : W_d\Lambda^{(0)} \times W_d\Lambda^{(0)} \to \mathbb{R} : a(\cdot,\cdot) := (d\cdot, d\cdot)_\Omega \\ & F(\cdot) : W_d\Lambda^{(0)} \to \mathbb{R} : F(\cdot) := (\cdot, f^{(0)})_\Omega. \end{aligned}$$

Given $\psi^{(0)} \in L^2\Lambda^{(0)}$, find $\psi^{(0)} \in W_d\Lambda^{(0)}$ such that,

$$a(w^{(0)}, \psi^{(0)}) = F(w^{(0)}), \ \forall w^{(0)} \in \Lambda_0^{(0)}.$$

Lax-Milgram proves existence of unique solution if $a(\cdot,\cdot)$ is coercive, and continuous, and $F(\cdot)$ is bounded. Using Cauchy-Schwarz (CS), and Poincaré (PC), we find

$$\begin{aligned} & |a(w^{(0)}, \psi^{(0)})| = (dw^{(0)}, d\psi^{(0)})_\Omega \overset{CS}{\leq} \|dw^{(0)}\| \|d\psi^{(0)}\| < \infty, \\ & a(w^{(0)}, w^{(0)}) = (dw^{(0)}, dw^{(0)})_\Omega = \|dw^{(0)}\|^2 \overset{PC}{\geq} C\|w^{(0)}\|^2, \\ & \|F\| = \sup_{\|w^{(0)}\| \leq 1} |F(w^{(0)})| \overset{CS}{\leq} \sup_{\|w^{(0)}\| \leq 1} \|w^{(0)}\| \|f^{(0)}\| = \|f^{(0)}\| < \infty. \end{aligned}$$

Note that we used the boundedness of norms that exists by definitions of function spaces $L^2\Lambda^{(0)}$ and $W_d\Lambda^{(0)}$. Hence by Lax-Milgram there exists an unique solution $\psi^{(0)} \in W_d\Lambda^{(0)}$ s.t. $a(w^{(0)}, \psi^{(0)}) = F(w^{(0)}), \ \forall w^{(0)} \in W_d^0\Lambda^{(0)}$.

In the second problem we will consider the volume, n-form, Poisson problem. This problem is equivalent to constrained optimization of a quadratic functional. These problems are solved numerically using a mixed Galerkin formulation.

Example D.2 (n-form Poisson problem, (Sec. 2.3 [23]))**.**
Consider the domain $\Omega = [0,1]^2 \subset \mathbb{R}^2$ with boundary $\partial\Omega = \Gamma_d \cup \Gamma_n$, where $\Gamma_d \cap \Gamma_n = \emptyset$. Given $f^{(2)} \in \Lambda^{(2)}$, find $\psi^{(2)} \in \Lambda^{(2)}$ such that,

$$\begin{cases} \Delta\psi^{(2)} &= f^{(2)}, \text{ in } \Omega, \\ \psi^{(2)} &= 0, \text{ on } \Gamma_d, \\ \partial_t\psi^{(2)} &= 0, \text{ on } \Gamma_n \end{cases}$$

Again we multiply with some test-function $w^{(2)}$ and perform integration by parts for reasons mentioned before to obtain,

$$\left(d^* w^{(2)}, d^*\psi^{(2)}\right)_\Omega = \left(w^{(2)}, f^{(2)}\right)_\Omega.$$

We could use a similar roadmap as for the 0-form Poisson case, using Lax-Milgram to prove well-posedness, and taking the dual Sobolev space $W_{d^*}\Lambda^{(2)}$. However, in the finite projection method, we will only be able to satisfy one of the DeRham Sobolov complexes simultaneously. Hence we want to limit ourselves to the use of the following sequence of function spaces in proving well-posedness of the problem.

$$W_d\Lambda^{(0)} \xrightarrow{d} W_d\Lambda^{(1)} \xrightarrow{d} L^2\Lambda^{(2)}$$

Consider the equivalent system of first-order-differential equations,

$$\begin{cases} d^*\psi^{(2)} &= v^{(1)}, \\ dv^{(1)} &= f^{(2)} \end{cases}$$

A weak formulation can be obtained taking inner product with $q^{(1)} \in W_d\Lambda_0^{(1)}$ and $w^{(2)} \in L^2\Lambda^{(2)}$ respectively, and performing integration by parts, where

$$\Lambda_0^{(1)} := \{\alpha^{(1)} \in \Lambda^{(1)} : \operatorname{tr}\alpha^{(1)} = 0 \text{ on } \Gamma_n\}.$$

We obtain,

$$\begin{cases} \left(dq^{(1)}, \psi^{(2)}\right)_\Omega + \left(q^{(1)}, \psi^{(2)}\right)_{\partial\Omega} &= \left(q^{(1)}, v^{(1)}\right)_\Omega, & \forall q^{(1)} \in W_d\Lambda_0^{(1)}, \\ \left(w^{(2)}, dv^{(1)}\right)_\Omega &= \left(w^{(2)}, f^{(2)}\right)_\Omega, & \forall w^{(2)} \in L^2\Lambda^{(2)}. \end{cases}$$

Note that the boundary integral reduces to zero due to the induced boundary conditions. We can define bilinear forms $a(\cdot,\cdot)$, and $b(\cdot,\cdot)$ and functional $F(\cdot)$,

$$\begin{aligned} &a(\cdot,\cdot) : \Lambda^{(2)} \times \Lambda^{(2)} \to \mathbb{R} : a(\cdot,\cdot) := (\cdot,\cdot)_\Omega \\ &b(\cdot,\cdot) : W_d\Lambda^{(1)} \times L^2\Lambda^{(1)} \to \mathbb{R} : b(\cdot,\cdot) := (d\cdot,\cdot)_\Omega \\ &F(\cdot) : W_d\Lambda^{(0)} \to \mathbb{R} : F(\cdot) := (\cdot, f^{(0)})_\Omega. \end{aligned}$$

Now we can rewrite the problem in the variational formulation. Given $f^{(2)} \in L^2\Lambda^{(2)}$, find $\psi^{(2)} \in L^2\Lambda^{(2)}$ and $v^{(1)} \in W_d\Lambda^{(1)}$ such that,

$$\begin{cases} a(q^{(1)}, v^{(1)}) - b(q^{(1)}, \psi^{(2)}) & = 0, \ \forall q^{(1)} \in \Lambda_0^{(1)} \\ b(v^{(1)}, w^{(2)}) & = F(w^{(2)}), \ \forall w^{(2)} \in \Lambda^{(2)}. \end{cases}$$

Let $\mathcal{Z}_d\Lambda^{(1)} = \{q^{(1)} \in W_d\Lambda^{(1)} : dq^{(1)} = 0\}$. Note that the exterior derivative on $(n-1)$-forms is surjective, Equation A.1, which implies that for any $\psi^{(2)} \in L^2\Lambda^{(2)}$, there exists some $q_\psi^{(1)} \in W_d\Lambda^{(1)}$, such that $\psi^{(2)} = dq_\psi^{(1)}$, and $\|\psi^{(2)}\| = \|dq_\psi^{(1)}\|$.

Brezzi's theorem, Theorem D.4, can now be used to prove well-posedness of this problem. We need to prove that $a(\cdot,\cdot)$ is coercive on $\mathcal{Z}_d\Lambda^{(1)} \times \mathcal{Z}_d\Lambda^{(1)}$, that $b(\cdot,\cdot)$ is continuous, and that the inf-sup condition is satisfied for $b(\cdot,\cdot)$.

$$a(q^{(1)}, q^{(1)}) = \|q^{(1)}\|^2_{W_d\Lambda^{(1)}} = \|q^{(1)}\|_{L^2\Lambda^{(1)}} + \cancel{\|dq^{(1)}\|_{L^2\Lambda^{(2)}}},$$

$$|b(q^{(1)}, \psi^{(2)})| = |(dq^{(1)}, \psi^{(2)})| \overset{CS}{\leq} \|dq^{(1)}\|\|\psi^{(2)}\| < \infty$$

$$\sup_{q^{(1)} \in W_d\Lambda^{(1)}} \frac{b(q^{(1)}, \psi^{(2)})}{\|q^{(1)}\|} \geq \frac{b(q_\psi^{(1)}, \psi^{(2)})}{\|q_\psi^{(1)}\|} = \frac{\|\psi^{(2)}\|^2}{\|q_\psi^{(1)}\|} \geq \frac{1}{C}\|\psi^{(2)}\|,$$

where we used that $\|q_\psi^{(1)}\| \overset{PC}{\leq} C\|dq_\psi^{(1)}\| = C\|\psi^{(2)}\|$. Hence there exists an unique solution set $(v^{(1)}, \psi^{(2)}) \in (W_d\Lambda^{(1)}, L^2\Lambda^{(2)})$. Note that well-posedness depended on the exact sequence that is satisfied by the Sobolev DeRham complex. In our discretization approach we must ensure that our finite-dimensional function spaces satisfy the exact sequence to prove well-posedness in the discrete setting. In the 0-form Poisson example this was not the case which poses less restrictions on the choice of finite-dimensional function spaces in the discretization process.

E

DERIVATION OF EDGE FUNCTIONS

The finite-dimensional function spaces are constructed by taking spans of combinations of nodal- and edge-type basis functions as is shown in section 3.3. In this chapter we derive the edge-type basis function and prove its unit mass property.

Consider the 1-form $v_h^{(1)} \in L^2\Lambda_h^{(1)}$ that satisfies $v_h^{(1)} = df_h^{(0)}$. The question is, how do we define $L^2\Lambda_h^{(1)}$? Do we let $L^2\Lambda_h^{(1)} := \mathscr{S}_n^p$ as well? Application of the exterior derivative on the 0-form $f_h^{(0)}$ yields the following,

$$
\begin{aligned}
df_h^{(0)}(\xi) &= \left(\frac{d}{d\xi}\sum_{i=1}^{n}\lambda_{i,p}(\xi)f_i\right)d\xi \\
&\overset{3.17}{=} \left(\sum_{i=1}^{n}\left(\frac{p}{\xi_{i+p}-\xi_i}\lambda_{i,p-1}(\xi) - \frac{p}{\xi_{i+p+1}-\xi_{i+1}}\lambda_{i+1,p-1}(\xi)\right)f_i\right)d\xi \\
&= \cancel{\frac{p}{\xi_p-\xi_0}\lambda_{1,p-1}(\xi)d\xi\cdot f_1} - \frac{p}{\xi_{p+1}-\xi_1}\lambda_{2,p-1}(\xi)d\xi\cdot f_1 \\
&\quad + \frac{p}{\xi_{p+1}-\xi_1}\lambda_{2,p-1}(\xi)d\xi\cdot f_2 - \cdots\cdots \\
&\quad \cdots\cdots - \frac{p}{\xi_{n+p}-\xi_n}\lambda_{n,p-1}(\xi)d\xi\cdot f_{n-1} \\
&\quad + \frac{p}{\xi_{n+p}-\xi_n}\lambda_{n,p-1}(\xi)d\xi\cdot f_n - \cancel{\frac{p}{\xi_{n+p+1}-\xi_{n+1}}\lambda_{n+1,p-1}(\xi)d\xi\cdot f_n} \\
&= \sum_{i=2}^{n}\left(\frac{p}{\xi_{i+p}-\xi_i}\lambda_{i,p-1}(\xi)d\xi\right)(f_i - f_{i-1})
\end{aligned}
$$

Where we used that $\xi_p - \xi_0 = \xi_{n+p+1} - \xi_{n+1} = 0$. If we let $v_i = (f_i - f_{i-1})$, and use B-spline basis functions of a polynomial degree lower with scaling $\frac{p}{\xi_{i+p}-\xi_i}$, then the relation $v_h^{(1)} = df_h^{(0)}$ is exact.

Unit mass. Take $v_h^{(1)} = df_h^{(0)}$ with,

$$f_i = \begin{cases} C, & \text{if } i < j \\ C+1, & \text{if } i \geq j \end{cases},$$

for some constant $C \in \mathbb{R}$, such that $v_i = \delta_i^j$. Now,

$$\begin{aligned} \int_{\xi_j}^{\xi_{j+p}} \lambda_j^{(1)}(\xi) d\xi &= \int_{\xi_j}^{\xi_{j+p}} \left(\sum_{i=2}^{n} \lambda_i^{(1)}(\xi) v_i \right) d\xi \\ &= \int_{\xi_j}^{\xi_{j+p}} v_h^{(1)} = \int_{\xi_j}^{\xi_{j+p}} df_h^{(0)} d\xi = f_h^{(0)} \Big|_{\xi_j}^{\xi_{j+p}} = (C+1) - C = 1 \end{aligned}$$

□

This property reduces integration of 1-forms to mere summation of the expansion coefficients, i.e. for some $v_h^{(1)} \in L^2$,

$$\int_\Omega v_h^{(1)} = \int_\Omega \left(\sum_{i=2}^{n} \lambda_i^{(1)}(\xi) v_i \right) d\xi = \sum_{i=2}^{n} v_i$$

F

CONSTRUCTION OF BOUNDED COCHAIN PROJECTIONS

We want to construct projection operators, $\Pi^{(k)}$, that commute with the exterior derivative conform,

$$\begin{array}{ccc} \Lambda^{(k)} & \xrightarrow{d} & \Lambda^{(k+1)} \\ \downarrow{\scriptstyle \Pi^{(k)}} & & \downarrow{\scriptstyle \Pi^{(k+1)}} \\ C^{(k)} & \xrightarrow{\delta} & C^{(k+1)} \end{array}$$

Such commuting projection operators are known as *cochain projection operators*. Bounded cochain operators are fundamental in analysis. These projection operators allow us to provide estimates of the discrete solution with respect to the continuous solution. More on bounded cochain projectors can be found in the work by Falk and Winter, [5, 40]. Construction of such operators is not trivial, standard Galerkin L^2 projections of a k-form and $k+1$-form do not yield the desired commutativity. However, one can construct such projection by introducing a Poisson problem. An example is given in Appendix F.

Example F.1 (Construction of bounded cochain projections for $\omega^{(2)} = d\nu^{(1)}$ in $\mathbb{R}^2$)**.** Consider the pair $\nu^{(1)} \in W_d\Lambda^{(1)}$ and $\omega^{(2)} \in L^2\Lambda^{(2)}$ on $\Omega = [0,1]^2$ given by,

$$\begin{aligned} \nu^{(1)} &= -\frac{1}{4\pi}\cos(2\pi x)\sin(2\pi y)\,dx - \frac{1}{4\pi}\sin(2\pi x)\cos(2\pi y)\,dy \\ \omega^{(2)} &= d\nu^{(1)} = \sin(2\pi x)\sin(2\pi y)\,dx\wedge dy. \end{aligned}$$

We want to define bounded projection operators satisfying commutativity $\delta\Pi^{(1)}\nu^{(1)} = \Pi^{(2)}d\nu^{(1)}$. We let $W_d\Lambda^{(1)} := \mathscr{S}^{2,3}_{7,8} \times \mathscr{S}^{3,2}_{8,7}$ and $L^2\Lambda^{(2)} := \mathscr{S}^{2,2}_{7,7}$. To define $\Pi^{(2)}$ we consider

standard L^2 projection, i.e.

$$\left(s_h^{(2)}, \omega_h^{(2)}\right)_\Omega = \left(s_h^{(2)}, \omega^{(2)}\right)_\Omega, \qquad \forall s_h^{(2)} \in L^2\Lambda_h^{(2)},$$

Using the existence of $q^{(1)}$, such that, $s^{(2)} = dq^{(1)}$, Equation A.1, and using $\omega^{(2)} = dv^{(1)}$, we find an equivalent formulation,

$$\left(dq_h^{(1)}, dv_h^{(1)}\right)_\Omega = \left(dq_h^{(1)}, dv^{(1)}\right)_\Omega, \qquad \forall q_h^{(1)} \in W_d\Lambda_h^{(1)}.$$

Integration by parts yields,

$$\left(\Delta q_h^{(1)}, v_h^{(1)}\right)_\Omega - \left(dq_h^{(1)}, v_h^{(1)}\right)_{\partial\Omega} = \left(\Delta q_h^{(1)}, dv^{(1)}\right)_\Omega - \left(dq_h^{(1)}, v^{(1)}\right)_{\partial\Omega}, \qquad q_h^{(1)} \in W_d\Lambda_h^{(1)}.$$

Hence we let,

$$\Pi^{(2)} : L^2\Lambda^{(2)} \to \mathscr{C}^{(2)}, \quad \omega^{(2)} \overset{\Pi^{(2)}}{\to} \omega_h^{(2)} \text{ with}, \quad \left(s_h^{(2)}, \omega_h^{(2)}\right)_\Omega = \left(s_h^{(2)}, \omega^{(2)}\right)_\Omega, \qquad \forall s_h^{(2)} \in L^2\Lambda_h^{(2)}$$

$$\Pi^{(1)} : W_d\Lambda^{(1)} \to \mathscr{C}^{(1)}, \quad v^{(1)} \overset{\Pi^{(1)}}{\to} v_h^{(1)} \text{ with}, \quad \left(\Delta q_h^{(1)}, v_h^{(1)}\right)_\Omega = \left(\Delta q_h^{(1)}, v^{(1)}\right)_\Omega, \quad \forall q_h^{(1)} \in W_d\Lambda_h^{(1)}$$

To reduce continuity constraints, conform the chosen space $W_d\Lambda^{(1)}$, we will work we the integrated-by-parts version of $\Pi^{(1)}$. We obtain systems of equations,

$$\mathbb{M}^{(2,2)}\boldsymbol{\omega} = \left(\boldsymbol{\phi}^{(2)}, \omega^{(2)}\right)_\Omega$$
$$\left(\mathbb{E}^{(2,1)}\right)^T \mathbb{M}^{(2,2)}\mathbb{E}^{(2,1)}\boldsymbol{v} - \left(\mathbb{E}^{(2,1)}\right)^T \left(\boldsymbol{\phi}^{(2)}, v_h^{(1)}\right)_{\partial\Omega} = \left(\mathbb{E}^{(2,1)}\right)^T \left(\boldsymbol{\phi}^{(2)}, dv^{(1)}\right)_\Omega - \left(\mathbb{E}^{(2,1)}\right)^T \left(\boldsymbol{\phi}^{(2)}, v^{(1)}\right)_{\partial\Omega}.$$

A reconstruction of $\delta\Pi^{(1)}v^{(1)}$ is shown in Figure F.1. We find,

$$\|\delta\Pi^{(1)}v^{(1)} - \Pi^{(2)}dv^{(1)}\|_{L^2} = 1.2469e-15,$$

with,

$$\|\boldsymbol{v}\|_{L^2}^2 := \sum_i^{\dim(\boldsymbol{v})} |v_i|^2.$$

F

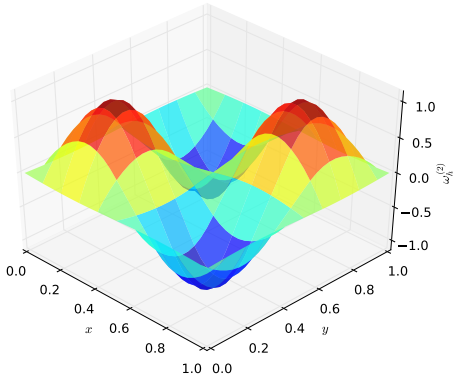

Figure F.1: Reconstruction of bounded cochain projection $\delta\Pi^{(1)}\nu^{(1)}$.

G

DERIVATION OF TRANSPORT PROBLEMS

We can derive the integral transport equations by analysing how some k-form $\alpha^{(k)}$ paired to some k-dimensional sub-manifold $V \subset \mathcal{M}$ evolves as it is advected with some velocity vector field $\boldsymbol{v}$. Let $\{\phi_t\}$ be the flow associated with $\boldsymbol{v}$, such that $V(t) = \phi^t V$. Theorem 4.1. From Theorem C.1 it follows that,

$$\int_{V(t)} \alpha^{(k)} = \int_V \phi_t^* \alpha^{(k)}. \tag{G.1}$$

We can derive the transport theorem by differentiating this relation with respect to t yields,

$$\begin{aligned}
\frac{d}{dt}\int_{V(t)} \alpha^{(k)}(t) &= \lim_{\Delta t\to 0} \frac{1}{\Delta t}\left(\int_{V(t+\Delta t)} \alpha^{(k)}(t+\Delta t) - \int_{V(t)} \alpha^{(k)}(t)\right) \\
&= \lim_{\Delta t\to 0} \frac{1}{\Delta t}\left(\int_{V(t+\Delta t)} \alpha^{(k)}(t+\Delta t) - \int_{V(t+\Delta t)} \alpha^{(k)}(t) \right. \\
&\qquad\qquad \left. + \int_{V(t+\Delta t)} \alpha^{(k)}(t) - \int_{V(t)} \alpha^{(k)}(t)\right) \\
&\overset{G.1}{=} \lim_{\Delta t\to 0} \frac{1}{\Delta t}\left(\int_V \phi_{t+\Delta t}^*[\alpha^{(k)}(t+\Delta t) - \alpha^{(k)}(t)] + \int_V [\phi_{t+\Delta t}^* - \phi_t^*]\alpha^{(k)}(t)\right) \\
&= \int_V \phi_t^* \lim_{\Delta t\to 0} \frac{\alpha^{(k)}(t+\Delta t) - -\alpha^{(k)}(t)}{\Delta t} + \int_V \phi_t^* \lim_{\Delta t\to 0} \frac{\phi_{\Delta t}^* - 1}{\Delta t}\alpha^{(k)}(t) \\
&\overset{4.3}{=} \int_V \phi_t^* \frac{\partial \alpha^{(k)}}{\partial t} + \int_V \phi_t^* \mathcal{L}_{\boldsymbol{v}} \alpha^{(k)} \\
&= \int_{V(t)} \left(\frac{\partial \alpha^{(k)}}{\partial t} + \mathcal{L}_{\boldsymbol{v}} \alpha^{(k)}\right).
\end{aligned}$$

The time-rate of change of a k-form $\alpha^{(k)} \in \Lambda^{(k)}$ paired to a k-dimensional sub-manifold $V \subset \mathscr{M}$ at some time-instant $t \in \mathbb{R}$ is thus given by,

$$\frac{d}{dt}\int_{V(t)} \alpha^{(k)} = \int_{V(t)} \left(\frac{\partial \alpha^{(k)}}{\partial t} + \mathscr{L}_{\boldsymbol{v}} \alpha^{(k)} \right). \tag{G.2}$$

Example G.1 (Conservation of mass, incompressible flow, and the advection-diffusion equation)**.**
Consider a volume $V(t) \subset \mathscr{M} \subset \mathbb{R}^n$ filled with some quantity with mass density $\rho^{(n)}$. The quantity's mass is given by,

$$M = \int_{V(t)} \rho^{(n)}.$$

Conservation of mass implies $\frac{d}{dt}M = 0$. Applying Theorem 4.2 yields,

$$0 = \frac{d}{dt}M = \frac{d}{dt}\int_{V(t)} \rho^{(n)} = \int_{V(t)} \left(\frac{\partial \rho^{(n)}}{\partial t} + \mathscr{L}_{\boldsymbol{v}} \rho^{(n)} \right), \tag{G.3}$$

Using Cartan's formula and the fact that $d\rho^{(n)} = 0$, we find that $\mathscr{L}_{\boldsymbol{v}}\rho^{(n)} = d i_{\boldsymbol{v}} \rho^{(n)}$. We can re-express the volume-form, $\rho^{(n)} = \rho \, \mathrm{vol}^{(n)}$. Now,

$$d i_{\boldsymbol{v}} \rho^{(n)} = d i_{\boldsymbol{v}} \rho \, \mathrm{vol}^{(n)} = d\rho \, i_{\boldsymbol{v}} \mathrm{vol}^{(n)} \overset{4.14}{=} d\rho \, v^{(n-1)} = dq^{(n-1)},$$

where $q^{(n-1)} := \rho v^{(n-1)}$ is the mass flux. Hence,

$$\int_{V(t)} \frac{\partial \rho^{(n)}}{\partial t} = -\int_{V(t)} dq^{(n-1)} = -\int_{\partial V(t)} q^{(n-1)}, \tag{G.4}$$

i.e. the time-rate of change of mass in the volume is balanced by the flux of the material through the volume's boundary. Additionally, we may want to take into account diffusive fluxes. Diffusive fluxes satisfy some constitutive law of the form,

$$q^{(n-1)}_{\text{diffusive}} = -\epsilon d^* \rho^{(3)},$$

where the material parameter $\epsilon > 0$ is the rate of diffusion. Examples of these constitutive laws are discussed in section 2.5. The total flux is then equal to the sum of the advective flux and the diffusive flux, $q^{(n-1)} = i_{\boldsymbol{v}} \rho^{(3)} - \epsilon d^* \rho^{(3)}$. Substituting this relation into Equation G.4 yields,

$$\begin{aligned} &\int_{V(t)} \frac{\partial \rho^{(n)}}{\partial t} = -\int_{V(t)} d(i_{\boldsymbol{v}} - \epsilon d^*)\rho^{(3)} \\ \Leftrightarrow &\int_{V(t)} \left(\frac{\partial \rho^{(n)}}{\partial t} + \mathscr{L}_{\boldsymbol{v}} \rho^{(n)} - \epsilon \Delta \rho^{(n)} \right) = 0, \end{aligned}$$

where we assumed ϵ to be constant. The result is known as the *scalar advection-diffusion equation*. Note that in the case of *convection*, when $\rho^{(3)}$ is the mass density of the flow itself, there cannot be an additional diffusive term. In that case all information governing

the flow of the material is contained in its velocity $\boldsymbol{v}$. In the case of a convection problem, conservation of mass is governed by,

$$\int_{V(t)} \left(\frac{\partial \rho^{(n)}}{\partial t} + \mathscr{L}_{\boldsymbol{v}} \rho^{(n)} \right) = 0. \tag{G.5}$$

Under the assumption of incompressible flow, variations of mass density $\rho^{(n)}$ are negligible within the volume $V(t)$, i.e. derivatives of ρ are assumed to be zero. For this case we find that,

$$\begin{aligned} 0 &= \int_{V(t)} \left(\cancel{\frac{\partial \rho^{(n)}}{\partial t}} + \mathscr{L}_{\boldsymbol{v}} \rho^{(n)} \right) \\ &= \int_{V(t)} d\rho\, v^{(n-1)} \\ &= \int_{V(t)} \rho\, dv^{(n-1)}. \end{aligned}$$

Hence an incompressible smooth flow in $V(t)$ satisfies $dv^{(n-1)} = 0$. We will refer to this condition as the *incompressibility constraint*. Note that by the Poincaré lemma, Theorem 2.1, there exists some potential function $\psi^{(n-2)}$, such that $d\psi^{(n-2)} = v^{(n-1)}$. This potential function is known as the *stream function*.

Example G.2 (Stream function $\psi^{(n-2)}$)**.**
We can retrieve the path of a fluid parcel by determining iso-surfaces of the stream function. Consider some fluid parcel with mass density $\rho^{(n)}$ that is advected along some flow with velocity field $\boldsymbol{v}$ on $\mathscr{M}$. Along its path we find that,

$$\mathscr{L}_{\boldsymbol{v}} \phi_t \rho^{(n)} \overset{4.3}{=} \frac{d}{dt} [\phi_t^* \phi_t \rho^{(n)}] = \frac{d}{dt} \left[\rho^{(n)} \big|_{t=0} \right] = 0.$$

Hence it follows that $d i_{\boldsymbol{v}} \rho^{(n)} = dq^{(n-1)} = 0$. By the Poincaré lemma, Theorem 2.1, there exists a potential function $\psi^{(n-2)}$, such that $d\psi^{(n-2)} = q^{(n-1)}$. Note that the stream function satisfies the equation $i_{\boldsymbol{v}} d\psi^{(n-2)} = i_{\boldsymbol{v}} q^{(n-1)} = i_{\boldsymbol{v}} i_{\boldsymbol{v}} \rho^{(n)} = 0$.

Now consider the case of incompressible flow, for which the there exists a stream function $\psi^{(n-2)}$, such that $d\psi^{(n-2)} = v^{(n-1)}$. Hence,

$$\begin{aligned} \mathscr{L}_{\boldsymbol{v}} \rho^{(n)} &= d(\rho^{(0)} \wedge v^{(n-1)}) \\ &= d\rho^{(0)} \wedge v^{(n-1)} + \cancel{\rho^{(0)} \wedge dv^{(n-1)}} \\ &= d\rho^{(0)} \wedge d\psi^{(n-2)} \end{aligned}$$

Let γ be a $(n-1)$-dimensional iso-contour of the stream function $\psi^{(n-2)}$, i.e. a submanifold on which $\psi^{(n-2)}$ equals some constant. Satisfying the conservation of mass, Equation G.5, along this iso-contour yields,

$$0 = \frac{\partial \rho^{(n)}}{\partial t} + \mathscr{L}_{\boldsymbol{v}} \rho^{(n)} = \frac{\partial \rho^{(n)}}{\partial t} + \cancel{d\rho^{(0)} \wedge d\psi^{(n-2)}}, \quad \forall x \in \gamma.$$

Hence the fluid parcel remains constant along γ, and γ is its path. If the flow field is time dependent, then iso-contours are streaklines. Now let A be the $(n-1)$-dimensional surface that is bounded by various iso-contours of $\psi^{(n-2)}$, e.g. as shown in Figure G.1. Then the integral flux through A is constant,

$$\int_A q^{(n-1)} = \int_A d\psi^{(n-2)} = \int_{\partial A} \psi^{(n-2)} = C.$$

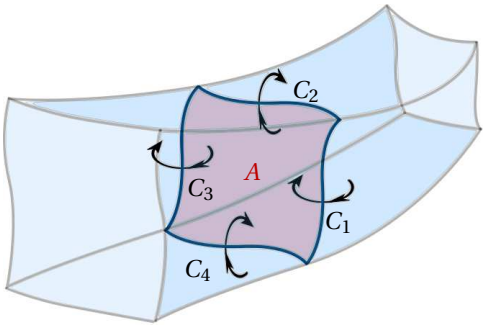

Figure G.1: Surface A (red) bounded by iso-surfaces (blue) of the stream function $\psi^{(1)} = \{C_1, C_2, C_3, C_4\}$. The integral flux is constant for any area bounded by the iso-surfaces, $\int_A q^{(2)} = \int_{\partial A} \psi^{(1)} = C_1 - C_2 - C_3 + C_4$.

From the principle of conservation of mass of some quantity with mass density $\rho^{(n)}$ that is transported along some incompressible flow with velocity field $\boldsymbol{v}$ we can formulate 4 equivalent formulations,

$$\frac{\partial \rho^{(n)}}{\partial t} + \mathcal{L}_{\boldsymbol{v}} \rho^{(n)} = 0, \tag{G.6}$$

$$\frac{\partial \rho^{(n)}}{\partial t} - \mathcal{L}^*_{\boldsymbol{v}} \rho^{(n)} = 0, \tag{G.7}$$

$$\frac{\partial \rho^{(0)}}{\partial t} + \mathcal{L}_{\boldsymbol{v}} \rho^{(0)} = 0, \tag{G.8}$$

$$\frac{\partial \rho^{(0)}}{\partial t} - \mathcal{L}^*_{\boldsymbol{v}} \rho^{(0)} = 0, \tag{G.9}$$

where $\rho^{(n)} = \rho \, \mathrm{vol}^{(n)} = \rho^{(0)} \wedge \mathrm{vol}^{(n)}$ or $\rho^{(0)} = \star \rho^{(n)}$. Equation G.6 and Equation G.9 are known as *conservative* formulations of the conservation of mass, whereas Equation G.7 and Equation G.8, are known as *non-conservative* formulations.

Proof. Equation G.6 follows from the integral conservation of mass, Equation G.5, under the assumption of smoothness within $V(t)$. We can derive Equation G.9 by taking the Hodge-$\star$ of Equation G.6,

$$\star \mathcal{L}_{\boldsymbol{v}} \rho^{(n)} = \star \mathcal{L}_{\boldsymbol{v}} \star \rho^{(0)} \overset{4.19}{=} -\mathcal{L}^*_{\boldsymbol{v}} \rho^{(0)}.$$

The same strategy can be used to derive Equation G.7 from Equation G.8. Equivalence of Equation G.6 and Equation G.8 can be shown by comparing $\mathscr{L}_{\boldsymbol{v}}\rho^{(n)}$ with $\star\mathscr{L}_{\boldsymbol{v}}\rho^{(0)}$,

$$\mathscr{L}_{\boldsymbol{v}}\rho^{(n)} = d\,i_{\boldsymbol{v}}(\rho^{(0)} \wedge \mathrm{vol}^{(n)}) = d(\rho^{(0)} \wedge v^{(n-1)}) = d\rho^{(0)} \wedge v^{(n-1)} + \rho^{(0)} \wedge \cancel{d v^{(n-1)}},$$
$$\star\mathscr{L}_{\boldsymbol{v}}\rho^{(0)} = \star\, i_{\boldsymbol{v}} d\rho^{(0)} = \star\star\,(\star d\rho^{(0)} \wedge v^{(1)}) = d\rho^{(0)} \wedge \star v^{(1)} = d\rho^{(0)} \wedge v^{(n-1)},$$

where we used the assumption of incompressible flow, $d\,v^{(n-1)} = 0$. And hence it follows that $\mathscr{L}_{\boldsymbol{v}}\rho^{(n)} = \star\mathscr{L}_{\boldsymbol{v}}\rho^{(0)}$. □

H

Construction of Periodic Basis

In this chapter we show how the periodic basis of Figure 4.5 can be constructed from an ordinary B-spline basis through knot insertion on the domain $\Omega = [0,1]$. The periodic basis can be seen as an interior part of an extended ordinary B-spline basis, Figure H.1. Through knot insertion we can lower the continuity of the basis at $\partial\Omega$, such that the interior part becomes an ordinary basis. From the knot insertion algorithm, Definition 3.6, we obtain the mapping $\mathbb{T}^p : \mathcal{T}_n^p \rightarrow \mathcal{S}_{n+2(p-1)}^p$. This mapping can be manipulated such that it links the basis functions crossing $\partial\Omega$.

Consider the B-spline shown in top of Figure H.1 with dimension $n = 8$ polynomial order $p = 2$, and knot vector,

$$\Xi = \frac{1}{4}\{-1,-1,-1,0,1,2,3,4,5,5,5\}.$$

To obtain C^0 at $\partial\Omega$, we insert the knots $\{0,1\}$. From Definition 3.6 we obtain the linear map to the new $n = 10$ dimensional basis,

$$\mathbb{T} = \begin{bmatrix} 1 & 0 & 0 & 0 & 0 & 0 & 0 & 0 \\ 0 & 1 & 0 & 0 & 0 & 0 & 0 & 0 \\ 0 & \frac{1}{2} & \frac{1}{2} & 0 & 0 & 0 & 0 & 0 \\ 0 & 0 & 1 & 0 & 0 & 0 & 0 & 0 \\ 0 & 0 & 0 & 1 & 0 & 0 & 0 & 0 \\ 0 & 0 & 0 & 0 & 1 & 0 & 0 & 0 \\ 0 & 0 & 0 & 0 & 0 & 1 & 0 & 0 \\ 0 & 0 & 0 & 0 & 0 & \frac{1}{2} & \frac{1}{2} & 0 \\ 0 & 0 & 0 & 0 & 0 & 0 & 1 & 0 \\ 0 & 0 & 0 & 0 & 0 & 0 & 0 & 1 \end{bmatrix}$$

We delete the first- and last $p = 2$ rows and $(p-1=1)$ columns corresponding to basis

functions supported outside the domain Ω,

$$\mathbb{T} = \begin{bmatrix} \frac{1}{2} & \frac{1}{2} & 0 & 0 & 0 & 0 \\ 0 & 1 & 0 & 0 & 0 & 0 \\ 0 & 0 & 1 & 0 & 0 & 0 \\ 0 & 0 & 0 & 1 & 0 & 0 \\ 0 & 0 & 0 & 0 & 1 & 0 \\ 0 & 0 & 0 & 0 & \frac{1}{2} & \frac{1}{2} \end{bmatrix}$$

The first- and final ($p = 2$) basis functions cross the boundary $\partial\Omega$. The ($p = 2$)nd basis function can be linked to the final ($n + p = 6$)th basis function, and the ($p - 1 = 1$)st basis function can be linked to the ($n + p - 1 = 5$)th basis function. Hence we add the 5th column to the 1st, and the 6th to the 2nd,

$$\mathbb{T} = \begin{bmatrix} \frac{1}{2} & \frac{1}{2} & 0 & 0 \\ 0 & 1 & 0 & 0 \\ 0 & 0 & 1 & 0 \\ 0 & 0 & 0 & 1 \\ 1 & 0 & 0 & 0 \\ \frac{1}{2} & \frac{1}{2} & 0 & 0 \end{bmatrix}$$

Hence we have obtained the map $\mathbb{T} : \mathscr{P}_4^2 :\rightarrow \mathscr{S}_6^2$. The reverse mapping that maps the ordinary basis to the periodic equals the transpose $\mathbb{T}^T : \mathscr{S}_6^2 \rightarrow \mathscr{P}_4^2$, hence,

$$(\mathbb{T}_{ij})^T \lambda_{i,p} = \lambda_{j,p}^{pd} \quad \Leftrightarrow \quad \mathbb{T}^T \lambda_p = \lambda_p^{pd}$$

We can use $\mathbb{T}$ to map mass matrices on periodic domains,

$$\begin{aligned} \mathbb{M}^{pd} &= \left(\lambda_p^{pd}, \lambda_p^{pd}\right)_\Omega \\ &= \int_\Omega \lambda_p^{pd} \wedge \star \lambda_p^{pd} \\ &= \int_\Omega \left(\mathbb{T}^T \lambda_p\right) \wedge \star \left(\mathbb{T}^T \lambda_p\right) \\ &= \mathbb{T}^T \left(\int_\Omega \lambda_p \wedge \star \lambda_p\right) \mathbb{T} \\ &= \mathbb{T}^T \mathbb{M} \mathbb{T}. \end{aligned}$$

This enables us to use the normal assembly routines to construct mass matrices on periodic domains.

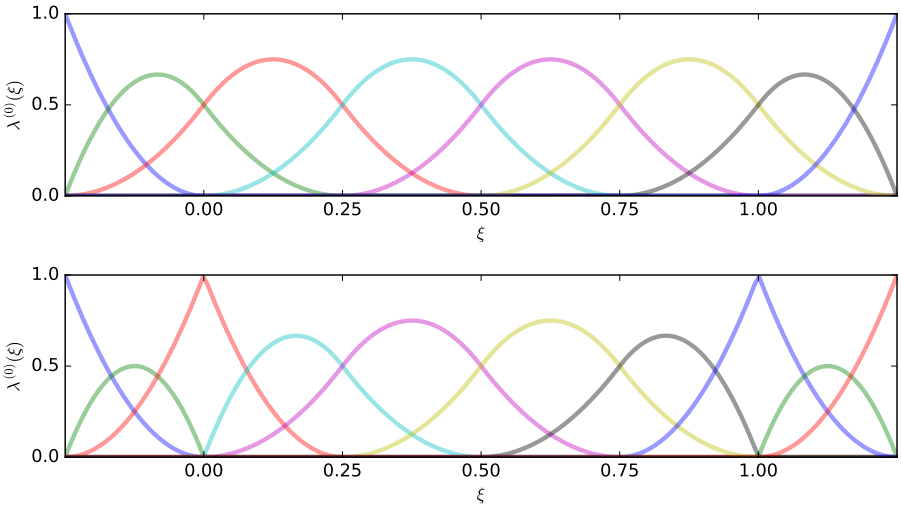

Figure H.1: The periodic basis can be constructed by taking the inner part of an extended basis (top) and linking the functions crossing the boundary of $\Omega = [0, 1]$. Through knot insertion we can obtain a second basis (bottom) whose inner part is an ordinary B-spline basis on Ω.

I

DERIVATION OF THE EULER EQUATIONS AND INVARIANTS

In *Euler equations* express conservation of mass, momentum, and energy in fluid dynamics. In Appendix G, we derived an invariant formulation for the conservation of mass using the transport theorem, Theorem 4.2. In this section we will derive and analyse the momentum equations. In incompressible flow, i.e. variations in mass density $\rho^{(n)}$ are assumed to be small, we can solve the mass and momentum equation without solving the energy equation. The conservation of momentum under the assumption of a perfect fluid (viscous effects and shear stresses are assumed to be zero) and incompressible flow in $\mathbb{R}^n$ is given by,

$$\frac{\partial v_j}{\partial t} + v_i \left(\frac{\partial v_j}{\partial x^i} \right) = -\frac{1}{\rho} \frac{\partial p}{\partial x^j} + b_j, \tag{I.1}$$

with v_i the components of the velocity field with $j = \{1, \cdots, n\}$, p the pressure, ρ the mass density, and b_i components of body force.

To transform to invariant formulation we consider the momentum 1-form, $P^{(1)}$. The momentum 1-form associates mass density with velocity along a line, dual to the mass flux $q^{(n-1)} = i_{\boldsymbol{v}} \rho^{(n)}$. We define,

$$P^{(1)} = \rho v^{(1)} = \rho \star v^{(n-1)} = \star \rho i_{\boldsymbol{v}} \mathrm{vol}^{(n)} = \star i_{\boldsymbol{v}} \rho^{(n)} = \star q^{(n-1)},$$

with $v^{(1)} = v_i dx^i$. The Lie-derivative of this velocity 1-form is given by,

$$\begin{aligned}
\mathscr{L}_{\boldsymbol{v}} v^{(1)} &= (d i_{\boldsymbol{v}} + i_{\boldsymbol{v}} d)\, v^{(1)} \\
&= d v_i^2 + i_{\boldsymbol{v}} \frac{\partial v_i}{\partial x^j} dx^j \wedge dx^i \\
&= 2 v_i \frac{\partial v_i}{\partial x^j} dx^j + v_i \frac{\partial v_j}{\partial x^i} dx^j - v_i \frac{\partial v_i}{\partial x^j} dx^j \\
&= v_i \frac{\partial v_j}{\partial x^i} dx^j + \frac{1}{2} \frac{\partial v_i^2}{\partial x^j} dx^j,
\end{aligned}$$

and so,

$$\frac{\partial v^{(1)}}{\partial t} + \mathscr{L}_{\boldsymbol{v}} v^{(1)} = \left(\frac{\partial v_j}{\partial t} + v_i \frac{\partial v_j}{\partial x^i} + \frac{1}{2} \frac{\partial v_i^2}{\partial x^j} \right) dx^j,$$

which contains the terms on the right-hand-side of Equation I.1 plus an additionaal term containing the kinetic energy $\frac{1}{2} v_i^2 = \frac{1}{2} i_{\boldsymbol{v}} v^{(1)} = \frac{1}{2} \| v^{(1)} \|^2$. Pressure and density are related through a constitutive equation or an *equation of state*, $p = p(\rho)$. Let $G(\rho) := \int \frac{dp}{\rho} = \frac{1}{\rho} \frac{dp}{d\rho} d\rho$, then

$$dG(\rho) = \frac{\partial G(\rho)}{\partial x^j} dx^j = G'(\rho) \frac{\partial \rho}{x^j} dx^j = \frac{1}{\rho} \frac{dp}{d\rho} \frac{\partial \rho}{\partial x^j} dx^j = \frac{1}{\rho} \frac{\partial p}{\partial x^j} dx^j.$$

Finally we assume the body force $b^{(1)}$ is uniform, e.g. gravity, such that $d b^{(1)} = 0$. Then there exists a potential function $\phi^{(0)}$, Theorem 2.1, such that $-d\phi^{(0)} = b^{(1)}$. Now by matching components with Equation I.1 we find the invariant form of the equations for conservation of momentum,

$$\frac{\partial v^{(1)}}{\partial t} + \mathscr{L}_{\boldsymbol{v}} v^{(1)} - \frac{1}{2} \| v^{(1)} \|^2 = -d \left(\phi^{(0)} + \int \frac{dp}{\rho} \right).$$

Note that this formulation of the momentum equations is known as

In Example G.1 we derived that conservation of mass for an incompressible fluid can be expressed as $d v^{(n-1)} = 0$, or $d^* v^{(1)} = 0$. Note that for this case there exists a potential function, the stream function $\psi^{(n-2)}$ or $\psi^{(2)}$, such that $d\psi^{(n-2)} = v^{(n-1)}$ or $d^* \psi^{(2)} = v^{(1)}$.

Theorem I.1 (Euler Equations for Incompressible Flow, (Sec. 4.3c [18]))**.** *The equations for conservation of mass and momentum for an ideal incompressible fluid on manifold $\mathcal{M} \subset \mathbb{R}^n$ are given by,*

$$d^* v^{(1)} = 0 \tag{I.2}$$

$$\frac{\partial v^{(1)}}{\partial t} + \mathscr{L}_{\boldsymbol{v}} v^{(1)} = -d f^{(0)}, \tag{I.3}$$

where $\boldsymbol{v}$ is the velocity-vector field, $v^{(1)}$ the velocity 1-form associated with $\boldsymbol{v}$, and $f^{(0)}$,

$$f^{(0)} = \int \frac{dp}{\rho} - \frac{1}{2} \| v^{(1)} \|^2 + \phi^{(0)},$$

with pressure p, mass density ρ, and potential $\phi^{(0)}$. We can solve for $f^{(0)}$ using the pressure Poisson equation, which can be obtained by taking the codifferetial d^* of Equation I.3, and substitute the incompressibility constraint, Equation I.2,

$$d^* \mathscr{L}_{\boldsymbol{v}} v^{(1)} = -\Delta f^{(0)}. \tag{I.4}$$

Next we introduce the vorticity 2-form $\omega^{(2)}$, which is a measure of rotation within the flow. We derive an equation for the vorticity by taking the exterior derivative d of equation Equation I.1,

$$d \left(\frac{\partial v^{(1)}}{\partial t} + \mathscr{L}_{\boldsymbol{v}} v^{(1)} \right) = \frac{\partial \omega^{(2)}}{\partial t} + \mathscr{L}_{\boldsymbol{v}} \omega^{(2)} = -d d f^{(0)} = 0.$$

From the incompressibility constraint we know that there exists a stream function such that $v^{(1)} = d^*\psi^{(2)}$. We find,

$$\omega^{(2)} = d v^{(1)} = d d^* \psi^{(2)} = \Delta \psi^{(2)}.$$

Vorticity and the stream function are related through a Poisson equation.

Example I.1 (Conservation of circulation)**.** We can pair Equation I.3 with some curve $\gamma(t) \subset \mathcal{M}$,

$$\int_{\gamma(t)} \frac{\partial v^{(1)}}{\partial t} + \mathcal{L}_{\boldsymbol{v}} v^{(1)} = -\int_{\gamma(t)} d f^{(0)} = -\int_{\partial\gamma(t)} f^{(0)}.$$

We define *circulation* $\Gamma := \int_{\gamma(t)} v^{(1)}$. Using the transport theorem, Theorem 4.2, we find,

$$\frac{d}{dt}\Gamma = \frac{d}{dt}\int_{\gamma(t)} v^{(1)} = -\int_{\partial\gamma(t)} f^{(0)}. \tag{I.5}$$

Hence along any closed curve $\gamma(t)$ the circulation Γ is constant in time. This result is known as *Kelvin's circulation theorem*.

Example I.2 (Conservation of Vorticity)**.** We can pair Equation 5.6 with some surface $A(t) \subset \mathcal{M}$ and use the transport theorem Theorem 4.2 to find,

$$\frac{d}{dt}\int_{A(t)} \omega^{(2)} = 0,$$

i.e. the integral vorticity within a surface is conserved over time. This result is simply a re-exprssion of Kelvin's theorem for conservation of circulation, Equation I.5,

$$\frac{d}{dt}\int_{A(t)} \omega^{(2)} = \frac{d}{dt}\int_{A(t)} d v^{(1)} = \frac{d}{dt}\int_{\partial A(t)} v^{(1)} = 0, \tag{I.6}$$

with $\partial A(t) = \gamma(t)$ the closed curve that bounds a surface. Note that we can Equation 5.6 as,

$$\mathcal{L}_{\boldsymbol{X}} \omega^{(2)} = 0,$$

with $\boldsymbol{X} = \frac{\partial}{\partial t} + \boldsymbol{v}$ the space-time velocity field. Hence vorticity is invariant under the flow related to $\boldsymbol{X}$.

Example I.3 (Conservation of Helicity)**.** Finally we consider the *helicity* 3-form $h^{(3)} := v^{(1)} \wedge \omega^{(2)}$. From the properties of the Lie-derivative,Definition 4.1, we find that,

$$\mathcal{L}_{\boldsymbol{X}} h^{(3)} = \mathcal{L}_{\boldsymbol{X}}\left(v^{(1)} \wedge \omega^{(2)}\right) = \mathcal{L}_{\boldsymbol{X}} v^{(1)} \wedge \omega^{(2)} + v^{(1)} \wedge \mathcal{L}_{\boldsymbol{X}} \omega^{(2)} = -d f^{(0)} \wedge \omega^{(2)} + \cancel{v^{(1)} \wedge 0}.$$

Now,

$$d\left(f^{(0)} \wedge \omega^{(2)}\right) = d\left(f^{(0)} \wedge d v^{(1)}\right) = d f^{(0)} \wedge d v^{(1)} + \cancel{f^{(0)} \wedge d d v^{(1)}} = d f^{(0)} \wedge \omega^{(2)}.$$

Again by applying the transport theorem after pairing helicity with some volume $V(t) \subset \mathcal{M}$, we find

$$\frac{d}{dt}\int_{V(t)} h^{(3)} = \int_{V(t)} \mathscr{L}_{\boldsymbol{X}} h^{(3)} = -\int_{V(t)} d\left(f^{(0)} \wedge \omega^{(2)}\right) = -\int_{\partial V(t)} f^{(0)} \wedge \omega^{(2)} = 0, \tag{I.7}$$

i.e. the integral helicity is conserved over time.

Example I.4 (Conservation of Kinetic Energy)**.** The weak formulation is valid for any test-function $w^{(1)}$, taking $w^{(1)} := v^{(1)}$, we obtain an equation for the evolution of kinetic energy,

$$\left(v^{(1)}, \partial_t v^{(1)}\right)_{\mathcal{M}} + \left(v^{(1)}, \mathscr{L}_{\boldsymbol{v}} v^{(1)}\right)_{\mathcal{M}} = -\left(v^{(1)}, d f^{(0)}\right)_{\mathcal{M}}, \tag{I.8}$$

where $\left(v^{(1)}, \partial_t v^{(1)}\right)_{\mathcal{M}} = \frac{1}{2}\partial_t \left(v^{(1)}, v^{(1)}\right)_{\mathcal{M}} = \frac{1}{2}\partial_t \|v^{(1)}\|^2$, i.e. the time-rate-of-change of the kinetic energy. We can substitute this identity and integrate by parts to obtain,

$$\begin{aligned}\frac{1}{2}\frac{\partial}{\partial t}\|v^{(1)}\|^2 + \cancel{\left(d^* v^{(1)}, i_{\boldsymbol{v}} v^{(1)}\right)_{\mathcal{M}}} + \cancel{\left(v^{(1)} \wedge v^{(1)}, d v^{(1)}\right)_{\mathcal{M}}} \\ = -\left(v^{(1)}, i_{\boldsymbol{v}} v^{(1)}\right)_{\partial\mathcal{M}} - \cancel{\left(d^* v^{(1)}, f^{(0)}\right)_{\mathcal{M}}} - \left(v^{(1)}, f^{(0)}\right)_{\partial\mathcal{M}}.\end{aligned}$$

By properties of the wedge product we find $v^{(1)} \wedge v^{(1)} = -v^{(1)} \wedge v^{(1)}$, such that $v^{(1)} \wedge v^{(1)} = 0$. Furthermore $d^* v^{(1)} = 0$ for incompressible flow, and so we obtain,

$$\frac{1}{2}\frac{\partial}{\partial t}\|v^{(1)}\|^2 = -\left(v^{(1)}, i_{\boldsymbol{v}} v^{(1)} + f^{(0)}\right)_{\partial\mathcal{M}}.$$

It follows that the integral amount of kinetic energy within the domain is balanced by some boundary flux-term, and hence conserved within boundary-less domains. A similar result by deriving a weak formulation of the dual formulation.

We obtain a weak formulation of the primal vorticity formulation of the momentum equation, Equation 5.6, by taking the inner product with some test function $s^{(2)} \in \Lambda^{(2)}(\mathcal{M})$, and obtain,

$$\left(s^{(2)}, \partial_t \omega^{(2)}\right)_{\mathcal{M}} + \left(s^{(2)}, d i_{\boldsymbol{v}} \omega^{(2)}\right)_{\mathcal{M}} = 0 \tag{I.9}$$

Example I.5 (Conservation of Enstrophy $\|\omega^{(2)}\|^2$ in $\mathbb{R}^2$)**.** We take $s^{(2)} := \omega^{(2)}$ in weak formulation, Equation I.9, to obtain an equation for the evolution *enstrophy*,

$$\frac{1}{2}\frac{\partial}{\partial t}\|\omega^{(2)}\|^2 + \left(\omega^{(2)}, \mathscr{L}_{\boldsymbol{v}} \omega^{(2)}\right)_{\mathcal{M}} = 0, \tag{I.10}$$

where $\left(\omega^{(2)}, \partial_t \omega^{(2)}\right)_{\mathcal{M}} = \frac{1}{2}\partial_t \left(\omega^{(2)}, \omega^{(2)}\right)_{\mathcal{M}} = \frac{1}{2}\partial_t \|\omega^{(2)}\|^2$, i.e. the time-rate-of-change of enstrophy. In $\mathcal{M} \subset \mathbb{R}^2$ vorticity $\omega^{(2)} = \omega^{(0)} \wedge \mathrm{vol}^{(2)} = \omega \mathrm{vol}^{(2)}$ is a scalar field, and hence,

$$\left(\omega^{(2)}, \mathscr{L}_{\boldsymbol{v}} \omega^{(2)}\right)_{\mathcal{M}} = \frac{1}{2}\int_{\mathcal{M}} d\|\omega\|^2 q^{(1)} = \int_{\partial\mathcal{M}} \|\omega\|^2 q^{(1)}, \tag{I.11}$$

where $q^{(1)}$ is the velocity $(n-1)$-form associated with the vector field $\boldsymbol{v}$. In $\mathbb{R}^2$ we use $v^{(1)}$ and $q^{(1)}$ to distinguish between the various 1-forms that are associated with $\boldsymbol{v}$. It follows that the enstrophy is balanced by some boundary flux-term. Note that this result is only valid in $\mathbb{R}^2$. In $\mathbb{R}^3$ vortex stretching leads to very different mechanics.

J

PROOF DISCRETE EULER EQUATIONS SATISFY CONSERVATION LAWS

In this chapter we prove that the semi-discrete equations introduced in section 5.2 satisfy conservation of integral mass, vorticity, kinetic-energy, and enstrophy at each time instant. Consider the vorticity-stream formulation,

$$\begin{bmatrix} -\mathbb{M}^{(1,1)} & \left(\mathbb{E}^{(2,1)}\right)^T \mathbb{M}^{(2,2)} \\ \mathbb{E}^{(2,1)} & \emptyset \end{bmatrix} \begin{bmatrix} \boldsymbol{h} \\ \boldsymbol{g} \end{bmatrix} = \begin{bmatrix} \mathbf{0} \\ -\mathbb{E}^{(2,1)} \left(\mathbb{M}^{(1,1)}\right)^{-1} \mathbb{C}^{(1,1)}_{\boldsymbol{\omega}_h} \boldsymbol{q} \end{bmatrix} \tag{J.1}$$

$$\mathbb{M}^{(1,1)} \frac{\partial \boldsymbol{q}}{\partial t} - \mathbb{C}^{(1,1)}_{\boldsymbol{\omega}_h} \boldsymbol{q} = \left(\mathbb{E}^{(2,1)}\right)^T \mathbb{M}^{(2,2)} \boldsymbol{g}. \tag{J.2}$$

1. **Conservation of Mass:**
   We obtain an equation for the evolution of the divergence of the velocity field by pre-multiplying the discrete momentum equation, Equation J.2, with $\mathbb{E}^{(2,1)} \left(\mathbb{M}^{(1,1)}\right)^{-1}$,

   $$\mathbb{E}^{(2,1)} \frac{\partial \boldsymbol{q}}{\partial t} - \cancel{\mathbb{E}^{(2,1)} \left(\mathbb{M}^{(1,1)}\right)^{-1} \mathbb{C}^{(1,1)}_{\boldsymbol{\omega}_h} \boldsymbol{q}} = \cancel{\mathbb{E}^{(2,1)} \left(\mathbb{M}^{(1,1)}\right)^{-1} \left(\mathbb{E}^{(2,1)}\right)^T \mathbb{M}^{(2,2)} \boldsymbol{g}},$$

   with the two terms cancel out by Equation J.1.

2. **Conservation of Vorticity:**
   Vorticity and velocity are related through $\omega_h^{(0)} = d^* q_h^{(1)}$, or

   $$\mathbb{M}^{(0,0)} \boldsymbol{\omega} = \left(\mathbb{E}^{(1,0)}\right)^T \mathbb{M}^{(1,1)} \boldsymbol{q}.$$

The integral vorticity is then given by,

$$\int_\Omega \omega_h^{(0)} d\Omega = \left(1, \omega_h^{(0)}\right)_\Omega = \mathbf{1}^T \mathbb{M}^{(0,0)} \boldsymbol{\omega} = \cancel{\mathbf{1}^T \left(\mathbb{E}^{(1,0)}\right)^T \mathbb{M}^{(1,1)} \boldsymbol{q}} = 0,$$

where again $\mathbb{E}^{(1,0)}\mathbf{1} = \mathbf{0}$. This is the discrete version of Kelvin's circulation theorem.

3. **Conservation of Kinetic Energy:**
We define the error $e_q^{(1)} = q^{(1)} - q_h^{(1)}$ with, $q_h^{(1)} = \boldsymbol{q}^T \boldsymbol{\phi}^{(1)}$. We find,

$$\begin{aligned} 0 = \frac{1}{2}\frac{\partial}{\partial t}\|q^{(1)}\|^2 &= \left(q_h^{(1)} + e_q^{(1)}, \partial_t q_h^{(1)} + \partial_t e_q^{(1)}\right)_\Omega \\ &= \frac{1}{2}\frac{\partial}{\partial t}\left(\|q_h^{(1)}\|^2 + \|e_q^{(1)}\|^2\right) + \cancel{\left(q_h^{(1)}, \partial_t e_q^{(1)}\right)_\Omega} + \cancel{\left(e_q^{(1)}, \partial_t q_h^{(1)}\right)_\Omega} \\ &\frac{1}{2}\frac{\partial}{\partial t}\left(\|q_h^{(1)}\|^2 + \|e_q^{(1)}\|^2\right). \end{aligned}$$

It follows that the discrete kinetic energy, $\frac{1}{2}\|q_h^{(1)}\|^2$ is balanced by the error's kinetic energy. Hence by constructing a scheme that conserves the discrete kinetic energy, we consistently approximate the continuous kinetic energy, and bound the growth of the error's kinetic energy. Th evolution of the discrete kinetic energy is given by,

$$\frac{1}{2}\frac{d}{dt}\int_\Omega q_h^{(1)} \wedge \star q_h^{(1)} = \left(q_h^{(1)}, \partial_t q_h^{(1)}\right)_\Omega = \boldsymbol{q}^T \mathbb{M}^{(1,1)} \frac{\partial \boldsymbol{q}}{\partial t}.$$

Hence by pre-multiplying Equation J.2 with $\boldsymbol{q}^T$ we obtain an equation for the evolution of the discrete kinetic energy,

$$\boldsymbol{q}^T \mathbb{M}^{(1,1)} \frac{\partial \boldsymbol{q}}{\partial t} - \cancel{\boldsymbol{q}^T \mathbb{C}^{(1,1)}_{\boldsymbol{\omega}_h} \boldsymbol{\omega}} = \cancel{\boldsymbol{q}^T \left(\mathbb{E}^{(2,1)}\right)^T \mathbb{M}^{(2,2)} \boldsymbol{g}}, \tag{J.3}$$

with the right-hand-side term reduces to zero by conservation of mass, $\mathbb{E}^{(2,1)}\boldsymbol{q} = \mathbf{0}$, and,

$$\begin{aligned} \boldsymbol{q}^T \mathbb{C}^{(1,1)}_{\boldsymbol{\omega}_h} \boldsymbol{\omega} &= \left(q_h^{(1)}, i^*_{\boldsymbol{\omega}_h} \star q_h^{(1)}\right)_\Omega = \left(q_h^{(1)}, i^*_{\boldsymbol{v}_h} \omega_h^{(0)}\right)_\Omega \\ &= \left(i_{\boldsymbol{v}_h} q_h^{(1)}, \omega_h^{(0)}\right)_\Omega = \left(i_{\boldsymbol{v}_h} i_{\boldsymbol{v}_h} \mathrm{vol}^{(2)}, \omega_h^{(0)}\right)_\Omega = 0. \end{aligned}$$

We find that the conservation of kinetic-energy depends on the nilpotency of the interior product.

4. **Conservation of Enstrophy:**
We obtain an equation for the evolution of enstrophy by taking the test function equal to the derivative of the vorticity,

$$\begin{aligned} \frac{1}{2}\frac{d}{dt}\int_\Omega \omega_h^{(0)} \wedge \star \omega_h^{(0)} &= \left(\omega_h^{(0)}, \partial_t \omega_h^{(0)}\right)_\Omega = \left(\omega_h^{(0)}, \partial_t d^* q_h^{(1)}\right)_\Omega \\ &= \left(d\omega_h^{(0)}, \partial_t q_h^{(1)}\right)_\Omega = \boldsymbol{\omega}^T \left(\mathbb{E}^{(1,0)}\right)^T \mathbb{M}^{(1,1)} \frac{\partial \boldsymbol{q}}{\partial t}. \end{aligned}$$

Hence, pre-multiplication of the discrete momentum equation, Equation J.2, with $\left(\mathbb{E}^{(1,0)}\boldsymbol{\omega}\right)^T$ yields,

$$\boldsymbol{\omega}^T\left(\mathbb{E}^{(1,0)}\right)^T\mathbb{M}^{(1,1)}\frac{\partial \boldsymbol{q}}{\partial t} - \cancel{\boldsymbol{\omega}^T\left(\mathbb{E}^{(1,0)}\right)^T\mathbb{C}^{(1,1)}_{\boldsymbol{\omega}_h}\boldsymbol{q}} = \cancel{\boldsymbol{\omega}^T\left(\mathbb{E}^{(1,0)}\right)^T\left(\mathbb{E}^{(2,1)}\right)^T\mathbb{M}^{(2,2)}\boldsymbol{g}},$$

where the right-hand-side term equals zero due to the exterior derivative's nilpotency. For the other term we find,

$$\boldsymbol{\omega}^T\left(\mathbb{E}^{(1,0)}\right)^T\mathbb{C}^{(1,1)}_{\boldsymbol{\omega}_h}\boldsymbol{q} = \left(d\omega_h^{(0)}, i^*_{\boldsymbol{v}_h}\omega_h^{(0)}\right)_\Omega = \left(i_{\boldsymbol{v}_h}d\omega_h^{(0)}, \omega_h^{(0)}\right)_\Omega \overset{J.6}{=} 0.$$

Next consider the velocity-pressure formulation,

$$\mathbb{M}^{(0,0)}\boldsymbol{\omega} + \left(\mathbb{E}^{(1,0)}\right)^T\mathbb{M}^{(1,1)}\mathbb{E}^{(1,0)}\boldsymbol{\psi} = \mathbf{0} \tag{J.4}$$

$$\mathbb{M}^{(0,0)}\frac{\partial \boldsymbol{\omega}}{\partial t} - \left(\mathbb{C}^{(0,1)}_{\boldsymbol{v}_h}\mathbb{E}^{(1,0)}\right)^T\boldsymbol{\omega} = \mathbf{0} \tag{J.5}$$

1. **Conservation of Mass:**
   Conservation of mass is trivial with $\boldsymbol{q} = \mathbb{E}^{(1,0)}\boldsymbol{\psi}$, such that $\mathbb{E}^{(2,1)}\boldsymbol{q} = \mathbf{0}$ with machine precision.

2. **Conservation of Vorticity:**
   We obtain an equation of the evolution of the integral vorticity by by taking the unit test-function, $1 = \mathbf{1}^T\boldsymbol{\phi}^{(0)}$,

   $$\frac{d}{dt}\int_\Omega \omega_h^{(0)}\,d\Omega = \left(1, \partial_t\omega_h^{(0)}\right)_\Omega = \mathbf{1}^T\mathbb{M}^{(0,0)}\frac{\partial \boldsymbol{\omega}}{\partial t}.$$

   Hence, pre-multiplying the discrete vorticity equation, Equation J.5, with the unit-vector $\mathbf{1}$ yields,

   $$\mathbf{1}^T\mathbb{M}^{(0,0)}\frac{\partial \boldsymbol{\omega}}{\partial t} - \cancel{\mathbf{1}^T\left(\mathbb{C}^{(0,1)}_{\boldsymbol{v}_h}\mathbb{E}^{(1,0)}\right)^T\boldsymbol{\omega}} = \mathbf{0},$$

   where $\mathbb{E}^{(1,0)}\mathbf{1} = \mathbf{0}$ trivially. So the discrete conservation of vorticity is satisfied through the exterior derivative.

3. **Conservation of Kinetic Energy:**
   We obtain an equation of the evolution of the integral kinetic energy by taking the test-function equal to the stream function,

   $$\frac{1}{2}\frac{d}{dt}\|q_h^{(1)}\|^2 = \left(q_h^{(1)}, \partial_t q_h^{(1)}\right)_\Omega = \left(d\psi_h^{(0)}, \partial_t q_h^{(1)}\right)_\Omega = \left(\psi_h^{(0)}, \partial_t\omega_h^{(0)}\right)_\Omega = \boldsymbol{\psi}^T\mathbb{M}^{(0,0)}\frac{\partial \boldsymbol{\omega}}{\partial t}.$$

   Pre-multiplication of Equation J.5 with $\boldsymbol{\psi}$ yields,

   $$\boldsymbol{\psi}^T\mathbb{M}^{(0,0)}\frac{\partial \boldsymbol{\omega}}{\partial t} - \cancel{\boldsymbol{\psi}^T\left(\mathbb{C}^{(0,1)}_{\boldsymbol{v}_h}\mathbb{E}^{(1,0)}\right)^T\boldsymbol{\omega}} = 0,$$

where,

$$\boldsymbol{\psi}^T \left(\mathbb{C}^{(0,1)}_{\boldsymbol{v}_h}\mathbb{E}^{(1,0)}\right)^T \boldsymbol{\omega} = \boldsymbol{q}^T \left(\mathbb{C}^{(0,1)}_{\boldsymbol{v}_h}\right)^T \boldsymbol{\omega} = \left(i_{\boldsymbol{v}_h} q_h^{(1)}, \omega^{(0)}\right)_\Omega = \left(i_{\boldsymbol{v}_h} i_{\boldsymbol{v}_h} \mathrm{vol}^{(2)}, \omega^{(0)}\right)_\Omega = 0.$$

Conservation of kinetic energy depends on the nilpotency of the interior product, which in this case is exactly satisfied due to the construction of $q_h^{(1)} = i_{\boldsymbol{v}_h}\mathrm{vol}^{(2)}$.

4. **Conservation of Enstrophy:**
Next we'll analyze the enstrophy. We define error $e_\omega^{(0)} = \omega^{(0)} - \omega_h^{(0)}$, and find,

$$\begin{aligned}
0 = \frac{1}{2}\frac{\partial}{\partial t}\|\omega^{(0)}\|^2 &= \frac{1}{2}\frac{\partial}{\partial t}\left(\omega_h^{(0)} + e_\omega^{(0)}, \partial_t \omega_h^{(0)} + \partial_t e_\omega^{(0)}\right)_\Omega \\
&= \frac{1}{2}\frac{\partial}{\partial t}\left(\|\omega_h^{(0)}\|^2 + \|e_\omega^{(0)}\|^2\right) + \cancel{\left(\omega_h^{(0)}, \partial_t e_\omega^{(0)}\right)_\Omega} + \cancel{\left(e_\omega^{(0)}, \partial_t \omega_h^{(0)}\right)_\Omega} \\
&= \frac{1}{2}\frac{\partial}{\partial t}\left(\|\omega_h^{(0)}\|^2 + \|e_\omega^{(0)}\|^2\right)
\end{aligned}$$

It follows that the discrete enstrophy, $\frac{1}{2}\|\omega_h^{(0)}\|^2$, is balanced by the error's enstrophy. Hence the error's enstrophy is bounded if we can construct a scheme that conserves the discrete enstrophy. Furthermore, the generalized Poincaré inequality, Equation D.2, states,

$$\|q_h^{(1)}\|^2 \overset{D.2}{\leq} C^2 \|d^* q_h^{(1)}\|^2 = C^2 \|\omega_h^{(0)}\|^2.$$

The discrete kinetic energy is bounded by the discrete enstrophy.

To obtain an equation for the evolution of enstrophy we take test function equal to the vorticity, $\omega_h^{(0)} = \boldsymbol{\omega}^T \boldsymbol{\phi}^{(0)}$,

$$\frac{1}{2}\frac{d}{dt}\int_\Omega \omega_h^{(0)} \wedge \star \omega_h^{(0)} = \left(\omega_h^{(0)}, \partial_t \omega_h^{(0)}\right)_\Omega = \boldsymbol{\omega}^T \mathbb{M}^{(0,0)} \frac{\partial \boldsymbol{\omega}}{\partial t}.$$

Hence, pre-multiplication of the discrete vorticity equation, Equation J.5, with the vorticity vector $\boldsymbol{\omega}$ yields,

$$\boldsymbol{\omega}^T \mathbb{M}^{(0,0)} \frac{\partial \boldsymbol{\omega}}{\partial t} - \cancel{\boldsymbol{\omega}^T \left(\mathbb{C}^{(0,1)}_{\boldsymbol{v}_h}\mathbb{E}^{(1,0)}\right)^T \boldsymbol{\omega}} = 0,$$

where,

$$\boldsymbol{\omega}^T \left(\mathbb{C}^{(0,1)}_{\boldsymbol{v}_h}\mathbb{E}^{(1,0)}\right)^T \boldsymbol{\omega} = \left(i_{\boldsymbol{v}_h} d\omega_h^{(0)}, \omega_h^{(0)}\right)_\Omega \overset{I.11}{=} \frac{1}{2}\int_\Omega d\|\omega_h^{(0)}\|^2 q_h^{(1)} = \frac{1}{2}\int_{\partial\Omega} \|\omega_h^{(0)}\|^2 q_h^{(1)} = 0. \tag{J.6}$$

Hence conservation of enstrophy depends on the incompressibility constraint, and on the exactness of the exterior derivative.

K

PICARD AND NEWTON LINEARISATION

The discrete vorticy- and momentum equations, Equation J.5 and Equation J.2, are non-linear systems of equations. We can write these equations in the following form.

$$\mathbb{A}(\boldsymbol{u})\boldsymbol{u} = \boldsymbol{f}, \tag{K.1}$$

where $\mathbb{A}(\boldsymbol{u})$ is the system matrix which is a function of the vector of unknown coefficients $\boldsymbol{u}$, and $\boldsymbol{f}$ is the right-hand-side vector. The system can be written as a fixed point,

$$\boldsymbol{u} = \mathbb{A}(\boldsymbol{u})^{-1}\boldsymbol{f},$$

which we can write as iterative process, $\boldsymbol{u}^{n+1} = \mathbb{A}(\boldsymbol{u}^n)^{-1}\boldsymbol{f}$.

Definition K.1 (Picard Iteration, (Sec. 9.7 [41]))**.** Consider the system of equations of the form Equation K.1. We generate a sequence $\boldsymbol{u}^n$ with $\boldsymbol{u}^n \to \boldsymbol{u}$ for $n \to \infty$, and initial guess $\boldsymbol{u}^0$, that satisfies,

$$\mathbb{A}(\boldsymbol{u}^n)\boldsymbol{u}^{n+1} = \boldsymbol{f}. \tag{K.2}$$

Iterative techniques that rely on Banach's fixed point iteration are known as *Picard iteration* techniques. Picard iteration converges linearly.

Alternatively, consider the vector of functionals $F(\boldsymbol{u})$,

$$F(\boldsymbol{u}) := \mathbb{A}(\boldsymbol{u})\boldsymbol{u} - \boldsymbol{f} = 0, \tag{K.3}$$

for which we take a Taylor expansion at $\boldsymbol{u}^{n+1}$,

$$\begin{aligned} 0 = F(\boldsymbol{u}) &= F\left(\boldsymbol{u}^n\right) + \left.\frac{\partial F(\boldsymbol{u})}{\partial \boldsymbol{u}}\right|_{\boldsymbol{u}^n}\left(\boldsymbol{u}-\boldsymbol{u}^n\right) + \mathcal{O}\left(\left(\boldsymbol{u}-\boldsymbol{u}^n\right)^2\right) \\ &= \left(\mathbb{A}\left(\boldsymbol{u}^n\right)\boldsymbol{u}^n - \boldsymbol{f}\right) + \left.\frac{\partial \mathbb{A}(\boldsymbol{u})\boldsymbol{u}}{\partial \boldsymbol{u}}\right|_{\boldsymbol{u}^n}\left(\boldsymbol{u}-\boldsymbol{u}^n\right) + \mathcal{O}\left(\left(\boldsymbol{u}-\boldsymbol{u}^n\right)^2\right), \end{aligned}$$

which we can evaluate at $\boldsymbol{u}^{n+1}$ to obtain,

$$0 = F(\boldsymbol{u}^{n+1}) = \left(\mathbb{A}\left(\boldsymbol{u}^n\right)\boldsymbol{u}^n - \boldsymbol{f}\right) + \left.\frac{\partial \mathbb{A}\left(\boldsymbol{u}\right)\boldsymbol{u}}{\partial \boldsymbol{u}}\right|_{\boldsymbol{u}^n}\left(\boldsymbol{u}^{n+1} - \boldsymbol{u}^n\right) + \mathcal{O}\left(\left(\boldsymbol{u}^{n+1} - \boldsymbol{u}^n\right)^2\right). \tag{K.4}$$

By neglecting higher order terms, we solve for $\boldsymbol{u}^{n+1}$, and define an iterative process.

Definition K.2 (Newton Iteration, (Sec. 9.7 [41]))**.** Consider the system of equations of the form Equation K.3. In the neighbourhood of root $\boldsymbol{u}^{n+1}$, we generate a sequence $\boldsymbol{u}^n$ using Taylor's theorem, Equation K.4, with some initial guess $\boldsymbol{u}^0$,

$$\boldsymbol{u}^{n+1} = \boldsymbol{u}^n - \left[\left.\frac{\partial \mathbb{A}\left(\boldsymbol{u}\right)\boldsymbol{u}}{\partial \boldsymbol{u}}\right|_{\boldsymbol{u}^n}\right]^{-1}\left(\mathbb{A}\left(\boldsymbol{u}^n\right)\boldsymbol{u}^n - \boldsymbol{f}\right), \tag{K.5}$$

where $\left.\frac{\partial \mathbb{A}(\boldsymbol{u})\boldsymbol{u}}{\partial \boldsymbol{u}}\right|_{\boldsymbol{u}^n}$ is the Jacobian matrix. This method is known as the *Newton iteration* techniques. Newton iteration converges quadratically. The method is less robust than Picard iteration, and more sensitive to the accuracy of the initial guess $\boldsymbol{u}^0$.

As an example non-linear test problem we consider *Burgers' equation* in $\mathbb{R}^1$. Burgers' equations describe a simplified Euler flow under the assumption that the function gradient equals zero. For this example we consider the non-conservative form of Burgers' equation (equivalent formulations for incompressible flows were derived in section 4.2), which is given by,

$$\frac{\partial v^{(0)}}{\partial t} + \mathscr{L}_{\boldsymbol{v}}\, v^{(0)} = 0. \tag{K.6}$$

Example K.1 (Linearization of Burgers' Equation)**.** Consider space-time domain $Q = \Omega \times T$, with unit-interval $\Omega = [0,1]$, and time-interval $T = [0,t]$. The discrete system of Burgers' equation, Equation K.6, using standard space-time Galerkin technique is given by,

$$\mathbb{A}^{(0,0)}_{\boldsymbol{v}}\,\boldsymbol{v} = 0, \tag{K.7}$$

$$\text{with } \mathbb{A}^{(0,0)}_{\boldsymbol{v}} = \mathbb{C}^{(0,1)}_{\boldsymbol{X}_h(\boldsymbol{v}^n)}\mathbb{E}^{(1,0)}, \tag{K.8}$$

where $\boldsymbol{X}_h(\boldsymbol{v}) = v_h\partial_x + c\partial t$ is the space-time velocity vector field, and $v_h = \boldsymbol{v}^T\boldsymbol{\phi}^{(0)}$ the reconstructed velocity field. To linearize the system of non-linear equations we consider sequences generated through Picard's and Newton's technique, where we take initial guess $\boldsymbol{v}^0$ equal to the initial solution at $t = 0$ over time $[0,t]$. Picard's technique, Equation K.2, requires iteratively solving of,

$$\mathbb{A}^{(0,0)}_{\boldsymbol{v}^n}\,\boldsymbol{v}^{n+1} = \boldsymbol{0}, \tag{K.9}$$

To generate a sequence through Newton, we need to compute the Jacobian matrix $\mathbb{J}\left(\mathbb{A}^{(0,0)}_{\boldsymbol{v}}\,\boldsymbol{v}\right)$. Using the product rule we find,

$$\mathbb{J}\left(\mathbb{A}^{(0,0)}_{\boldsymbol{v}}\right) := \frac{\partial}{\partial \boldsymbol{v}}\left[\mathbb{A}^{(0,0)}_{\boldsymbol{v}}\,\boldsymbol{v}\right] = \frac{\partial}{\partial \boldsymbol{v}}\left[\mathbb{A}^{(0,0)}_{\boldsymbol{v}}\right]\boldsymbol{v} + \mathbb{A}^{(0,0)}_{\boldsymbol{v}}\frac{\partial}{\partial \boldsymbol{v}}\left[\boldsymbol{v}\right],$$

with,

$$\frac{\partial}{\partial v_j} v_i = \delta_i^j,$$

and,

$$\begin{aligned}\frac{\partial}{\partial v_j}\left[\left(\mathbb{A}_{\boldsymbol{v}}^{(0,0)}\right)_{i,:}\right]\boldsymbol{v} &= \left(\frac{\partial}{\partial v_j}\int_Q \left(\left[\phi_i^{(0)}(\boldsymbol{v}^T\boldsymbol{\phi}^{(0)})(\boldsymbol{\phi}_x^{(1)})^T \quad \phi_i^{(0)} c(\boldsymbol{\phi}_t^{(1)})^T\right]\right) dQ\right)\mathbb{E}^{(1,0)}\boldsymbol{v} \\ &= \left(\int_Q \left(\left[\phi_i^{(0)}\phi_j^{(0)}(\boldsymbol{\phi}_x^{(1)})^T \quad \mathbf{0}^T\right]\right) dQ\right)\mathbb{E}^{(1,0)}\boldsymbol{v}\end{aligned}$$

Newton's methods, Equation K.5, then yields,

$$\boldsymbol{v}^{n+1} = \boldsymbol{v}^n - \left[\mathbb{J}\left(\mathbb{A}_{\boldsymbol{v}^n}^{(0,0)}\right)\right]^{-1}\left[\mathbb{A}_{\boldsymbol{v}^n}^{(0,0)}\boldsymbol{v}^n\right]. \tag{K.10}$$

As an initial condition we take the sinusoid, Equation 4.26 with $\sigma = 0.4$ and $x_0 = 0.5$. For the discretization we took linear splines, $\Lambda_h^{(0)} = \mathscr{S}_{64,24}^{1,1}$. Finally we took time $t = 0.2$. Results are shown in Figure K.1. The initially smooth sinusoid steepens at its front, and will eventually become discontinuous.

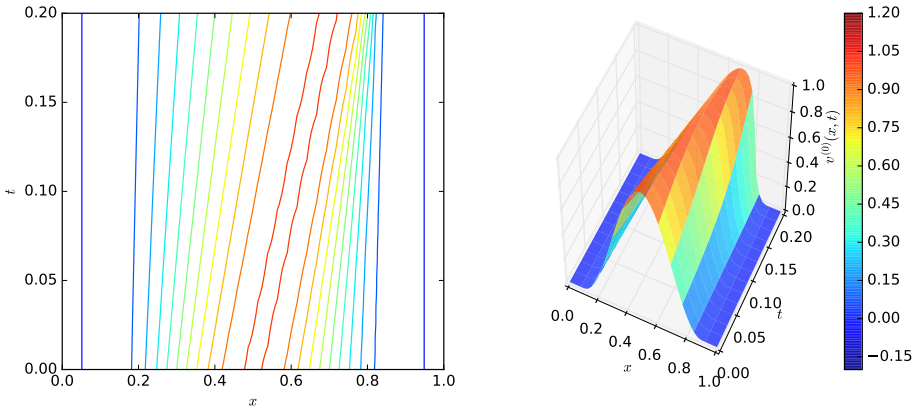

Figure K.1: Steepening in Burgers' equation of initial distribution. Contour plot (left) show the characteristic lines. Surf plot is also given (right).

To analyze the convergence behaviour of both methods we look at the residual r^n,

$$r^{n+1} = \|\boldsymbol{u}^{n+1} - \boldsymbol{u}^n\|_\infty.$$

Convergence is achieved when r^{n+1} is within the range of machine precision, i.e. $r^{n+1} = \mathscr{O}(10^{-14})$. Convergence can be considered linear if the linear convergence speed v_{lin} equals to some constant $C < 1$. Similarly, convergence can be considered quadratic if the quadratic convergence speed v_{qua} equals to some constant $C < 1$.

$$v_{\text{lin}} := \frac{\|\boldsymbol{u}^{n+1}-\boldsymbol{u}^n\|_\infty}{\|\boldsymbol{u}^n-\boldsymbol{u}^{n-1}\|_\infty} \qquad v_{\text{qua}} = \frac{\|\boldsymbol{u}^{n+1}-\boldsymbol{u}^n\|_\infty}{\|\boldsymbol{u}^n-\boldsymbol{u}^{n-1}\|_\infty^2} \tag{K.11}$$

Results are shown in Figure K.2. Both techniques converged with machine precision. Picard iteration converged with 27 iterations, whereas Newton iteration required 5 iterations.

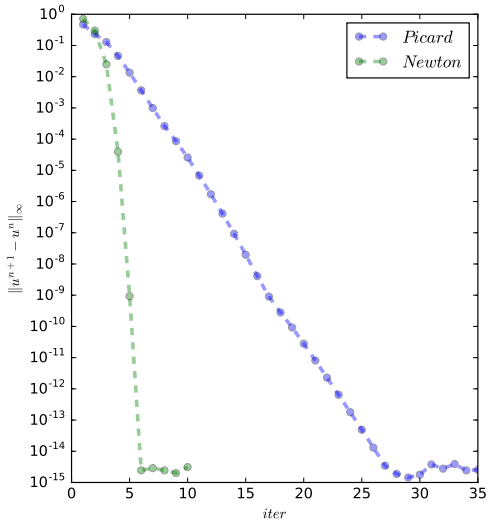

(a) Iteration residual. Methods are converged when $\|\boldsymbol{u}^{n+1} - \boldsymbol{u}^n\|_\infty = \mathcal{O}(10^{-14})$.

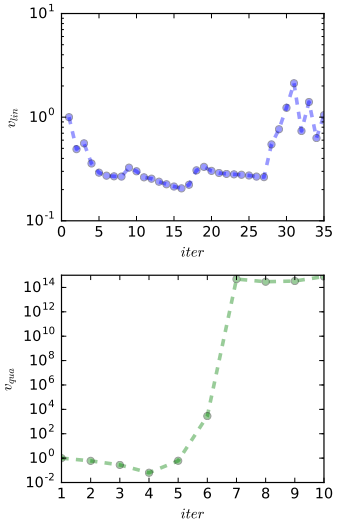

(b) Convergence speed versus iteration number, Equation K.11, of Picard (top) and Newton (bottom) iteration technique. Observed convergence speeds are near $C < 1$ until convergence is achieved.

Figure K.2

REFERENCES

[1] E. Tonti, *Why starting from differential equations for computational physics?* Journal of Computational Physics **257, Part B**, 1260 (2014).

[2] J. Donea and A. Huerta, *Finite Element Methods for Flow Problems* (John Wiley & Sons, Ltd, 2005).

[3] J. Hyman and M. Shashkov, *Mimetic discretizations for maxwell's equations,* Journal of Computational Physics **151**, 881 (1999).

[4] M. Desbrun, A. Hirani, M. Leok, and J. Marsden, *Discrete exterior calculus,* ArXiv Mathematics e-prints (2005), math/0508341 .

[5] D. N. Arnold, R. S. Falk, and R. Winther, *Finite element exterior calculus: from Hodge theory to numerical stability,* Bulletin of the American Mathematical Society (2010), arXiv:0906.4325 [math.NA] .

[6] P. Bochev and J. Hyman, *Principles of mimetic discretizations of differential operators,* in *Compatible Spatial Discretizations*, The IMA Volumes in Mathematics and its Applications, Vol. 142 (Springer New York, 2006) pp. 89–119.

[7] P. Bochev and M. Gerritsma, *A spectral mimetic least-squares method,* Computers & Mathematics with Applications **68**, 1480 (2014), minimum Residual and Least Squares Finite Element Methods.

[8] T. Hughes, J. Cottrell, and Y. Bazilevs, *Isogeometric analysis: Cad, finite elements, nurbs, exact geometry and mesh refinement,* Computer Methods in Applied Mechanics and Engineering **194**, 4135 (2005).

[9] I. B. J.A. Evans, Y. Bazilevs and T. Hughes, *nwidths, supinfs, and optimality ratios for the k-version of the isogeometric finite element method,* Computer Methods in Applied Mechanics and Engineering **198**, 1726 (2009), advances in Simulation-Based Engineering Sciences, Honoring J. Tinsley Oden.

[10] T. Hughes, J. Evans, and A. Reali, *Finite element and {NURBS} approximations of eigenvalue, boundary-value, and initial-value problems,* Computer Methods in Applied Mechanics and Engineering **272**, 290 (2014).

[11] A. Buffa, J. Rivas, G. Sangalli, and R. Vázquez, *Isogeometric discrete differential forms in three dimensions,* SIAM Journal on Numerical Analysis **49**, 818 (2011), http://dx.doi.org/10.1137/100786708 .

[12] A. Buffa, G. Sangalli, and R. Vázquez, *Isogeometric methods for computational electromagnetics: B-spline and t-spline discretizations,* Journal of Computational Physics **257, Part B**, 1291 (2014), physics-compatible numerical methods.

[13] J. Evans and T. Hughes, *Isogeometric divergence-conforming b-splines for the unsteady navier-stokes equations,* Journal of Computational Physics **241**, 141 (2013).

[14] A. Majda and A. Bertozzi, *Vorticity and Incompressible Flow (Cambridge Texts in Applied Mathematics)*, 1st ed. (Cambridge University Press, 2001).

[15] V. Arnold, *Sur la géométrie diffeérentielle des groupes de lie de dimensione infinie et ses application à l'hydrodynamique des fluides parfaits,* Ann. Inst. Fourier , 319 (1966).

[16] M. Olshanskii and L. Rebholz, *Velocity-vorticity-helicity formulation and a solver for the navier-stokes equations,* Journal of Computational Physics **229**, 4291 (2010).

[17] A. Palha and M. Gerritsma, *A mass, energy, enstrophy, and vorticity conserving (meevc) mimetic spectral element discretization for the 2d incompressible navier-stokes equations,* (2016).

[18] T. Frankel, *The Geometry of Physics: An Introduction* (Cambridge University Press, 2011).

[19] W. Burke, *Applied Differential Geometry* (Cambridge University Press, 1987).

[20] J. Kreeft, A. Palha, and M. Gerritsma, *Mimetic framework on curvilinear quadrilaterals of arbitrary order,* (2011).

[21] J. Kreeft and M. Gerritsma, *Mixed mimetic spectral element method for stokes flow: A pointwise divergence-free solution,* Journal of Computational Physics **240**, 284 (2013).

[22] F. Brezzi and M. Fortin, *Mixed and hybrid finite elements methods*, Springer series in computational mathematics (Springer-Verlag, 1991).

[23] P. Bochev, *A discourse on variational and geometric aspects of stability of discretizations,* 33rd Computational Fluid Dynamics Lecture Series, VKI LS (2003-05).

[24] L. Piegl. and W. Tiller, *The NURBS book*, Monographs in visual communications (Springer, Berlin, New York, 1997) nURBS : Non-Uniform Rational B-Splines.

[25] J. A. Cottrell, T. J. R. Hughes, and Y. Bazilevs, *Isogeometric Analysis: Toward Integration of CAD and FEA*, 1st ed. (Wiley Publishing, 2009).

[26] R. Hiemstra, D. Toshniwal, R. Huijsmans, and M. Gerritsma, *High order geometric methods with exact conservation properties,* Journal of Computational Physics **257, Part B**, 1444 (2014), physics-compatible numerical methods.

[27] R. Hiemstra, *IsoGeometric Mimetic Methods*, Master's thesis, Delft University of Technology (2011).

[28] Hirani and A. Nirmal, *Discrete Exterior Calculus*, Ph.D. thesis, Pasadena, CA, USA (2003), aAI3086864.

[29] M. Rudman, *Volume-tracking methods for interfacial flow calculations,* (2009).

[30] R. Abedi, S.-H. Chung, J. Erickson, Y. Fan, M. Garland, D. Guoy, R. Haber, J. M. Sullivan, S. Thite, and Y. Zhou, *Spacetime meshing with adaptive refinement and coarsening,* in *Proceedings of the Twentieth Annual Symposium on Computational Geometry*, SCG '04 (ACM, New York, NY, USA, 2004) pp. 300–309.

[31] A. Bossavit, *Extrusion, contraction: their discretization via whitney forms,* COMPEL - The international journal for computation and mathematics in electrical and electronic engineering **22**, 470 (2003), http://dx.doi.org/10.1108/03321640310474877 .

[32] H. Heumann and R. Hiptmair, *Extrusion contraction upwind schemes for convection-diffusion problems*, Tech. Rep. 2008-30 (Seminar for Applied Mathematics, ETH Zürich, Switzerland, 2008).

[33] P. Mullen, A. McKenzie, D. Pavlov, L. Durant, Y. Tong, E. Kanso, J. E. Marsden, and M. Desbrun, *Discrete Lie Advection of Differential Forms,* ArXiv e-prints (2009), arXiv:0912.1177 [math.NA] .

[34] A. Palha, *High Order Mimetic Discretization*, Ph.D. thesis, Delft University of Technology (2013).

[35] P. Rebelo, *Physically Accurate Advection - A discrete representation of the Lie derivative,* Master's thesis, Delft University of Technology (2011).

[36] B. d. H. M. Gerritsma, J. Kunnen, *Discrete lie derivative,* .

[37] R. Granger, *Fluid Mechanics* (Courier Corporation, 1995).

[38] A. Palha and M. Gerritsma, *Mimetic spectral element method for hamiltonian systems,* arXiv preprint arXiv:1505.03422 (2015).

[39] V. Goldshtein and M. Troyanov, *Sobolev inequalities for differential forms andl q,p -cohomology,* The Journal of Geometric Analysis **16**, 597 (2006).

[40] R. Falk and R. Winther, *Local bounded cochain projections,* Mathematics of **83**, 2631 (2014).

[41] J. van Kan, A. Segal, and F. Vermolen, *Numerical Methods in Scientific Computing* (Delft Academic Press / VSSD, 2014).

INDEX